SISSA - SCUOLA
INTERNAZIONALE
SUPERIORE
I STUDI AVANZATI
TRIESTE
Strada Costiera 11

ISAS - INTERNATIONAL SCHOOL FOR ADVANCED STUDIES

Thesis submitted for the degree of
"Doctor Philosophiae"

Concentration Fluctuations in Liquid Metal Alloys

CANDIDATE:
Wang Li

SUPERVISOR:
Prof. Mario P. Tosi

Academic Year 1988/89

TRIESTE

Acknowledgement

I would like to express my gratitude to Professor Mario P. Tosi for his supervision and constant help throughout this work.

Contents

Introduction

The focus of this thesis is on the thermodynamic properties of liquid alloys, with special attention to the description of concentration fluctuations in these systems and how they relate to their phase diagram. Together with the question of phase stability in relation to thermodynamic state (temperature, pressure and composition), we shall be discussing also the compressibility and the concentration dependence of the molar volume in the alloy. Our main interest will concern the microscopic electron theory of these thermodynamic properties.

The partial structure factors in an alloy give information on the spacial arrangement of pairs of metal ions. These structural functions can be determined experimentally by neutron diffraction using the technique of isotopic enrichment. Using thermodynamic fluctuation theory, Kirkwood and Buff[1] showed that the partial structure factors at long wavelength are related to a set of thermodynamic properties. In a binary alloy these are the isothermal compressibility, the difference in partial molar volumes of the alloy components, and the dependence of the chemical potential of the solute of its concentration. The latter quantity in particular is related to the concentration-concentration structure factor introduced by Bhatia and Thornton[2]. The above thermodynamic quantities can be measured by appropriate thermodynamic techniques,

as we shall see in the following.

From the point of view of microscopic theory, the approach based on pseudopotentials for the electron-ion interactions and screening by the conduction electrons has been extensively used to deal with the electronic and atomic properties of metals and alloys. The original part of this thesis is concerned with examining the usefulness of this approach in relation to the thermodynamic properties of liquid alloys that we have mentioned above. We shall discuss the construction of effective pair potentials in an alloy, with specific attention to alkali metal alloy, and relate the potentials in Fourier transform and in the long wavelength limit to the concentration-concentration structure factor, the isothermal compressibility and the difference in partial molar volumes of the alloy components.

We shall also see in the course of the discussion that the concentration-concentration structure factor has a very close relation to the so-called stability function and the phase diagrams. Different type of phase diagrams will also be discussed in relation to transport properties.

The layout of the thesis is as follows. In Chapter 1 we give a general descriptive introduction to the structure factors and the thermodynamic properties of liquid metals and alloys. In the last part of this chapter, we collect experimental data on phase diagrams, concentration-concentration structure factors and electrical resistivities of binary liquid metal alloys. The data show the relations between the behavior of the concentration-concentration structure factor, as a function of concentration, and the other properties (such as the complex-forming composition, the glass-forming range, the high-melting composition in the phase diagram and anomalies of the transport properties). In Chapter 2 a brief

description of pseudopotential theory is presented. Some typical model potentials and their applications are introduced. In Chapter 3, we first derive an exact formula for the concentration-concentration structure factor in a binary liquid alloy, showing how mechanical stress contributions and electron transfer contributions enter its determination, and relate it within pseudopotential theory to the pair potentials in the alloy. The long wavelength limit of the effective ion-ion interaction is of interest and will be derived in full detail. Our numerical calculation for some alkali-metal alloys are compared with the experiments. Chapter 4 is a short summary of this work.

Chapter 1

Structure and Thermodynamic fluctuations in Liquid Metals and Alloys

1.1 Structure factor and thermodynamics of a monatomic liquid[3–5]

The most basic characteristic of a liquid is that it possesses short-range order, as opposed to the long-range periodicity of a crystalline solid. Just as the structure of a crystal is determined experimentally by observing the Bragg reflections of X-rays, a quantitative description of the liquid structure can be given via the intensity I of X-rays scattered through an angle 2θ from the liquid. If we introduce the wavenumber variable $k = 4\pi\, sin\theta/\lambda$, λ being the X-ray wavelength, then the liquid structure factor $S(k)$ is defined by

$$S(k) = I/Nf^2 \tag{1.1}$$

where N is the total number of atoms in the liquid, assumed monatomic. In equation (1.1), $f(k)$ is the atomic scattering factor, *i.e.* the Fourier transform of the electron density in the atom. $f(k)$ falls from a value Z, the atomic number, at $k = 0$ to zero at large k, the asymptotic behaviour being proportional to k^{-4}.

1.1.1 Definition of radial distribution function $g(r)$ and structure factor $S(k)$

To gain insight into the relation between the liquid structure factor $S(k)$ in (1.1) and the atomic arrangement, one now uses the Debye theory of the diffraction of X-ray by a liquid* . One has

$$I = Nf^2[1 + \sum_n{}' \frac{sin\, kR_{nm}}{kR_{nm}}]. \tag{1.2}$$

Here the R_{nm} denote the interatomic distances in the system, while the prime denotes the exclusion of the term $R_{nm} = 0$ from the summation. Eqn. (1.2), on which the statistical average is still to be taken for a fluid, reveals an interference pattern between scattered X-rays from pairs of atoms. Therefore, it is helpful to introduce the pair distribution function $g(r)$, which, following Zernike and Prins*, is defined by setting $\rho\, g(r) 4\pi\, r^2 dr$ equal to the total average number of atoms in a spherical shell of radius r and thickness dr centered on a chosen atom at the origin of coordinates. Here $\rho = N/V$ is the average number density of N atoms in volume V. Replacing the summation in Eqn. (1.2) by an integration, and subtracting the X-ray scattering from a uniform density of electrons (merely a delta function at $k = 0$ in the limit of a

* For details and references see [3].

large liquid sample), we find from Eqns. (1.1) and (1.2) that

$$S(k) = 1 + \rho \int_0^\infty 4\pi r^2 [g(r) - 1] \frac{sinkr}{kr} dr. \qquad (1.3)$$

Here, the liquid structure factor is related by Fourier transform to the atomic arrangement around a given atom chosen at the origin. By noting that $sinkr/kr$ is the s wave ($l = 0$ term) in the expansion of the plane wave $\exp(i\mathbf{k} \cdot \mathbf{r})$ in spherical waves, $S(k)$ in (1.3) can be rewritten as

$$S(k) = 1 + \rho \int [g(r) - 1] exp(i\mathbf{k} \cdot \mathbf{r}) \mathbf{dr}. \qquad (1.4)$$

In a crystalline solid, $g(r)$ in (1.4) would not be isotropic but (neglecting atomic vibrations and choosing the origin at lattice site) would be a sum of delta functions centered on the crystal lattice sites. Evidently, Eqn. (1.4) would lead then to non-zero $S(k)$ only when $\mathbf{k}$ is a reciprocal lattice vector. These reflections can be thought of, roughly, as blurred out and spherically averaged in the liquid, leading to a continuous function $S(k)$ reflecting directly the short-range order via $g(r)$. We would view Eqns. (1.3) and (1.4) as the route by which X-ray intensity could be predicted from a calculated pair distribution function $g(r)$. Alternatively, one can invert the Fourier transform and hence derive $g(r)$ from the measured $S(k)$ via

$$\begin{aligned} g(r) &= \frac{1}{8\pi^3 \rho} \int [S(k) - 1] exp(-i\mathbf{k} \cdot \mathbf{r}) \mathbf{dk} \\ &= 1 + \frac{1}{2\pi^2 \rho r} \int_0^\infty [S(k) - 1] k \, sin \, kr \, dk. \end{aligned} \qquad (1.5)$$

Of course, the determination of $g(r)$ from the measured $S(k)$ is subject to some problems and the kinds of errors which can arise have been discussed by Paalman and Pings [3].

Fig. 1.1 reports the liquid structure factor $S(k)$ of the three alkali metals Na, K, and Cs near their respective freezing points, from X-ray

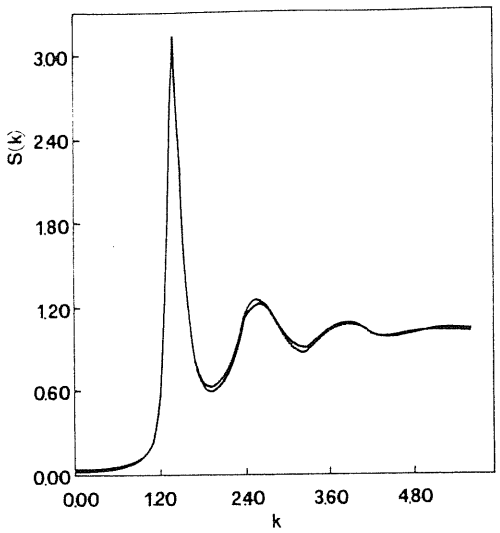

Figure 1.1: Structure factor $S(k)$ of molten Na, K and Cs near freezing versus scaled wavenumber (from [6]).

diffraction data[6]. The wave number k for the three systems has been scaled so as to bring out the striking affinity of their liquid structure, as far as the main peak and the high-k features are concerned. At low wave number (below $1\mathring{A}^{-1}$, say) the differences between these structure factors, which are not visible on the scale of the figure, can only be appreciated through a quantitative comparison.

1.1.2 Internal energy and equation of state in liquids with pair forces

In this section expressions will be reported for the internal energy E and the equation of state. The assumption will be made that the intermolecular potential energy Φ can be decomposed into a sum of pair

potentials

$$\Phi(\mathbf{R}_1 ... \mathbf{R}_N) = \sum_{i<j} \phi(\mathbf{R}_{ij}). \tag{1.6}$$

The objectives will be to obtain E and the pressure p in terms of the pair distribution function $g(r)$ and the potential $\phi(r)$.

In a classical monatomic liquid at temperature T, the kinetic energy per degree of freedom is $\frac{1}{2}k_BT$ and hence

$$E = \frac{3}{2}Nk_BT + < \Phi > . \tag{1.7}$$

The mean potential energy $< \Phi >$ is simply

$$< \Phi >= Z^{-1} \int ... \int exp(-\Phi/k_BT)\Phi d\mathbf{R}_1 ... d\mathbf{R}_N, \tag{1.8}$$

where Z is the partition function. From the assumption (1.6) of pair forces, the sum consists of $N(N-1)/2$ terms, all of which make equal contributions to $< \Phi >$. Hence we have

$$< \Phi >= \frac{N(N-1)}{2} \int \int \phi(R_{12}) [\frac{\int ... \int exp(-\Phi/k_BT)\, d\mathbf{R}_3 ... d\mathbf{R}_N}{Z}] d\mathbf{R}_1 d\mathbf{R}_2. \tag{1.9}$$

But from the definition of the radial distribution function we can write

$$\begin{aligned} < \Phi > &= \frac{N(N-1)}{2} \int \int \phi(R_{12}) \frac{(N-2)!}{N!} \rho^2 g(R_{12}) d\mathbf{R}_1 d\mathbf{R}_2 \\ &= \frac{1}{2}\rho^2 V \int_0^\infty \phi(r) g(r) 4\pi r^2 dr, \end{aligned} \tag{1.10}$$

one of the integrations yielding immediately the volume V of the fluid. Hence we have finally

$$E = \frac{3}{2}Nk_BT + \frac{N\rho}{2} \int_0^\infty \phi(r) g(r) 4\pi r^2 dr. \tag{1.11}$$

The potential energy term exhibited in this equation could have been written down directly on physical grounds, since the number of molecules

on average within a distance between r and $r + dr$ of a given molecule is $\rho g(r) 4\pi^2 dr$ and the factor $\frac{1}{2}$ avoids counting interactions twice over.

Similarly, the equation of state can be obtained. To do so, we make use of the classical virial theorem, which relates the average of the kinetic energy, $\overline{K}$ say, to the virial of the forces. The virial of the pressure p is $3pV$, yielding for a perfect gas

$$2\overline{K} = 3pV. \tag{1.12}$$

When there is a force $\mathbf{F}_i$ acting on the ith molecule at $\mathbf{R}_i$, the average of $-\sum \mathbf{R}_i \cdot \mathbf{F}_i$ has to be calculated, the summation extending over all the molecules. For central pair forces, this becomes again the average of $N(N-1)/2$ terms, one term being

$$\int R_{12} \frac{\partial \phi(R_{12})}{\partial R_{12}} [\int \frac{exp(-\Phi/k_B T)}{Z} d\mathbf{R}_3 ... d\mathbf{R}_N] d\mathbf{R}_1 d\mathbf{R}_2. \tag{1.13}$$

Expressing this once more in terms of the radial distribution function yields, since $\overline{K} = \frac{3}{2} N k_B T$, as used in the calculation of E,

$$3pV = 3Nk_B T - \frac{N(N-1)}{2} \int R_{12} \frac{\partial \phi}{\partial r} g(r) d\mathbf{r}, \tag{1.14}$$

or

$$p = \rho k_B T - \frac{\rho^2}{6} \int r \frac{\partial \phi}{\partial r} g(r) dr. \tag{1.15}$$

In principle then, from an assumed law of force and knowledge of the corresponding radial distribution function, the internal energy E and the fluid pressure p can be estimated from Eqns. (1.11) and (1.15).

The results derived here are valid for insulating fluids, where the effects of conduction electrons are absent. For a metal, we have to include also contributions from the conduction electrons to the energy, which are volume dependent; in addition, the pair potential is also density

dependent, via the screening due to the conduction electrons. We can thus write the total potential energy U for a metal as

$$U(\mathbf{R}_1, ...\mathbf{R}_N) = U_0(\rho) + U_s(\mathbf{R}_1, ...\mathbf{R}_N; \rho),$$

where $U_0(\rho)$ expresses the volume-dependent part of the energy, which is entirely independent of structure, and $U_s(\mathbf{R}_1, ...\mathbf{R}_N)$ is the structure- and volume-dependent remainder. If the structure-dependent part of the potential energy can be written in a pair approximation with pair potential $\phi(r;\rho)$, then the pressure p, for a metal, can be written[7]

$$p = \rho k_B T + \rho^2 \frac{dU_0}{d\rho} - \frac{1}{2}\rho^2 \int dr 4\pi r^2 g(r)\{\frac{r}{3}\frac{\partial \phi}{\partial r} - \rho\frac{\partial \phi}{\partial \rho}\} \qquad (1.16)$$

where ρ is the mean ionic density.

It is important to note at this point that while Equation (1.15), or (1.16), requires knowledge of both $g(r)$ and $\phi(r)$, there is another route to the equation of state of a fluid, which is more fundamental in that it does not require the assumption (1.6) of pair potentials. However, to derive this further relation we must go from the canonical ensemble used above to the grand canonical ensemble.

1.1.3 Relation of liquid structure factor at $k = 0$ to compressibility

Let us consider an open region, *i.e.* one in which particles can come and go freely, drawn in a system of infinite extent. We shall now show that the fluctuation in the number of particles in this region is given by the volume integral of $g(r) - 1$ and is specifically related to the isothermal compressibility of the fluid. Another interesting example of such relation

between fluctuations and thermodynamical quantities yields the specific heat C_V [3].

One reason for the interest in the above relation between the volume integral of the radial distribution function, or equivalently, from Eqn (1.3), the long wavelength limit of $S(k)$, and the compressibility, is because of the difficulty of extending the diffraction experiments, referred to in section 1.1.1, to small scattering angles.

Consider a member of the grand canonical ensemble in which the open region, of volume V, contains exactly N particles. For a specified configuration of the particles, $\mathbf{R}_i$ say, the singlet density $\rho(\mathbf{r}_1)$ at point $\mathbf{r}_1$ in this region, and the density $\rho^{(2)}(\mathbf{r}_1\mathbf{r}_2)$ of pairs of particles at point $\mathbf{r}_1$ and $\mathbf{r}_2$ are respectively given by

$$\rho(\mathbf{r}_1) = \sum_{i=1}^{N} \delta(\mathbf{R}_i - \mathbf{r}_1) \tag{1.17}$$

and

$$\rho^{(2)}(\mathbf{r}_1\mathbf{r}_2) = \sum_{i\neq j=1}^{N} \delta(\mathbf{R}_i - \mathbf{r}_1)\delta(\mathbf{R}_i - \mathbf{r}_2). \tag{1.18}$$

It follows immediately from these definitions that

$$\int_V d\mathbf{r}_1 \rho(\mathbf{r}_1) = \mathrm{N} \tag{1.19}$$

$$\int_V \int_V d\mathbf{r}_1 d\mathbf{r}_2 \rho^{(2)}(\mathbf{r}_1\mathbf{r}_2) = \mathrm{N}^2 - \mathrm{N} \tag{1.20}$$

The distribution function for single particle and for pair of particles are obtained by averaging the respective densities over phase space and over all number N of particles with the probability distribution of the grand canonical ensemble,

$$W_{GC} = exp[(\Omega + N\mu - H_N)/k_B T)], \tag{1.21}$$

where $\Omega = -pV$, μ is the chemical potential, and H_N is the Hamiltonian of the set of N particles. In a fluid the averaged densities have the form $< \rho(\mathrm{r}_1) >=< \mathrm{N} > /\mathrm{V} = \rho$ and $< \rho^{(2)}(\mathrm{r}_1\mathrm{r}_2) >= \rho^2\mathrm{g}(\mathrm{r}_{12})$, where ρ is the bulk number density of the fluid and $g(r_{12})$ is the radial distribution function, dependent only on the scalar distance r_{12}. By taking the average of Eqn (1.20) it therefore follows that

$$\lim_{k\to 0} S(k) = 1 + \rho \int dV[g(r_{12}) - 1] = \frac{< N^2 > -(< N >)^2}{< N >} \qquad (1.22)$$

which is the desired relation between the structure factor at long wavelengths and the particle number fluctuations.

Next, we recall from fluctuation theory that the particle number fluctuations are related to thermodynamic properties of the system. The grand partition function is

$$exp(-\Omega/k_BT) = \sum_{N=0}^{\infty} exp[N\mu - F(N,T,V)]/k_BT \qquad (1.23)$$

where $F(N,T,V)$ is the Helmholtz free energy of a member of the grand ensemble containing N particles. By differentiating Ω and the average number of particles,

$$< N >= \sum_{N=0}^{\infty} N exp[\Omega + N\mu - F(N,T,V)]/k_BT, \qquad (1.24)$$

with respect to the chemical potential we find

$$(\frac{\partial \Omega}{\partial \mu})_{T,V} = - < N > \qquad (1.25)$$

and

$$(\frac{\partial N}{\partial \mu})_{T,V} = \frac{1}{k_BT}[< N > [(\frac{\partial \Omega}{\partial \mu})_{T,V} + < N^2 >], \qquad (1.26)$$

whence it follows that

$$< N^2 > -(< N >)^2 = k_BT(\frac{\partial N}{\partial \mu})_{T,V}. \qquad (1.27)$$

Finally, by using the thermodynamic identity

$$(\frac{\partial \mu}{\partial N})_{T,V} = -\frac{1}{\rho^2}(\frac{\partial \rho}{\partial N})_{T,N} \equiv \frac{1}{\rho^2 V \kappa_T}$$

where κ_T is the isothermal compressibility, we arrive at the Ornstein-Zernike relation,

$$\lim_{k \to 0} S(k) = \rho k_B T \kappa_T. \tag{1.28}$$

1.1.4 Direct correlation function

As a final point, in this brief review, we note that there is a further correlation function, introduced by Ornstein and Zernike, and commonly refer to as the direct correlation function $c(r)$, which is much more intimately related to the pair potential $\phi(r)$ than is $g(r)$. Here we introduce the definition of $c(r)$ through the relation[3-5]

$$h(\mathbf{r}) = \mathrm{c}(\mathbf{r}) + \rho \int \mathrm{h}(\mid \mathbf{r} - \mathbf{r}' \mid)\mathrm{c}(\mathbf{r}')\mathrm{d}\mathbf{r}' \tag{1.29}$$

where $h(\mathbf{r}) = \mathrm{g}(\mathbf{r}) - 1$ is the total correlation function. By a Fourier transform, with

$$\tilde{c}(\mathbf{k}) = \rho \int \mathrm{c}(\mathbf{r})\mathrm{e}^{\mathrm{i}(\mathbf{k}\cdot\mathbf{r})}\mathrm{d}\mathbf{r} \tag{1.30}$$

we obtain almost immediately

$$\tilde{c}(\mathbf{k}) = \frac{\mathrm{S}(\mathbf{k}) - 1}{\mathrm{S}(\mathbf{k})} \tag{1.31}$$

$\tilde{c}(\mathbf{k})$ is dominated, for simple metals, by short-range behavior. At large r, $c(r)$ is directly proportional to the pair potential, the proportionality constant being simply $-(k_B T)^{-1}$ [4,5].

1.2 Structure factors and thermodynamics of a mixture

In this section we want to turn from the discussion of pure one-component liquids to deal with mixtures. Although many of the arguments presented are easy to generalize, we shall present the treatment in terms of binary mixtures[3].

1.2.1 Partial structure factors in a binary mixture

In a binary mixture, three pair correlation functions are evidently required for a complete description of static two-body correlation functions. Partial structure factors $a_{\alpha\beta}$ for a binary system with a total of N atoms in a volume V are often defined by

$$a_{\alpha\beta}(q) = 1 + 4\pi\rho \int_0^\infty [g_{\alpha\beta}(r) - 1] \frac{sin\, qr}{qr} r^2 dr \qquad (1.32)$$

where $g_{\alpha\beta}(r)$ represent the pair distribution functions and $\rho = N/V$. The definition of $g_{\alpha\beta}(r)$ is such that the quantity $4\pi\rho_\beta g_{\alpha\beta}(r)r^2 dr$ gives the number of particles of type β within a spherical shell at distance r from a particle of type α. Here, $\rho_\alpha = N_\alpha/V$ is the number of particles of type α per unit volume.

The above definition is usually adopted in dealing with thermodynamic properties of the mixture, but is not directly comparable with the structure factor in a one-component liquid. Structure factors giving directly the various contributions to the scattering intensity from the mixture are alternatively defined by

$$S_{\alpha\beta} = \delta_{\alpha\beta} + 4\pi(\rho_\alpha\rho_\beta)^{1/2} \int_0^\infty [g_{\alpha\beta}(r) - 1] \frac{sinqr}{qr} r^2 dr \qquad (1.33)$$

It is sometimes convenient to build other structure factors as linear combinations of those defined above, to describe correlations between fluctuations of properties of the mixture which can be expressed as linear combinations of the partial density fluctuations. One such combination is the number N-concentration c correlations, which are defined by

$$g_{NN}(r) = c_1^2 g_{11}(r) + c_2^2 g_{22}(r) + 2c_1 c_2 g_{12}(r) \quad (1.34)$$

$$g_{cc}(r) = c_1^2 c_2^2 [g_{11}(r) + g_{22}(r) - 2g_{12}(r)] \quad (1.35)$$

and

$$g_{Nc} = c_1 c_2 [c_1 g_{11}(r) - c_2 g_{22}(r) + (c_2 - c_1) g_{12}(r)] \quad (1.36)$$

where $c_\alpha = \rho_\alpha / \rho$ are the number concentrations. It is easily seen that these represent correlations between fluctuations in the total particle number density (irrespective of the species) and between fluctuations in the concentration and cross-correlations between these fluctuations, respectively. The corresponding structure factors are

$$\begin{aligned} S_{NN}(q) &= 1 + \rho \int d\mathbf{r} \exp(\mathrm{i}\mathbf{q}\cdot\mathbf{r})[\mathrm{g_{NN}(r)} - 1] \\ &= c_1 S_{11}(q) + c_2 S_{22}(q) + 2(c_1 c_2)^{1/2} S_{12}(q) \quad (1.37) \\ S_{cc}(q) &= c_1 c_2 + \rho \int d\mathbf{r} \exp(\mathrm{i}\mathbf{q}\cdot\mathbf{r})\mathrm{g_{cc}(r)} \\ &= c_1 c_2 [c_2 S_{11}(q) + c_1 S_{22}(q) - 2(c_1 c_2)^{1/2} S_{12}(q)] \quad (1.38) \end{aligned}$$

and

$$\begin{aligned} S_{Nc} &= \rho \int d\mathbf{r} \exp(\mathrm{i}\mathbf{q}\cdot\mathbf{r})\mathrm{g_{Nc}(r)} \\ &= c_1 c_2 [S_{11}(q) - S_{22}(q) + \frac{c_2 - c_1}{(c_1 c_2)^{1/2}} S_{12}(q)] \quad (1.39) \end{aligned}$$

The X-ray diffraction intensity itself is a linear combination of the partial structure factors $S_{\alpha\beta}(k)$, with weighting factors given by prod-

ucts of the scattering amplitudes of the component species. Specifically,

$$I(k) \propto f_1^2 S_{11}(k) + f_2^2 S_{22}(k) + 2 f_1 f_2 S_{12}(k) \tag{1.40}$$

where f_α are the atomic scattering factors. An X-ray diffraction experiment is obviously insufficient to determine separately the three partial structure factors. Such a determination becomes possible by neutron diffraction, if one takes advantage of the fact that different isotopes of the same element have sometimes very different scattering lengths. Mixtures built with identical chemical composition but different isotopic composition have different neutron scattering factors and hence experiments on such mixtures allow a complete determination of the $S_{\alpha\beta}$. The results of such an experiment on the $Cu - Sn$ system[8] are reported in Figure 1.2 while Figure 1.3 reports the number- concentration structure factors for the same system as constructed from the neutron scattering data by Bhatia and Thornton[2]. Figure 1.4 reports data by Ruppersberg[9] on the scattering intensity from a $Li - Pb$ alloy spanning the whole range of concentration.

Finally, we give the relations between the $a_{\alpha\beta}$ and the structure factors $S_{NN}(q)$, $S_{cc}(q)$ and $S_{Nc}(q)$ defined above. Since

$$S_{\alpha\beta} = \delta_{\alpha\beta} + (c_\alpha c_\beta)^{1/2}[a_{\alpha\beta}(q) - 1], \tag{1.41}$$

we have

$$c_1^2 a_{11}(q) = c_1^2 S_{NN}(q) + 2c_1 S_{Nc}(q) + S_{cc}(q) - c_1 c_2, \tag{1.42}$$

$$c_2^2 a_{22}(q) = c_2^2 S_{NN}(q) - 2c_2 S_{Nc}(q) + S_{cc}(q) - c_1 c_2 \tag{1.43}$$

and

$$c_1 c_2 a_{12}(q) = c_1 c_2 S_{NN}(q) + (c_2 - c_1) S_{Nc}(q) - S_{cc}(q) + c_1 c_2. \tag{1.44}$$

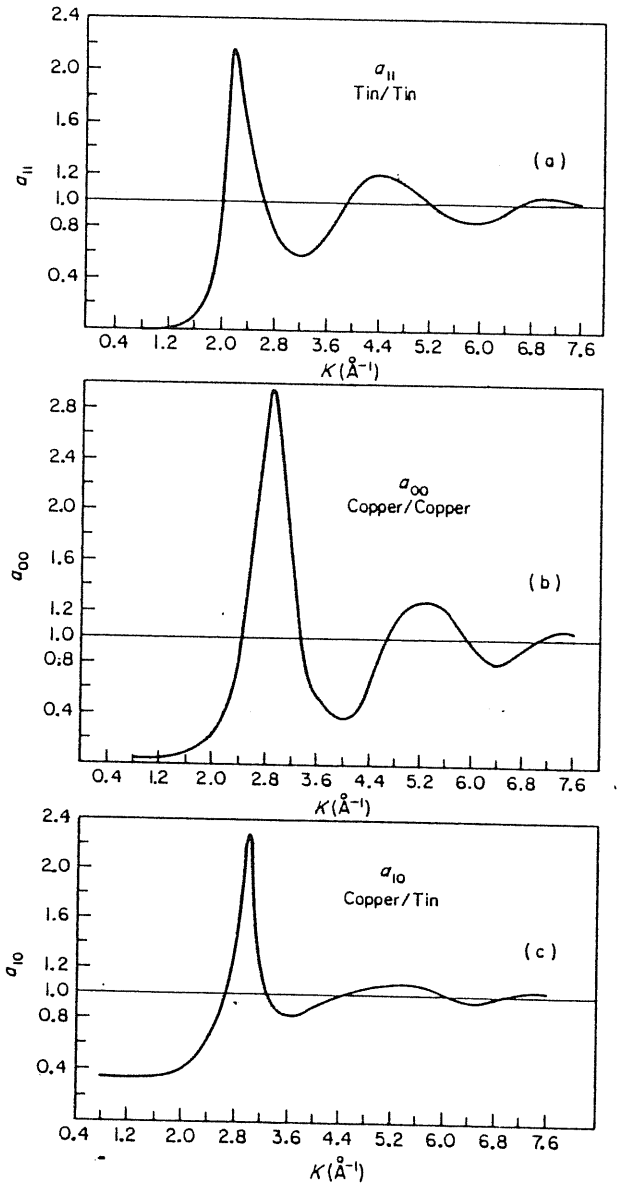

Figure 1.2: Partial structure factors in liquid Cu_6Sn_5 system, as obtained by neutron scattering through isotopic substitution (from [8]).

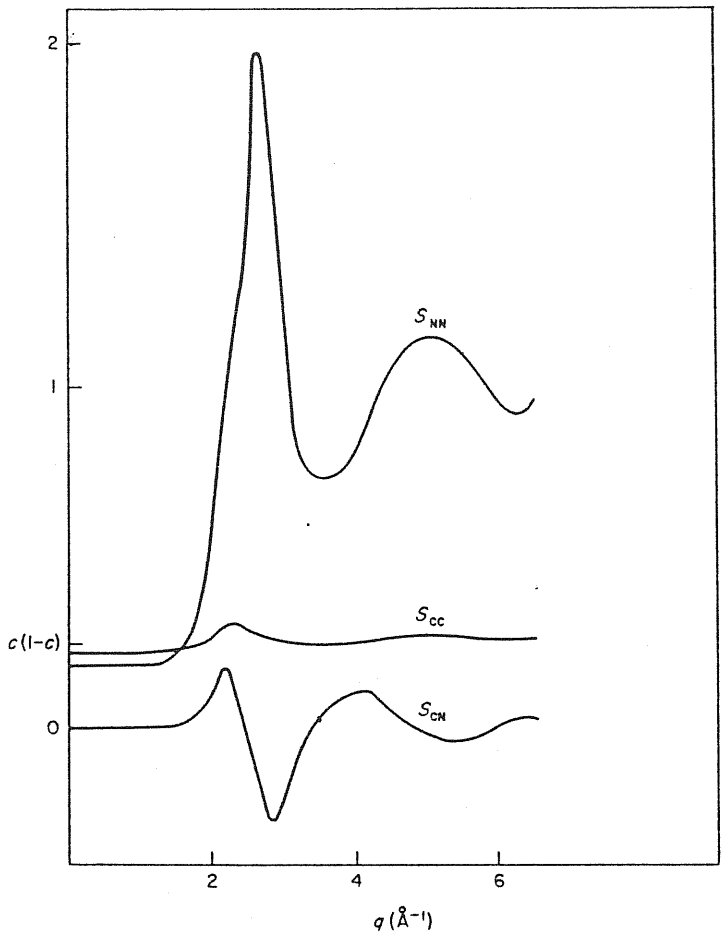

Figure 1.3: Number-concentration structure factors for the copper-tin alloy of figure 1.2 (from [2]).

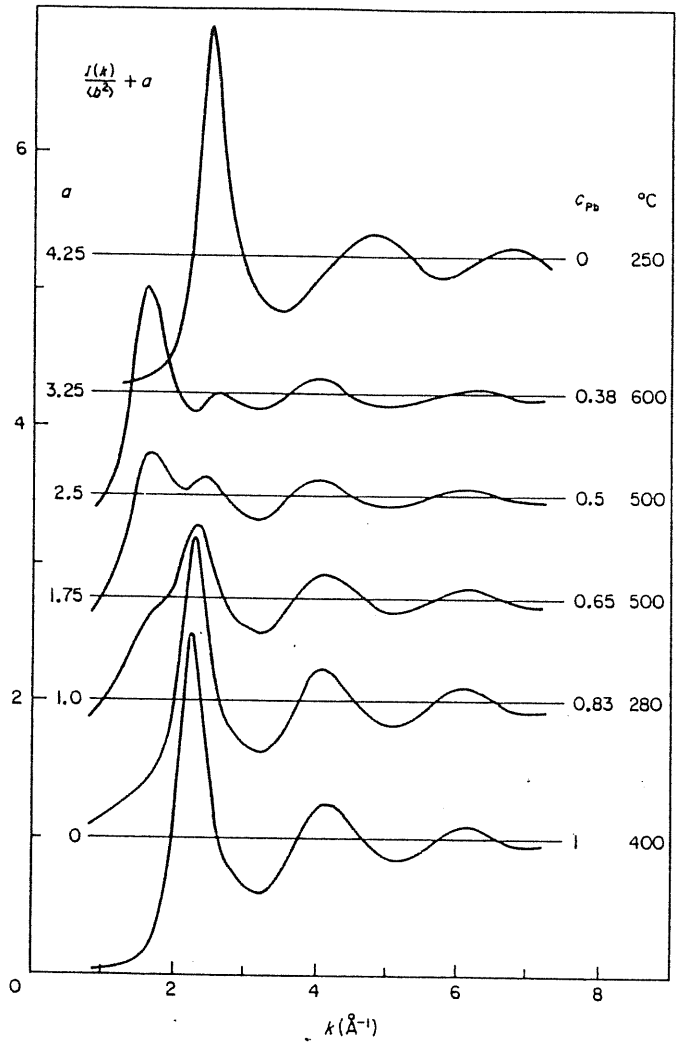

Figure 1.4: Neutron scattering intensities from $Li - Pb$ alloys at various concentrations, indicated on the right of the figure (from [9]). The scattering lengths are such as to give a more pronounced effect from concentration fluctuations for c between 50% and 11%Pb. The pre-peaks at such concentrations are due to $S_{cc}(k)$.

1.2.2 Partial structure factors in the long wavelength limit

In the long wavelength ($q \rightarrow 0$) limit, the structure factors defined in Eqns. (1.37)-(1.39) have simple physical meaning for liquid mixtures, namely[2,10]

$$S_{NN}(0) =< (\Delta N)^2 > /N, \tag{1.45}$$

$$S_{cc}(0) = N < (\Delta c)^2 > \tag{1.46}$$

and

$$S_{Nc}(0) =< \Delta N \Delta c > \tag{1.47}$$

where $< (\Delta N)^2 >$ is the mean square fluctuation in the number of particles in a subvolume, $< (\Delta c)^2 >$ the mean square fluctuation in concentration and $< \Delta N \Delta c >$ the correlation between the two fluctuations.

As it has been shown[2,10], one may write the above structure factors ($S_{NN}(0), S_{cc}(0)$ and $S_{Nc}(0)$) in terms of thermodynamic properties,

$$S_{NN}(0) = \theta + \delta^2 S_{cc}(0) \tag{1.48}$$

$$S_{Nc}(0) = -\delta S_{cc}(0) \tag{1.49}$$

and

$$S_{cc}(0) = \frac{N k_B T}{(\partial^2 G/\partial c^2)_{T,P}} \tag{1.50}$$

where

$$\theta = (N/V) k_B T \kappa_T, \tag{1.51}$$

$c \equiv c_2$, κ_T is the isothermal compressibility at constant composition, P, T are pressure and temperature respectively, G is the Gibbs free en-

ergy and δ is a dilation factor defined by

$$\delta = -\frac{1}{V}(\frac{\partial V}{\partial c})_{P,T,N} = \frac{v_1 - v_2}{(1-c)v_1 + cv_2} \tag{1.52}$$

where v_1 and v_2 are the partial molar volumes of the two species.

If the partial molar volumes of the two species are the same, then $\delta = 0$ and the fluctuations in number density are independent of those in concentration ($S_{Nc}(0) = 0$) and $S_{NN}(0)$, like the expression for the structure factor of a pure liquid, is equal to θ (see Eqn. (1.28)).

1.3 Models and applications for long wavelength fluctuations in alloys .

To calculate $S_{cc}(0)$ we need to know G or the free energy of mixing G_m which is defined by

$$G = (1-c)G_1 + cG_2 + G_m \tag{1.53}$$

where G_1 and G_2 are the Gibbs free energies of the pure species 1 and 2 at the same pressure and temperature as the mixture. On one hand, we can calculate $\partial^2 G/\partial c^2$, which is often called the stability function, on the basis of some simple theoretical models for G_m for different types of mixtures. On the other hand, $\partial^2 G/\partial c^2$ and hence $Scc(0)$ can be evaluated from the experimental data on G_m, or more conveniently, from the thermodynamic activity a_α of the solute as

$$S_{cc}(0) = -(1-c_\alpha)[(\partial ln a_\alpha/\partial c_\alpha)_{T,P}]^{-1}. \tag{1.54}$$

The commonly used method to get $S_{cc}(0)$ from the experiment is to measure the electromotive force (EMF) ε by using a suitable electromo-

tive cell. The formula (1.54) now becomes

$$S_{cc}(0) = -\frac{RT}{F}\frac{1-c}{(\partial\varepsilon/\partial c)_{T,P}} \tag{1.55}$$

where R is the universal gas constant and F the Faraday constant.

1.3.1 Model of conformal solutions.

The simplest realistic model for liquid mixtures is perhaps the conformal solution model of Longuet-Higgins[11] for which the Gibbs free energy is given by

$$G = (1-c)G_1 + cG_2 + Nk_BT\{clnc + (1-c)ln(1-c)\} + c(1-c)Nw \tag{1.56}$$

where the third term is just $(-T)$ times the entropy of random mixing and w is an interchange energy, which is assumed to be concentration independent. Its meaning is such that if a nearest neighbour $A-A$ atoms pair and a similar $B-B$ atoms pair are replaced by two $A-B$ pairs, the increase in the energy of the mixture is $2w/Z$, where Z is number of nearest neighbours of an atom. A positive w implies that like-atom nearest neighbour pairs are energetically preferred over unlike-atom pairs and viceversa for w negative.

According to Eqns. (1.50) and (1.56), $S_{cc}(0)$ can be written in the model of conformal solutions as

$$S_{cc}(0) = \frac{c(1-c)}{1 - \frac{2w}{k_BT}c(1-c)} \tag{1.57}$$

which is symmetric about $c = 0.5$ when w is independent of c.

The special case of this model is when $w = 0$. Then we come to the "ideal solution"

$$G_m^{id} = Nk_BT\{c\,ln\,c + (1-c)ln(1-c)\} \tag{1.58}$$

and

$$S_{cc}^{id}(0) = c(1-c) \tag{1.59}$$

which means the two types of atoms in the mixture are distributed at random .

Any deviation of $S_{cc}(0)$ from the ideal value $S_{cc}^{id}(0)$ is of great interest to visualize the degree of interaction in the mixture. If, at a given composition, $S_{cc}(0) \gg S_{cc}^{id}(0)$, then there is a tendency for segregation or phase separation; $S_{cc}(0) \ll S_{cc}^{id}(0)$ is an indication of strong association or the existence of the chemical complexes in the mixture. Figure 1.5 illustrates the behaviour of $S_{cc}(0)$ for several values of w. In this figure the experimental values for $Na-K$ alloy has been given, comparing with the theoretical curve for $w = 1.1k_BT$.

Here we recall the partial structure factors $a_{\alpha\beta}$ which are defined through Eqn. (1.32). We can rewrite them in the long-wavelength limit, by using Eqns. (1.48)-(1.50), as

$$a_{11} = \theta + [\frac{1}{(1-c)^2} - \frac{2\delta}{1-c} + \delta^2]S_{cc} - \frac{c}{1-c} \tag{1.60}$$

$$a_{22} = \theta + [\frac{1}{c^2} - \frac{2\delta}{c} + \delta^2]S_{cc} - \frac{c}{1-c} \tag{1.61}$$

$$a_{12} = \theta + [\delta^2 - \frac{(2c-1)\delta}{c(1-c)} - \frac{1}{c(1-c)}]S_{cc} + 1 \tag{1.62}$$

The quality of the predictions of these partial structure factors in the long-wavelength limit is shown by comparing the conformal solution theory with the experimentally derived results of McAlister and Turner[12] in Figure 1.6 for the $Na-K$ alloy[13]. The salient features of the experiments in this alloy are all faithfully reflected by the conformal solution theory.

Conformal solution theory should not be used in the case of large size differences. It fails, for instance, for liquid $Na-Cs$, where the

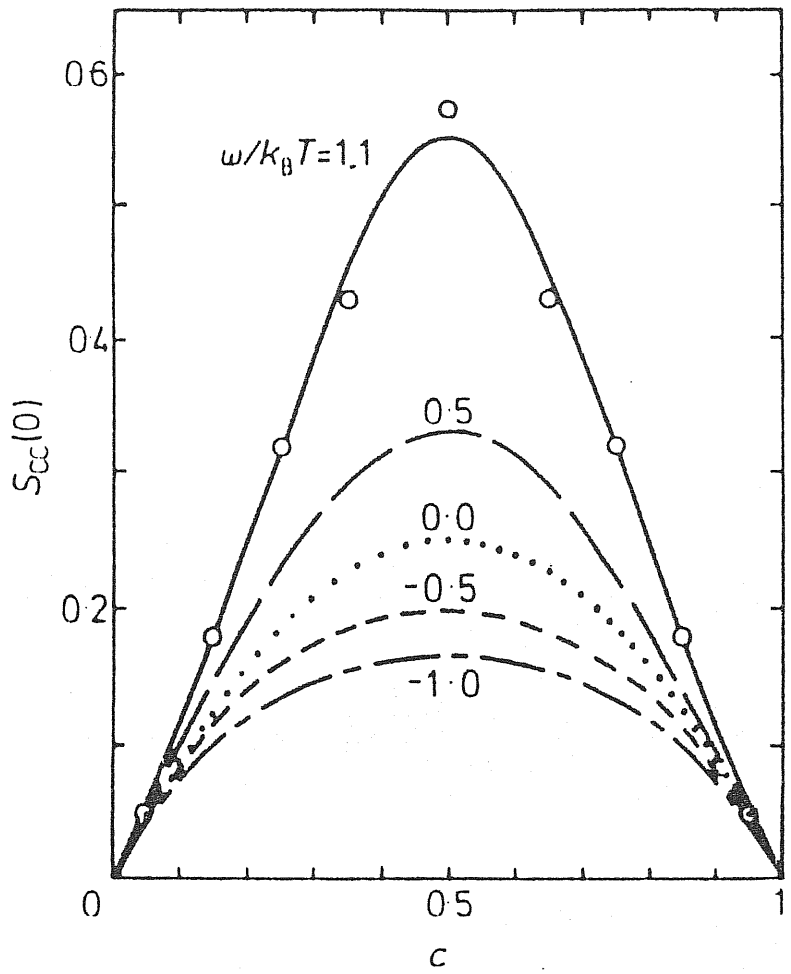

Figure 1.5: $S_{cc}(0)$ as a function of concentration for conformal solution for different values of w/k_BT. $w = 0.0$ is the ideal solution curve. $\circ$ data for $Na - K$ with $c = c_K$ (from [10]).

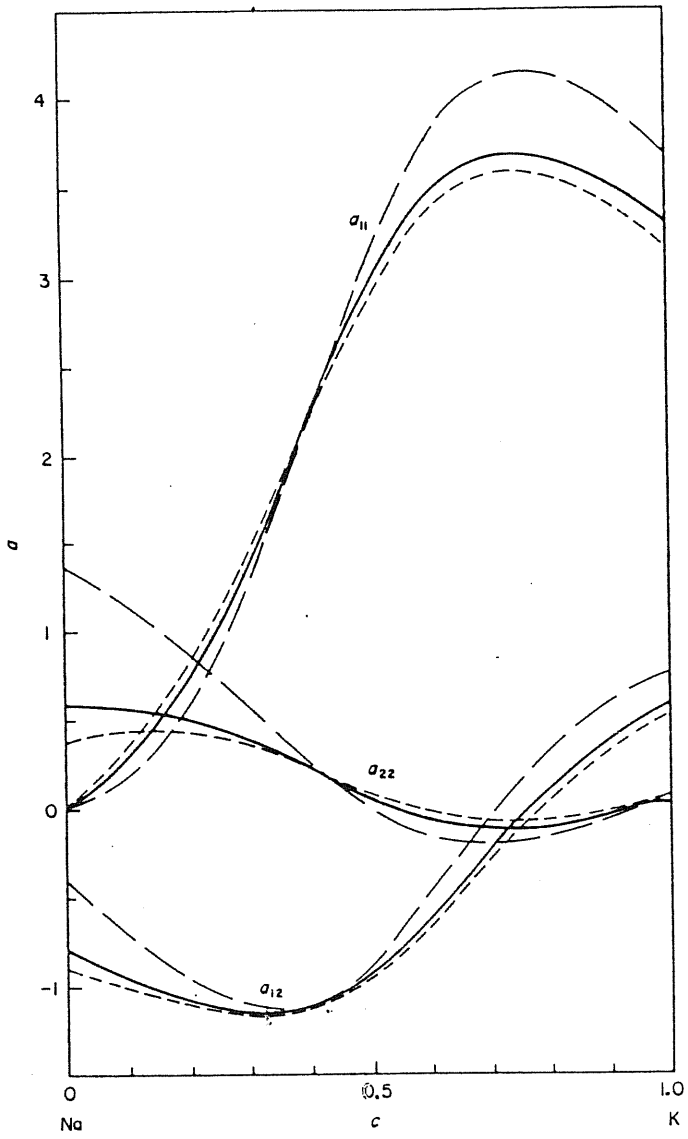

Figure 1.6: Long-wavelength limit of structure factors in liquid $Na - K$ alloys for various sets of parameters in conformal solution theory, compared with experiment (from [13]).

ratio of atomic volume is 3. This case is discussed separately below by a modified approach of Flory's work.

1.3.2 Phase diagrams and concentration fluctuations

As a further application of conformal solution theory for liquid metal alloys, we shall now outline the calculation of the phase diagram of $Na - K$[14].

The liquidus curve of an ideal solution has long been known to have the approximate form

$$ln(1 - c_2) = (L_{10}/R)(T_1^{-1} - T^{-1}) \tag{1.63}$$

c_2 being the concentration of the element 2 and L_{10} the latent heat at freezing temperature T_1 of pure liquid 1. To clarify the assumptions underlying (1.63) we shall summarize the thermodynamic equations along the liquidus[14]. When no mixed crystals are present, we have, in terms of chemical potentials

$$\mu_{10}^S(T) = \mu_1(T, c_2) \tag{1.64}$$

with the differential form

$$\begin{aligned} \frac{\Delta T}{\Delta c_2} &= -(\frac{\partial \mu_1}{\partial c_2})_{P,T} / [(\frac{\partial \mu_1}{\partial T})_{c_2,P} - (\frac{\partial \mu_{10}^s(T)}{\partial T})_P] \\ &= (\frac{\partial \mu_1}{\partial c_2})_{P,T} / (L/T) = -c_2 (\frac{\partial^2 G}{\partial c_2^2})_{P,T} / (L/T) \\ &= \frac{RT^2 c_2}{S_{cc} L} \end{aligned} \tag{1.65}$$

where subscript zero reflects to a pure substance and subscript s denote solid. Hence it can be seen that the liquidus curve depends crucially on

the concentration fluctuations $< (\Delta c)^2 >$. In the above equation for the slope of the liquidus curve, L is a generalized concentration-dependent latent heat defined by

$$\frac{L}{T} = \frac{L_{10}}{T} + \int_{T_1}^{T} \frac{\Delta c_{P10}}{T} dT - \frac{\partial}{\partial T}\{RTln[\gamma_1(1-c_2)]\} \qquad (1.66)$$

γ_1 being the activity, while $\Delta c_{P10} = c_{P10}^L - c_{P10}^S$.

If we now expand Δc_{P10} around T_1 and neglect higher terms than the first, and calculate the activity γ_1 from conformal solution theory ($RTln\gamma_1 \div wc^2$), then the equation of the liquidus curves is obtained in the form[3,4]

$$c(t) - 1 = (c_{ideal} - 1)exp(-Wc^2/t) \qquad (1.67)$$

where $t = T/T_1$ and $W = w/RT_1$ (for detailed derivations see [3]). If the value $w^{Na}/RT_1 = 1.1$ is used, the liquidus of the eutectic $Na - K$ mixture are found to be in good agreement with experiment, as shown

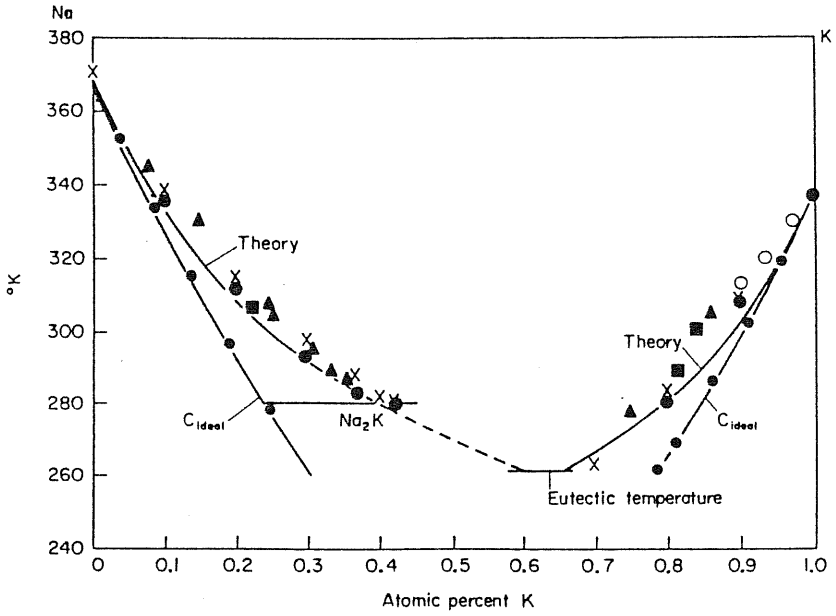

Figure 1.7: Liquidus curves in $Na - K$ alloys. Points refer to measurements and curves are from conformal solution theory (from [14]).

in Figure 1.7.

1.3.3 Size effects in mixtures.

Conformal solution theory is valid when (a) size differences are not too large, and (b) weak interaction theory is applicable. When the atomic volumes $v_1^{(0)}$ and $v_2^{(0)}$ differ considerably each other, Flory's formula for Gibbs free energy of mixing is a more valid approximation and is given by

$$G_m = Nk_BT[cln\phi + (1-c)ln(1-\phi)] + Nw\phi(1-\phi)[c + (1-c)/\beta] \quad (1.68)$$

where ϕ is the concentration by volume:

$$\phi = \frac{cv_1^{(0)}}{cv_1^{(0)} + (1-c)v_2^{(0)}}, \qquad \beta = \frac{v_1^{(0)}}{v_2^{(0)}}. \quad (1.69)$$

From Eqns. (1.50) and (1.68) we can get the expression for $S_{cc}(0)$,

$$S_{cc}(0) = \frac{c(1-c)}{1 + c(1-c)\delta^2\{1 - [2\beta\delta w/(\beta-1)^3 k_BT]\}} \quad (1.70)$$

where

$$\delta = \frac{v_1^{(0)} - v_2^{(0)}}{cv_1^{(0)} + (1-c)v_2^{(0)}} = \frac{\beta - 1}{(1-c) + c\beta}. \quad (1.71)$$

From Eqn. (1.70) we can see that when $w = 0$, $S_{cc}(0)$ is not equal to $S_{cc}^{id}(0) = c(1-c)$ and is asymmetric about $c = 0.5$. The comparison of theory and experiment for $S_{cc}(0)$ is shown in Figure 1.8 for the $Na - Cs$ alloy. The overall agreement between theory and experiment is quite reasonable.

It is noteworthy that the liquidus of $Na - Cs$ is also described quite reasonable by the model of Flory. The slope of the liquidus curve was earlier seen to be given by (Eqn. (1.65))

$$\frac{\Delta T}{\Delta c} = -\frac{RT^2 c}{S_{cc}(0)L} \quad (1.72)$$

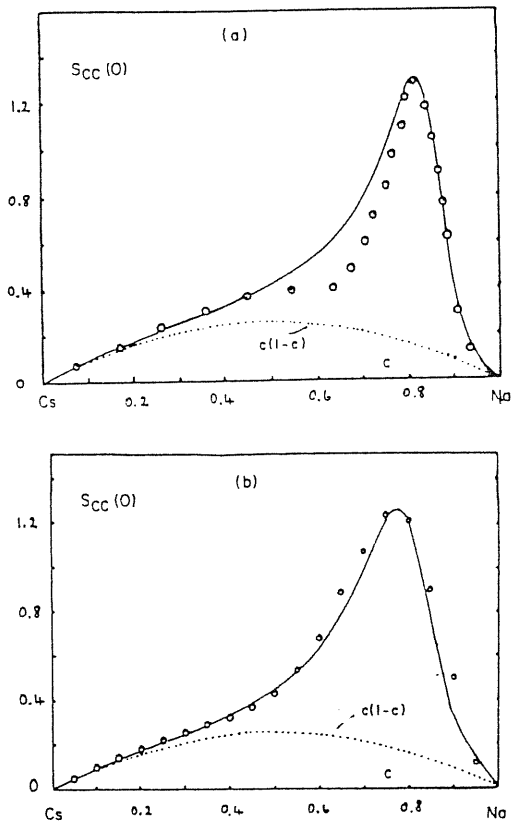

Figure 1.8: $S_{cc}(0)$ in $Na - Cs$ at $383K$. (a) Theory, by Bhatia and March [15] uses (1.70) and $w/k_BT = 1.14$. Observed points are due to Ichikawa *et.al.*[16]. (b) Calculated line and observed points by Neale and Cusack[17]. These writers use a version of (1.70) in which w depends on the actual volume of the alloy (from [18]).

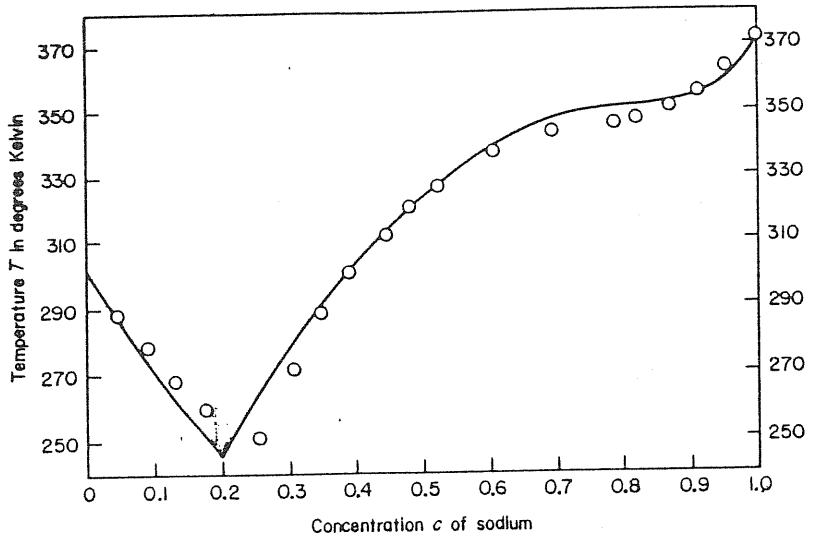

Figure 1.9: Liquidus curve of the $Na - Cs$ system against Na concentration: symbols are as in Figure 1.7(from [15]). The flat portion of the liquidus curve coincides with the concentration at which $S_{cc}(0)$ peaks in Figure 1.8.

so it is evident that a rather flat portion of the liquidus curve will be found where there is a large peak in $S_{cc}(0)$ and, of course, this is observed near $c = 0.75 - 80$ in Figure 1.9.

1.3.4 Relation of Miedema's work to solution theories[3,19]

The interchange energy w in conformal solution theory is calculable from the properties of a suitably chosen reference liquid [in fact from its ϕ and $g(r)$]. However, how to find such a reference liquid for a given alloy system remains somewhat of a problem.

From the work of Miedema and his colleagues (see, for example, [20]), the heats of solution of i in j [say $\Delta H_s(\mathrm{i\,in\,j})$] of binary ab metal

alloys can be expressed as

$$\Delta H_s(b\,in\,a) = \frac{V_b^{2/3}}{(n^{-1/3})_{av}}[-P(n_a^{1/3} - n_b^{1/3})^2 + Q(x_a - x_b)^2] \qquad (1.73)$$

where V_b is the atomic volume of pure metal b; n_i and x_i are the Wigner-Seitz cell boundary densities of electrons and the electronegativities in pure metals i, respectively; P and Q are almost constant through a wide class of alloys.

As mentioned in section 1.3.1, w is in fact an interchange energy such that if we start with two pure metals a and b and exchange an interior a atom with an interior b atom, the total change of the energy of the metals is $2w$. Then one can write

$$w = \frac{1}{2}[\Delta H_s(a\,in\,b) + \Delta H_s(b\,in\,a)]. \qquad (1.74)$$

Using Miedema's results this yields

$$w = \frac{V_a^{2/3} + V_b^{2/3}}{n_a^{-1/3} + n_b^{1/3}}[-P(n_a^{1/3} - n_b^{1/3})^2 + Q(x_a - x_b)^2]. \qquad (1.75)$$

This equation therefore provides a link between n_a and n_b, which can be obtained from the electron theory of pure metals, the electronegativity difference $(x_a - x_b)$, and the interchange free energy w of solution theory.

Table 1.1 summarizes the numerical consequency of the above equation for liquid mixtures of two alkalis. Actually, w as obtained by this method is about a factor of 2 too large for $Na - K$; this is an unacceptable error in calculating the concentration fluctuations $S_{cc}(0)$. Refinements of Miedema's work are therefore clearly needed, but the gross trends of the measured interchange energy are illustrated by this treatment.

Table 1.1: Interchange energy w for liquid alkali mixtures as extracted from experiment compared with that obtained using Miedema's work[19]

Alloy (a b)	w (units are KJ/g at. solute)	Experiment
NaK	5.5	2.9
CsK	0.0	0.45
(NaCs)	10.0	5.0
RbCs	0.0	-0.5
KRb	0.0	0.5
NaRb	7.5	5.4

1.4 Chemical short-range order in liquid alloys.

As stated before, in liquid solutions the magnitude of the concentration-concentration structure factor S_{cc} is dependent on the nature of the solution formed and can vary considerably from ideal ($S_{cc}^{id}(0)$) to non-ideal solutions. The concentration dependence of $S_{cc}(0)$ in a binary system also varies depending on the nature of the solution and the type of interaction between the species.

Extensive investigations[2,10,15–18,22–25,34–37] have shown that the magnitude of $S_{cc}(0)$ may be greater than, equal to or less than that of an ideal solution. In systems with phase separation tendency the magnitude of $S_{cc}(0)$ may become very large, while in strongly associated or compound-forming systems it may approach zero at compositions corresponding to the stoichiometry of such complex or compound. Many investigators also often use the so called "excess stability function" de-

fined by Darken[21]

$$ES = (\frac{\partial^2 G^E}{\partial c_i^2})_{T,P} = \frac{RT}{1-c_i}(\frac{\partial ln\gamma_i}{\partial c_i})_{T,P} \tag{1.76}$$

where $G^E(G_m - Nk_BT\{clnc + (1-c)ln(1-c)\})$ is the excess Gibbs free energy, R is the universal gas constant, γ_i and c_i are the activity coefficient and the number concentration respectively, referring to the ith component in the system. This excess stability function is directly related to $S_{cc}(0)$ by Eqn. (1.50) (see Figures 1.10 and 1.11).

In the following figures (1.10-1.20) some examples are given, showing how $S_{cc}(0)$ varies with concentration in liquid binary alloys and how the dependence of $S_{cc}(0)$ on concentration relates to the nature of chemical short-range order. Together with $S_{cc}(0)$ we also give the phase diagrams and the transport properties of some binary alloys. Through these experimental data of concentration fluctuations, phase diagrams and electrical resistivity we can see that the variations of $S_{cc}(0)$ with composition deviate from the ideal solution in some ranges of composition. The dips in the $S_{cc}(0) - c$ curve, or peaks in the $ES - c$ curve, correspond to the compositions at which complexes are found in compound-forming liquid alloys. The observed electrical resistivity also shows anomalous properties in these ranges of composition. These data shows that the concentration fluctuation $S_{cc}(0)$ is closely related to the other physical properties of the alloys, such as the phase diagrams, the stability of the complexes in the compound-forming liquid alloys, metallic glass forming composition range, the extrema of the electrical resistivity, *etc.*

As a summary of this chapter, we stress again that the structure factors of liquid metals and alloys are very important quantity to describe the systems. The long-wavelength limit of the concentration-

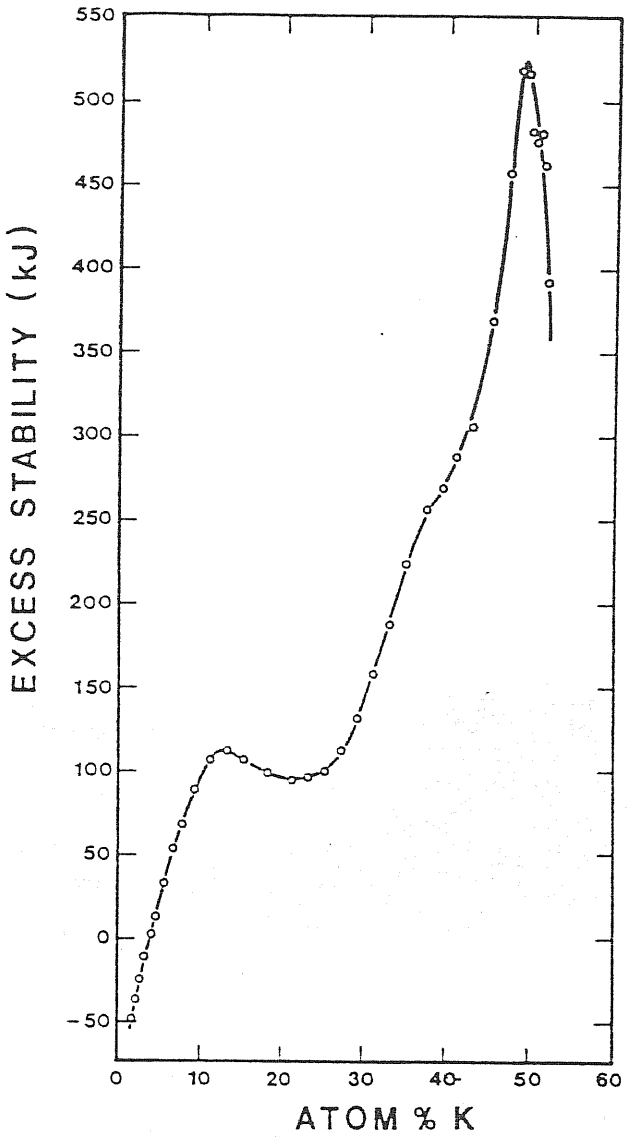

Figure 1.10: The excess stability function of liquid $K - Te$ alloys at $773K$ (from [22]).

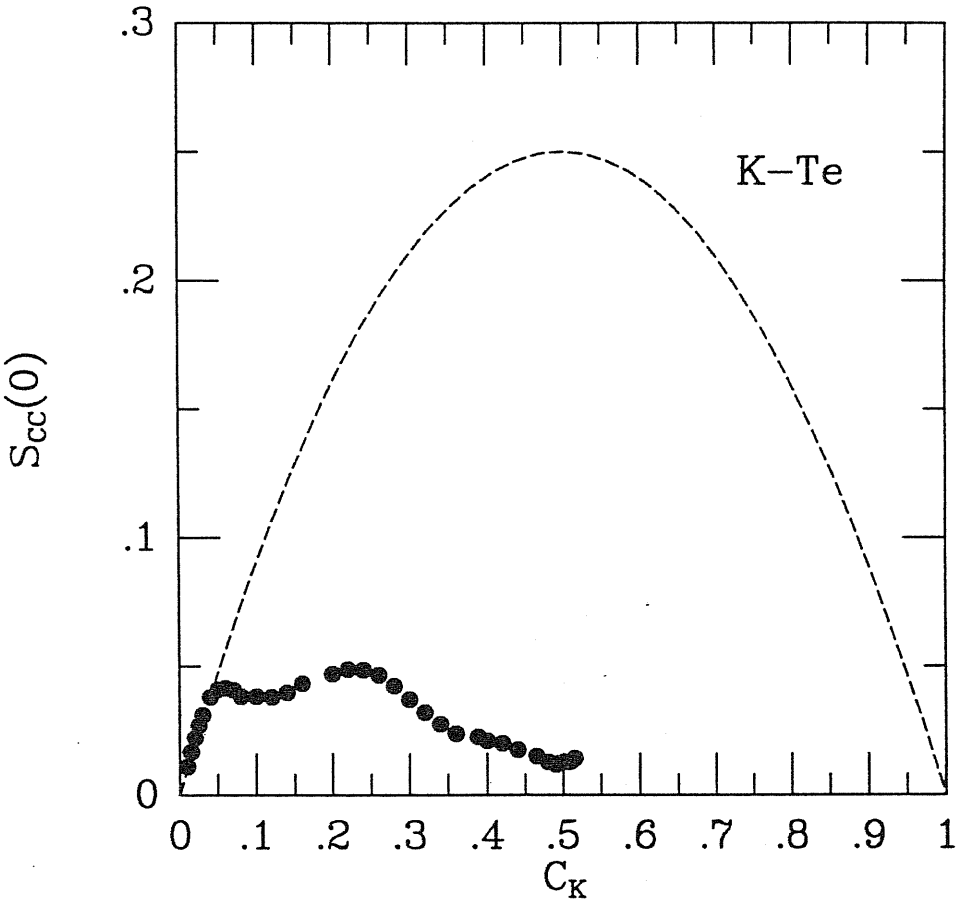

Figure 1.11: The $S_{cc}(0)$ vs composition for $K-Te$ liquid alloys calculated form th ES data in Fig.10. The dips correspond to the peaks in $ES-c$ curve, indicating maximum ordering in the liquid near those compositions related to the dips. The dashed line is for $S_{cc}^{id}(0) = c(1-c)$.

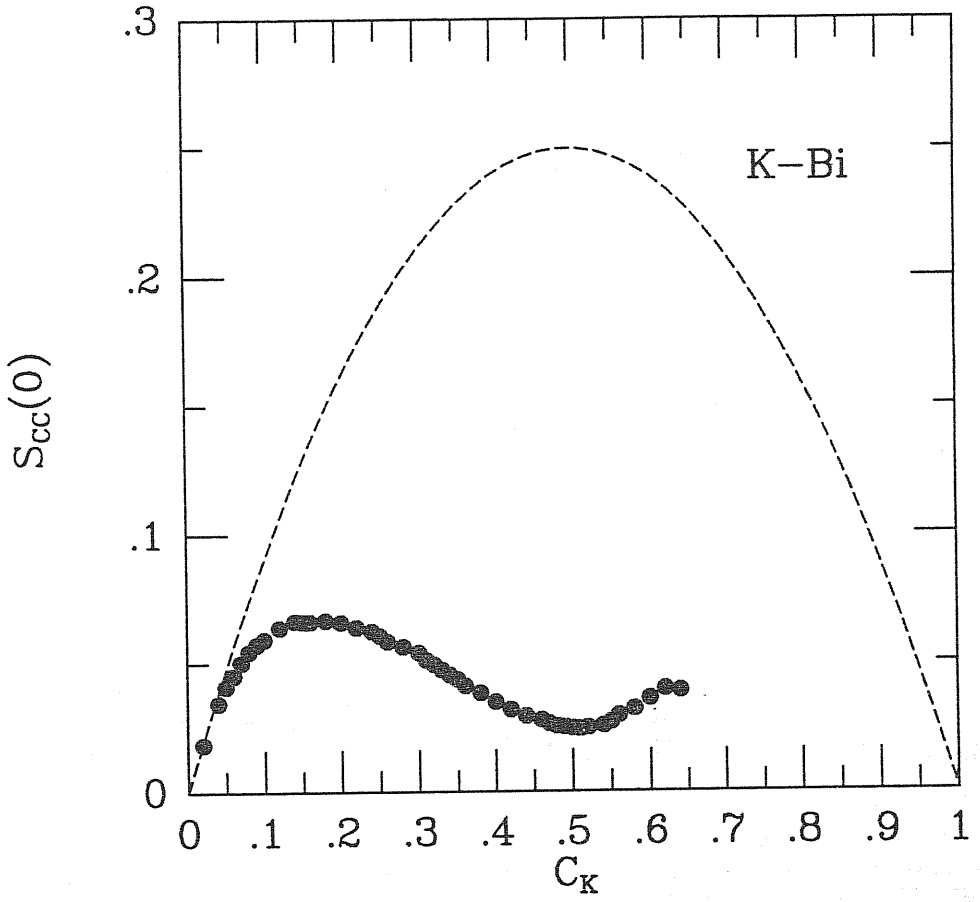

Figure 1.12: The $Scc(0)$ vs composition for liquid $K - Bi$ alloys at temperature $873K$. This is calculated from the measured EMF's (ES)[23]. Two dips (one at $50at.\%K$ and the other near $75at.\%K$) appear to be strong ordering-one near the equimolar composition KBi and the other near the composition corresponding to the ratio of the chemical valences of the elements, that is K_3Bi (see also Figure 1.13). The dashed line is for the $S^{id}_{cc}(0) = c(1 - c)$.

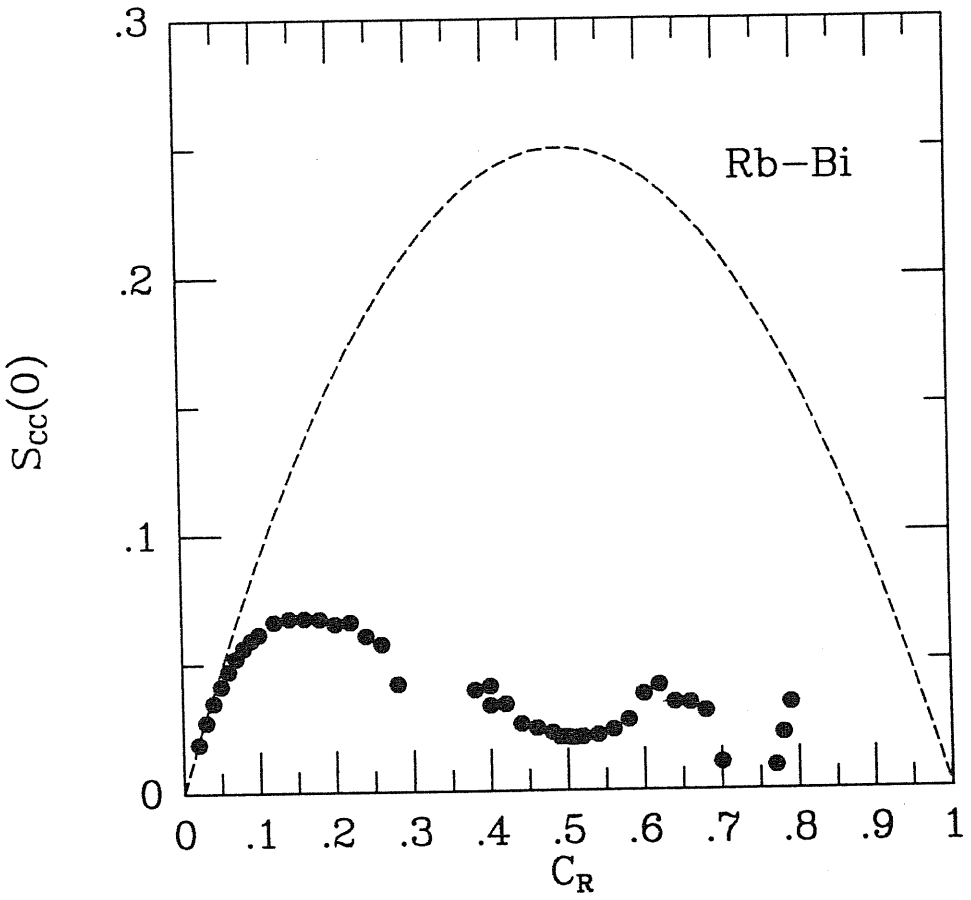

Figure 1.13: The $S_{cc}(0)$ vs composition for liquid $Rb - Bi$ alloys at $873K$. The data (dots) are calculated from the measured EMF's (ES)[25]. Similar to $K - Bi$ alloys (see Figure 1.12), there are two dips appear to be strong ordering, $Rb - Bi$ and Rb_3Bi.

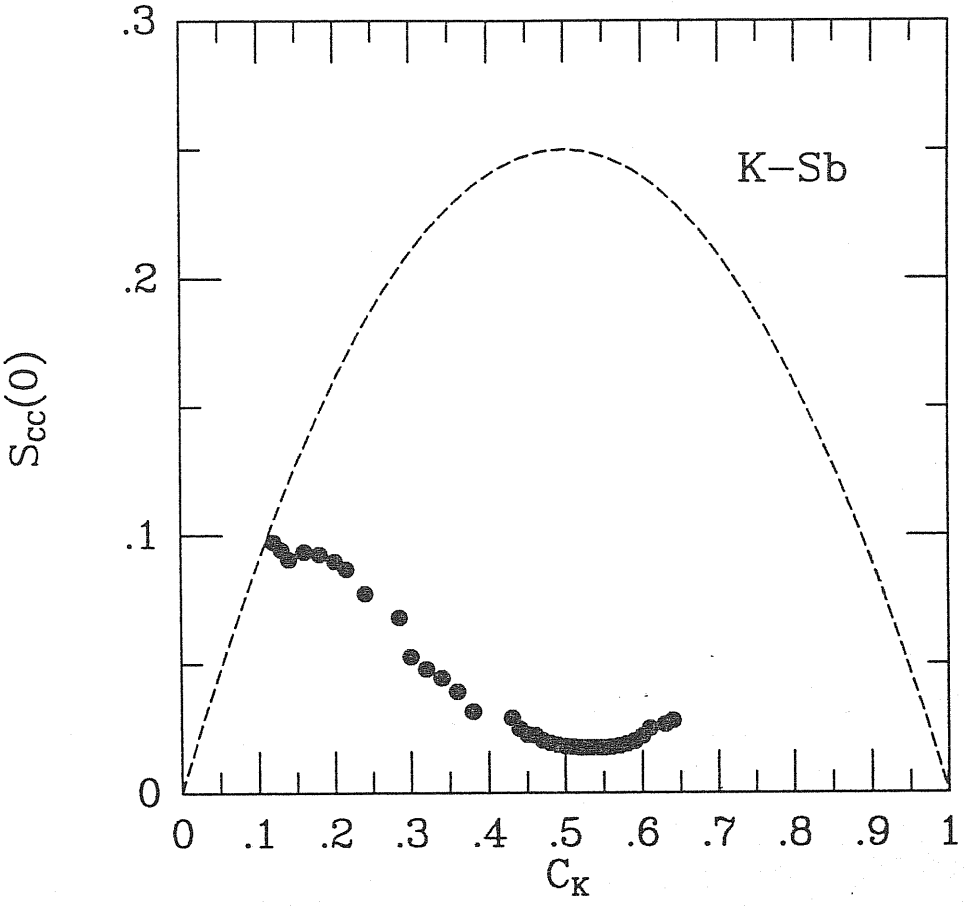

Figure 1.14: The S_{cc} vs composition for liquid $K - Sb$ alloys at $873K$. The data (dots) are calculated from the EMF's (ES)[24]; the dashed line is for the $S_{cc}^{id}(0) = c(1-c)$. A deep dip at the equiatomic composition, along with an excess heat capacity of about $8 - 14 Jmol^{-1}K^{-1}$, support the possible presence of "clusters" such as, $K_n Sb_m (n > 2)$[24].

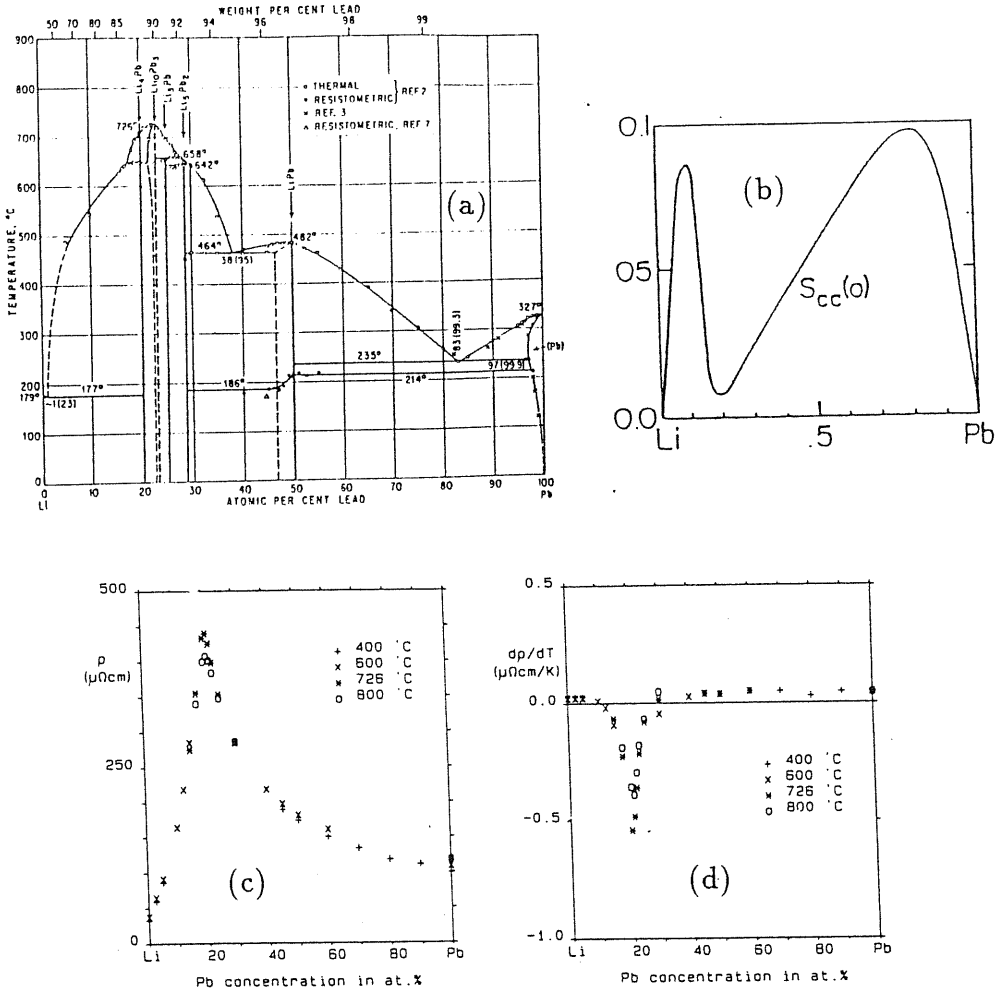

Figure 1.15: (a) The $Li - Pb$ Phase diagram[26]. The composition between $20(Li_4Pb)$ and $28.6(Li_5Pb_2)at.\%Pb$ is dominated by a number of high-melting compounds. (b) The $S_{cc}(0)$ vs composition for liquid $Li - Pb$ alloys[27]. The sharp dip corresponds to the composition at which the compound Li_4Pb is formed. (c) Resistivity ρ vs composition for liquid $Li - Pb$ alloys[28]. There is a sharp peak near the composition $20at.\%Pb(Li_4Pb)$. (d) $d\rho/dT$ vs composition for liquid $Li-Pb$ alloys[28]. The deep dip is near the composition $20at.\%Pb(Li_4Pb)$. Notice that the temperature coefficient of the resistivity is negative in this region.

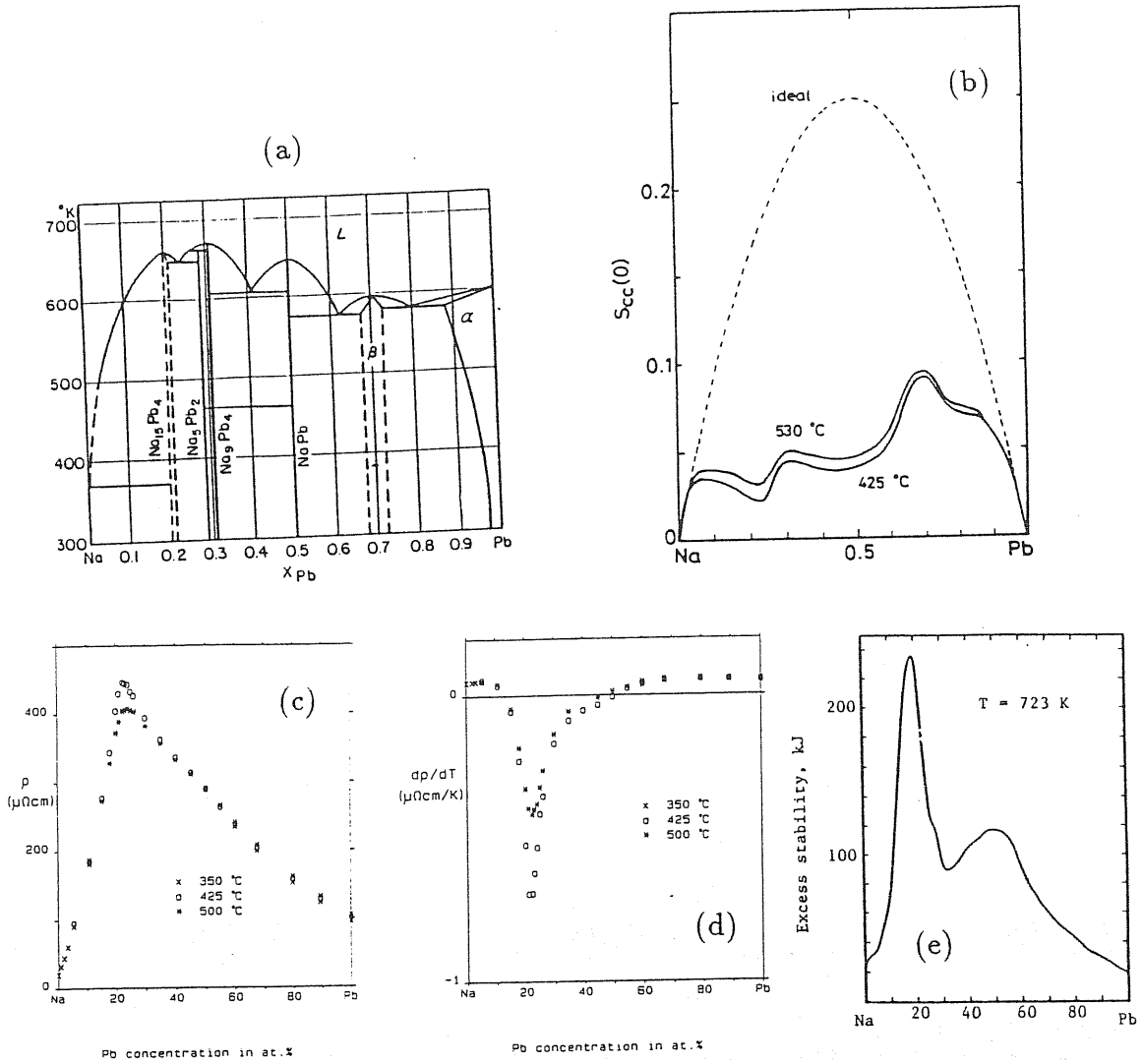

Figure 1.16: (a) The $Na-Pb$ phase diagram[29]. As in the $Li-Pb$ phase diagram , there are some high-melting compounds which are found in the composition range $\sim 20-30at.\%Pb$. But there also exists the equiatomic compound $NaPb$. (b) The $S_{cc}(0)$ vs composition for liquid $Na-Pb$ alloys[30]. The two dips corresponds to the two position, at which the compounds Na_4Pb and $NaPb$ are formed. (c) Resistivity ρ vs composition for liquid $Na-Pb$ alloys[31]; a peak appears near the composition $20at.\%Pb$. (d) $d\rho/dT$ vs composition for liquid $Na-Pb$ alloys[31]; a dip appears near the composition $20at.\%Pb$. (e) ES vs composition for liquid $Na-Pb$ alloys[32]. Two peaks appears - one is near the composition $20at.\%Pb(Na_4Pb)$, the other $50at.\%Pb(NaPb)$.

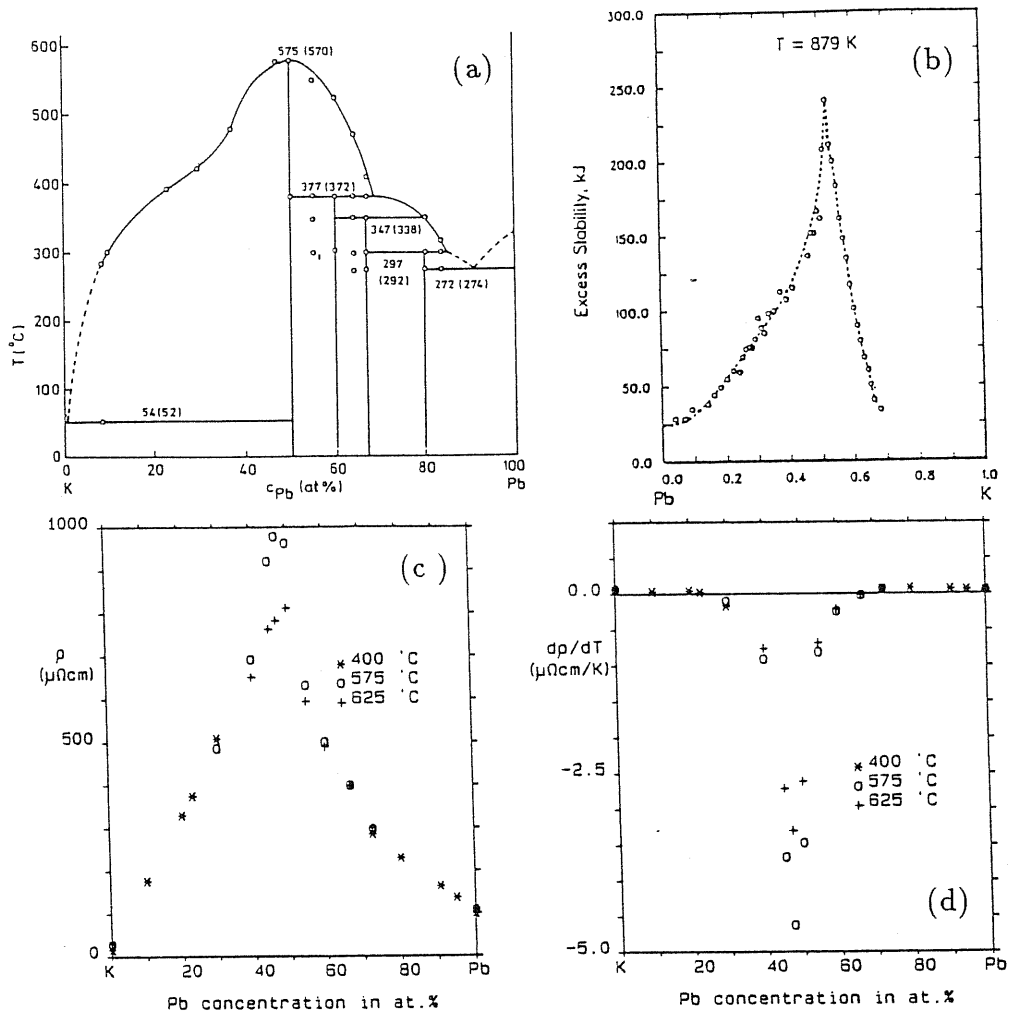

Figure 1.17: (a) The $K-Pb$ phase diagram[28,33]. There is no K_4Pb compound (see the $Li-Pb$ and $Na-Pb$ phase diagrams). Instead, the phase diagram is dominated by the equiatomic compound, KPb. (b) ES vs composition for liquid $K-Pb$ alloys[34]. Three is a sharp peak, which corresponds to a deep dip in $S_{cc}(0)$, at the equiatomic composition. (c) Resistivity ρ vs composition for liquid $K-Pb$ alloys[28]. The sharp peak appears near the equiatomic composition. (d) $d\rho/dT$ vs composition for liquid $K-Pb$ alloys[28]. The deep dip appears near the equiatomic composition.

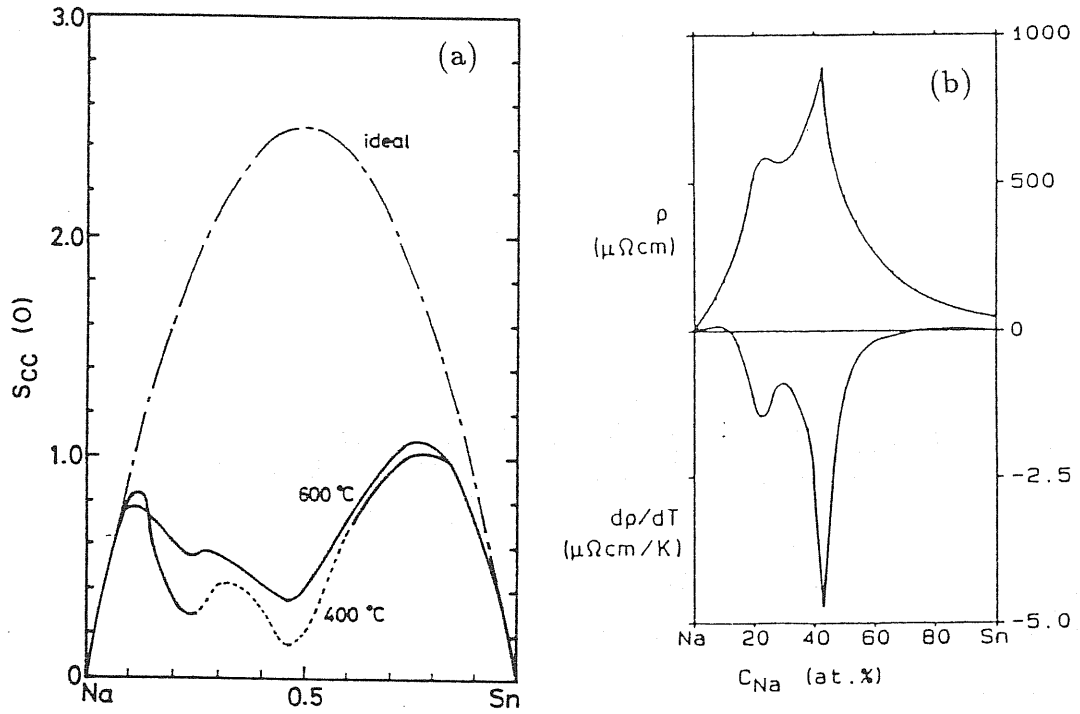

Figure 1.18: (a) $S_{cc}(0)$ vs composition for $Na - Sn$ alloys[35]. (b) Resistivity ρ (top) and its temperature derivative $d\rho/dT$ vs composition[31]. The two dips in $S_{cc}(0)$ corresponds to the two peaks in ρ and two dips in $d\rho/dT$.

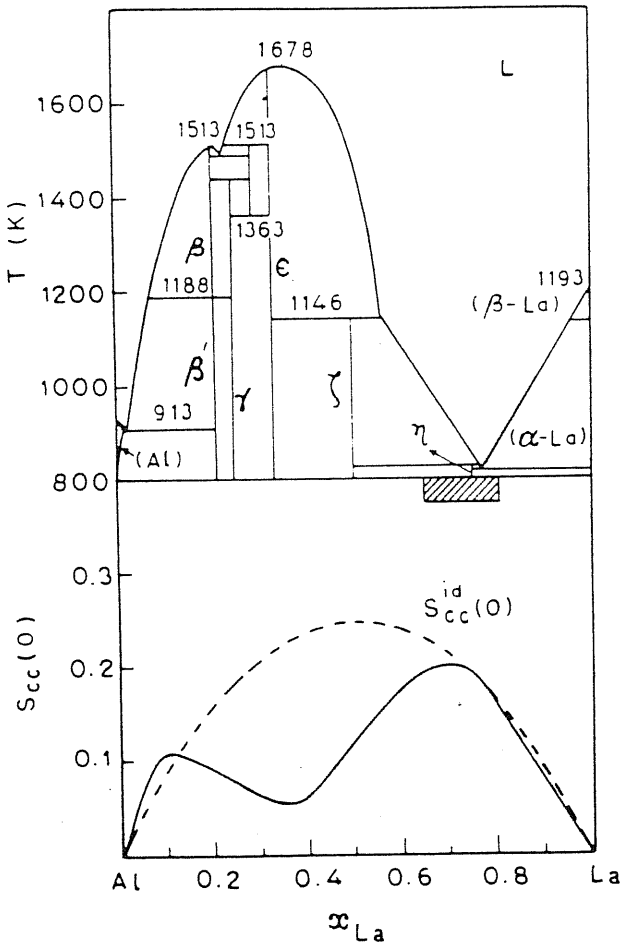

Figure 1.19: The phase diagram and the composition dependence of $S_{cc}(0)$ at $1693K$ in the $Al-La$ system[36]. The peak in $S_{cc}(0)$ (approach the $S^{id}_{cc}(0)$ value) corresponds to the glass formation range. The very low value of $S_{cc}(0)$ at $33at.\%La$ is a measure of the strong chemical interaction between Al and La leading to the formation of Al_2La complexes.

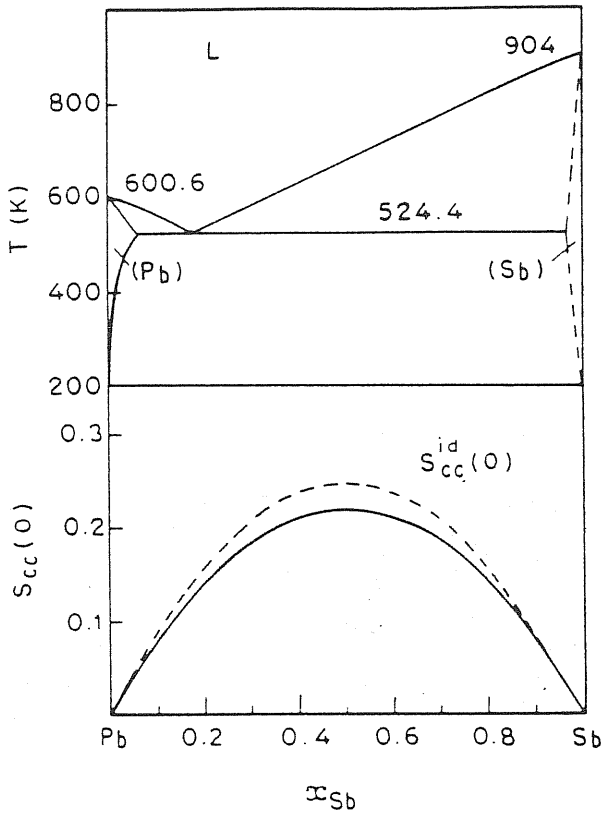

Figure 1.20: The phase diagram and the composition dependence of $S_{cc}(0)$ at $905K$ in the system $Pb - Sb$[36]. The lack of a sufficient strong interaction between Pb and Sn leads to a nearly ideal mixing.

concentration structure factors, $S_{cc}(0)$, plays an important role in describing the concentration fluctuations in the liquid alloys.

Chapter 2

Pseudopotential Theory of Metals and Alloys

In this chapter we shall give some basic descriptions of pseudopotential theory, *e.g.*, the approximations introduced in this theory, the pseudopotential formulations, the selection of a pseudopotential, the evaluation of the total energy, *etc.* We shall also discuss model pseudopotential calculations for a few specified model pseudopotentials and some applications of these model pseudopotentials.

2.1 The Pseudopotential Method

As we know, the calculation of the states of a valence electron in a metal is a very complicated problem. One has to consider not only its interaction with nuclei and core electrons, but also the interactions and the exchange with the other valence electrons and the correlations that arise from these effects. Since a complete solution of the many-body Schődinger equation for the interacting electrons and nuclei is impossi-

ble, one has to resort to various approximations. An efficient method to tackle the problem is provided by the theory of pseudopotentials.

2.1.1 The approximations

There are three fundamental approximations which enter the theory[38]: (1) the self-consistent-field approximation, (2) the separation of the electron states into core states and conduction-band (valence) states and the treatment of the core states as localized and essentially atomic-like, (3) the use of perturbation theory in computing the conduction-band states. The first approximation means that we replace the interaction between electrons by a potential which is to represent some average interaction. This potential depends upon the states which are occupied by electrons, and these states, in turn, depend on the potential, thus we must compute the potential self-consistently. The second approximation implies that all the states beyond the last filled rare-gas shells are delocalized and determined by the interaction with ionic cores assumed to be small and essentially rigid. The number of conduction electrons per atom is thus equal to the column number in the periodic table, or the valence, of the element in question; all low-lying levels are core levels. The application of the small-core approximation is very good for alkali and polyvalent metals and is not expected to introduce appreciable errors[38]. The third approximation is the basis of the theory and distinguishes it from traditional band calculations. It is this feature which enables us to explore the vast array of metallic properties. (The detailed explanation of the validity of the perturbation expansion is given in [38]).

Pseudopotential theory began as an extension of the orthogonalized-plane-wave (OPW) method. We will give in the next section the deriva-

tion of pseudopotentials.

2.1.2 The pseudopotential formulation

Let $V(\mathbf{r})$ be the self-consistent potential seen by each electron. Then each energy eigenfunction will satisfy the Schrődinger equation (atomic units will be used in the following,

$$H\psi_i = (T + V(\mathbf{r}))\psi_i = \mathrm{E_i}\psi_i \tag{2.1}$$

where T is the kinetic energy, $-\nabla^2/2$, and E_i is the energy of the ith state. We use the indices α and $\mathbf{k}$ for core states and conduction-band states, respectively. According to the second assumption, the core states are the same as in the isolated ion, but have a different energy E_α

$$(T + V(\mathbf{r}))\psi_\alpha = \mathrm{E}_\alpha\psi_\alpha. \tag{2.2}$$

The subscript α denotes the position of the ion as well as the energy and angular-momentum quantum numbers of the state in question.

We write the normalized plane waves and normalized core wave functions as

$$\mid \mathbf{k} > \equiv \Omega^{-1/2}e^{i\mathbf{k}\cdot\mathbf{r}} \tag{2.3}$$

$$\mid \alpha > \equiv \psi_\alpha(\mathbf{r}) \tag{2.4}$$

where Ω is the volume of the metal. Thus the OPW's can be written as [38,39]

$$OPW_\mathbf{k} = \mid \mathbf{k} > - \sum_\alpha \mid \alpha >< \alpha \mid \mathbf{k} >, \tag{2.5}$$

where

$$< \alpha \mid \mathbf{k} > \equiv \Omega^{-1/2} \int \psi_\alpha^*(\mathbf{r})\mathrm{e}^{\mathrm{i}\mathbf{k}\cdot\mathbf{r}}\mathrm{d}\mathbf{r}.. \tag{2.6}$$

If we introduce the projection operator,

$$P = \sum_{\alpha} \mid \alpha >< \alpha \mid, \tag{2.7}$$

which projects any function onto the core states, then we can write

$$OPW_{\mathbf{k}} = (1 - P) \mid \mathbf{k} > . \tag{2.8}$$

Now we may expand the conduction-band state in terms of a general linear combination of OPW's,

$$\psi_{\mathbf{k}} = \sum_{\mathbf{q}} a_{\mathbf{q}}(\mathbf{k})(1 - \mathrm{P}) \mid \mathbf{k} + \mathbf{q} >, \tag{2.9}$$

and substitute it into the Schődinger equation (2.1). Then we obtain:

$$\sum_{\mathbf{q}} a_{\mathbf{q}}(\mathbf{k})\mathrm{H}(1 - \mathrm{P}) \mid \mathbf{k} + \mathbf{q} >= \mathrm{E}_{\mathbf{k}} \sum_{\mathbf{q}} \mathrm{a}_{\mathbf{q}}(\mathbf{k})(1 - \mathrm{P}) \mid \mathbf{k} + \mathbf{q} > . \tag{2.10}$$

If we rewrite this equation by taking all the terms involving the projection operator P to the left side, we can obtain the form

$$T\varphi_{\mathbf{k}} + W\varphi_{\mathbf{k}} = E_{\mathbf{k}}\varphi_{\mathbf{k}} \tag{2.11}$$

where W is called the "pseudopotential" and is defined by[40]

$$W = V(\mathbf{r}) + \sum_{\alpha}(\mathrm{E}_{\mathbf{k}} - \mathrm{E}_{\alpha}) \mid \alpha >< \alpha \mid = \mathrm{V}(\mathbf{r}) + (\mathrm{E}_{\mathbf{k}} - \mathrm{H})\mathrm{P}, \tag{2.12}$$

and $\varphi_{\mathbf{k}}$ is called the "pseudo wave function" and is defined by

$$\varphi_{\mathbf{k}} = \sum_{\mathbf{q}} a_{\mathbf{q}}(\mathbf{k}) \mid \mathbf{k} + \mathbf{q} > . \tag{2.13}$$

The relation between the true wave function and the pseudo wave function is, according to (2.9),

$$\psi_{\mathbf{k}} = (1 - P)\varphi_{\mathbf{k}}. \tag{2.14}$$

From (2.12) we see that (i) W is energy-dependent and (ii) $V(\mathbf{r})$ has to be known. In actual applications, $V(\mathbf{r})$ may sometimes be taken as the Hartree-Fock (HF) potential. Even in this approximation, the solution of Eqn. (2.11) is by no means easy.

In other approaches, instead, it is assumed that the poseudopotential W can be constructed from model potentials for the electron-core interaction, having a simple analytic form and involving parameters to be determined by fitting some experimental data[41]. In this way, the need of knowing the core states is bypassed and a precise knowledge of $V(\mathbf{r})$ is not necessary. This class of pseudopotentials is usually called "model pseudopotentials" to avoid confusion. Because of its simplicity, such approach is very useful in studying the electronic states in solids or liquids.

2.2 Model Pseudopotentials

Before we come to specific model pseudopotentials, let us see a particular pseudopotential, that is the Austin form[42]

$$W\varphi(\mathbf{r}) = \mathrm{V}(\mathbf{r})\varphi(\mathbf{r}) - \sum_{\alpha}[\int \psi_{\alpha}^{\star}(\mathbf{r}')\mathrm{V}(\mathbf{r}')\mathrm{d}^3\mathrm{r}']\psi_{\alpha}(\mathbf{r}). \qquad (2.15)$$

In (2.15) the second term on the right is the expansion of $V\varphi$ in terms of the set of core functions ψ_{α}. If these were a complete set, the right side of (2.15) would be identically zero. Of course, the ψ_{α} are only finite in number and cannot form a complete set, but inside the core they provide a fairly satisfactory expansion set so that the right side is small for r smaller than the core radius (R_c, say).

Let us present now some model potentials for electron-core interaction that have been presented in the literature. We shall return later to

discuss how the full W is constructed from these. In essence, once the electron-core interaction has been chosen, the solid or liquid is viewed as a collection of ions, while the effect of all the conduction electrons is introduced through the notion of dielectric screening.

2.2.1 Empty-core model pseudopotential

Bearing in mind the comment made above on the Austin model, Ashcroft proposed the so-called empty-core model pseudopotential[42]:

$$v_{ps}^{ion}(r) = \begin{cases} 0 & \text{for } r < R_e \\ -Z/r & \text{for } r > R_e \end{cases} \tag{2.16}$$

Here the empty-core parameter R_e is approximately the radius R_c of the physical atomic core and may be varied somewhat around that value. Figure 2.1 gives the schematic picture of the empty-core model potential generated by a bare ion.

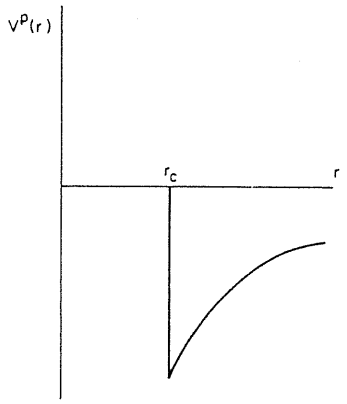

Figure 2.1: The empty-core model pseudopotential of a bare ion (schematic picture).

2.2.2 Heine-Abarankov (HA) model pseudopotential

The model pseudopotential introduced by Abarenkov and Heine[43] is that the model radius R_m is chosen at some convenient value greater than the core radius R_c, and outside R_m the pseudopotential is the bare Coulomb potential of the bare ion (ionic charge Z)

$$v_{ps}^{HA} = -Z/r, \qquad for \qquad r > R_m. \tag{2.17}$$

Inside R_m the potential is instead taken as a constant,

$$v_{ps}^{HA} = -\sum_l A_l(E)P_l, \qquad for \qquad r < R_m. \tag{2.18}$$

(see Figure 2.2). The quantities $A_l(E)$ are energy and angular momentum dependent and are adjusted to give the observed energy levels E_{3s}, E_{sp}, E_{4s}, *etc.* for an extra electron in the field of the isolated ion, the

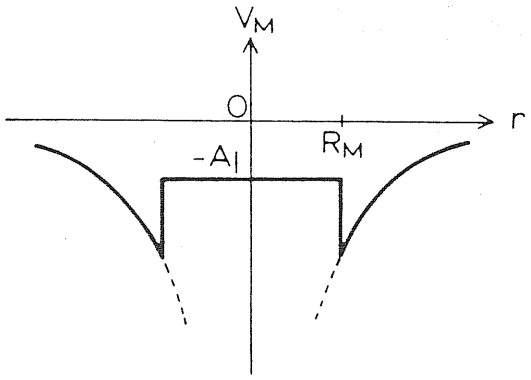

Figure 2.2: HA model potential of a bare ion, shown in real space (schematic figure).

latter being taken from spectroscopic measurements on free ions. Here P_l is the projection operator that picks out the component of the same function with angular momentum l. Shaw and Harrison[44] reformulated the HA pseudopotential and considered a model potential which is sufficiently general to include both the HA model and a limited class of other pseudopotentials. They take the model potential operator for an isolated atom to have the form

$$v_m = v - \sum_l A_l(E) \mid l >< l \mid \tag{2.19}$$

where the $\mid l >$ are a set of angular-momentum eigenstates and E is the energy of the state under consideration.

The r representation of (2.19) is

$$< \mathbf{r} \mid \mathrm{v_m} \mid \mathbf{r}' >= \mathrm{v}(\mathbf{r})\delta(\mathbf{r} - \mathbf{r}') - \sum_l A_l(E) \mid l >< l \mid \mathbf{r}' > \tag{2.20}$$

The potential $v(\mathbf{r})$ has been taken to be local (diagonal) in the r representation. It is clear that the second term in (2.20) is not diagonal in the r representation and is consequently referred to as a nonlocal contribution. If we set

$$v(r) = -(Z/r)\Theta(r - R_m)$$
$$A_l(r, E) = A_l(E)\Theta(R_m - r)$$

where

$$\Theta(r) = \begin{cases} 0 & r < 0 \\ 1 & r > 0 \end{cases}$$

one recovers the HA model potential.

2.2.3 Shaw's model potential[45]

Some features of the HA model potential should now be discussed. First, a single value of R_m is chosen for all l. This is an unnecessary restriction but was made largely for simplicity. The choice of R_m for each element actually seems to have been somewhat arbitrary. Secondly, all the A_l for $l > 2$ were set arbitrarily equal to A_2. The reason for doing this is that there are essentially no spectroscopic term values available for $l > 2$, and therefore no direct way of calculating the A_l for these l's. Thirdly, the discontinuity in the potential at R_m (see Figure 2.2) causes the model potential form factors to have oscillatory tails of short-wavelength.

To overcome these problems, Shaw introduce an optimum form for a modified HA model potential. His first modification of the HA model potential is to include the core potential only those A_l's for which there

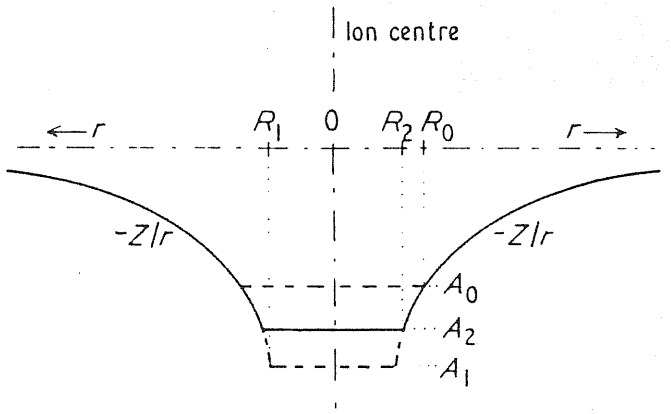

Figure 2.3: Shaw's model pseudopotential of a bare ion. The relative magnitudes of R_0, R_1 and R_2 and of A_0, A_1 and A_2 are arbitrary illustrations.

are core states. For higher l the true potential is instead used. The further modification that he made is that the model radius $R_l(E)$ is allowed to depend on l and on energy. Introducing a whole set of new parameters, the $R_l(E)$, makes the model potential flexible enough to be optimized. In fact, the optimization of the potential leads to a relation between $A_l(E)$ and $R_l(E)$, so that the number of parameters is not increased.

The new form of the bare model potential w_0 for a single ion can be written as

$$w_0 = v_b(r) - \sum_{l=0}^{l_0} \Theta(R_l - r)[A_l + v_b(r)]P_l \qquad (2.21)$$

where $v_b(r)$ is the bare ion potential and l_0 is the largest angular momentum quantum number for which there are core states. The model parameters A_l are still computed by assuming that $v_b(r) = -Z/r$ for $r > R_l$. The optimization condition leads to[45] $A_l = Z/R_l$ (see Figure 2.3).

Table 2.1 gives the general optimized model potential parameters, which are calculated from spectroscopic term values. The $A_l(E)$ for any element can be obtained directly by interpolating this table. Table 2.2 gives the optimized model potential parameters evaluated at the Fermi energy.

Hallers *et.al.*[46] pointed out that for cesium this optimized model potential gives rise to an unphysically large core radius for the $l = 2$ level, so that the small core approximation is violated. In order to avoid this problem, they dropped the dependence of R_l on l and E by taking $R_l(E) = R_m$. This means that they ignore the optimization of the model potential and return to a bare-ion potential which is a combination of the HA potential and the Shaw model potential.

Table 2.1: General optimized model potential parameters (in atomic units). The $A_l(E)$ for any element can be obtained directly by interpolating this table (from [45]).

	$l=0$				$l=1$				$l=2$	
E/Z^2	ZR_l		A_l/Z^2		ZR_l		A_l/Z^2		ZR_l	A_l/Z^2
0.2958	1.450		0.6894							
0.2551	1.991		0.5020							
0.2222	2.532		0.3948							
0.1953	3.115		0.3210							
0.1730	3.735		0.2677							
0.1543	4.387		0.2279							
0.1385	5.083		0.1967							
0.1250	5.842		0.1712							
0.1133	6.628		0.1509		2.650		0.3773			
0.1033	7.421		0.1347		3.756		0.2662			
0.0945	8.298		0.1205		4.767		0.2097			
0.0868	9.196	2.066	0.1087	0.4840	5.809		0.1721			
0.0799	10.135	2.653	0.0987	0.3768	6.808		0.1469			
0.0739	11.151	3.296	0.0897	0.3033	7.805		0.1281			
0.0685	12.155	3.992	0.0823	0.2505	8.877		0.1126			
0.0637	13.236	4.766	0.0755	0.2098	9.954		0.1005			
0.0594	14.351	5.612	0.0697	0.1782	11.135		0.0898			
0.0555		6.517		0.1534	12.261		0.0816			
0.0520		7.496		0.1334	13.444	2.498	0.0744	0.4003	6.285	0.1591
0.0488		8.546		0.1170	14.706	3.587	0.0680	0.2788	8.192	0.1221
0.0459		9.644		0.1037		4.594		0.2176	9.873	0.1013
0.0432	2.087	10.864	0.4790	0.0920		5.657		0.1768	11.534	0.0867
0.0408	2.693	12.120	0.3712	0.0825		6.681		0.1497	13.070	0.0765
0.0385	3.365	13.437	0.2971	0.0744		7.728		0.1294	14.604	0.0685
0.0365	4.114	14.821	0.2431	0.0675		8.864		0.1128		
0.0346	4.956		0.2017			10.034		0.0997		
0.0328	5.898		0.1695			11.296		0.0885		
0.0312	6.936		0.1442			12.578		0.0795		
0.0297	8.074		0.1239		2.475	13.940	0.4039	0.0717	5.852	0.1709
0.0283	9.313		0.1074		3.533		0.2830		7.621	0.1312
0.0270					4.544		0.2200		9.259	0.1080

Table 2.2: Optimized model potential parameters (in atomic units) evaluated at Fermi energy (from [45]).

Element	$R_0(E_F)$	$A_0(E_F)$	$\partial A_0/\partial E$	$R_1(E_F)$	$A_1(E_F)$	$\partial A_1/\partial E$	$R_2(E_F)$	$A_2(E_F)$	$\partial A_2/\partial E$
Li	3.02	0.331	−0.186						
Be	2.00	1.000	−0.202						
Na	3.26	0.307	−0.231	2.71	0.369	−0.196			
Mg	2.58	0.776	−0.286	2.19	0.912	−0.058			
Al	2.15	1.395	−0.326	1.82	1.647	−0.044			
K	4.20	0.238	−0.294	4.00	0.250	−0.120			
Rb	4.46	0.224	−0.336	4.48	0.223	−0.159	[a]	[a]	[a]
Zn	2.03	0.984	−0.355	1.45	1.380	−0.484	2.33	0.860[b]	0
Cd	2.24	0.892	−0.424	1.75	1.144	−0.513	2.16	0.924[b]	−0.571
In	2.24	1.341	−0.454	2.01	1.494	−0.224	2.75	1.089	+0.094

[a] No values are obtainable using the range of parameters in Abarenkov's tables.
[b] Obtained by extrapolation beyond the range of Abarenkov's tables.

2.2.4 Energy independent model pseudopotential (EIMP)

In general, the pseudopotential operator, like the atomic potential operator v_a, is strongly state dependent, that is it depends on the entire distribution of the electron cloud it operates on, and not only on its energy. Therefore, characterizing the action of the pseudopotential operator just by the energy of the state on which it operates is probably an oversimplified picture[47,48].

On the basis of appropriate physical arguments (for details see [48]), the form of the model potential proposed by Wang *et.al.* is

$$v_a^{ps} = \sum_l V_l \mid l >< l \mid \tag{2.22}$$

where

$$V_l = \overline{V}_l(r) + \Delta_l \tag{2.23}$$

and

$$\Delta_l = [V_{1l}(r) - \overline{V}_l(r)] \mid R_{1l} >< R_{1l} \mid \tag{2.24}$$

$1l$ being a label for the first valence state of angular momentum l and $\mid R_{1l} >$ is the radial part of $\mid 1l >$.

To make use of equation (2.22) in an actual calculation, the model pseudopotential has been introduced for V_{1l},

$$V_{1l} = \begin{cases} -B_{1l} + Z_l/r & \text{for } r < R_l \\ -Z/r & \text{for } r > R_l \end{cases} \tag{2.25}$$

where B_{1l}, Z_l and R_l are parameters related by the continuity condition for the potential, $B_{1l} = (Z + Z_l)/R_l$. The corresponding form for $\overline{V}_l$ is then given by equation (2.25) with B_{1l} replaced by $\overline{B}_l$. The determination of the model parameters has been made by using the known

Table 2.3: Parameters for the model potentials V_{1l} and $\overline{V}_l$ for 12 simple metals (from [48]).

	R_0	B_{10}	$\bar{B}_0$	R_1	B_{11}	$\bar{B}_1$	R_2	B_{12}	$\bar{B}_2$
Li	2·7	0·452037	0·432494	2·4	−0·118654	−0·118568	3·4	−0·025036	−0·026054
Na	2·9	0·421999	0·395763	2·7	0·430142	0·423917	3·8	−0·094218	−0·096650
K	3·7	0·331569	0·299859	3·9	0·295924	0·285978	3·9	−0·463302	−0·463096
Rb	3·9	0·315109	0·278805	4·4	0·266928	0·256136	4·6	−0·316954	−0·316674
Cs	4·3	0·285014	0·245756	4·9	0·254362	0·242365	5·0	−0·310661	−0·310291
Be	1·9	1·097448	1·006343	1·5	−0·256042	−0·254348	3·5	−0·004084	−0·004223
Mg	2·4	0·913763	0·816893	2·2	0·906447	0·893666	2·9	−0·140825	−0·140902
Ca	3·3	0·651669	0·541316	3·3	0·637317	0·612581	2·5	−1·446672	−1·387579
Zn	1·9	1·132345	0·937060	1·5	1·462519	1·304832	2·0	1·121472	1·069575
Cd	2·1	1·000238	0·735190	1·9	1·001948	0·847148	2·7	0·804686	0·773042
Hg	1·8	1·180163	0·700763	1·7	1·119794	0·426535	3·0	0·669270	0·638592
Al	2·1	1·459164	1·213692	1·8	1·724312	1·705608	1·9	−0·518438	−0·519523

spectroscopic term values. We will not give the detailed procedures here. Table 2.3 gives the parameters for the model potentials V_{1l} and $\overline{V}_l$ for 12 simple metals.

2.3 The total energy

In the previous sections we have given the pseudopotential formulation and some examples of model pseudopotentials that are used in the theory of metals. These model potentials refer to each bare ion. When we plant these ions into the conduction electron gas to form a metal the following procedure must be followed: (i) an electron sees all the cores as the sum of bare ion model potentials; (ii) the other conduction electrons enter the problem by screening the bare potentials through the static dielectric function of the electron gas. In this section we will talk about depletion charges, screening of the model potential, and effective ion-ion interaction.

2.3.1 Depletion charge

From Eqn. (2.11) we can see that the exact wave equation has been replaced by a model wave equation in terms of the model wave function. Thus, the real electron density can be regarded as the sum of two terms, a term $\mid \varphi_{\mathbf{k}}(\mathbf{r}) \mid^2$ from the model wave function, and a contribution from the difference between the above and that due to the oscillating part of the real wave function localized in the core region (see Figure 2.4) We define the total charge coming from the second contribution as the depletion charge ρ_d:

$$\rho_d = \sum_{k \leq k_F} \int_{\Omega_m} d^3r [\mid \Psi_{\mathbf{k}}(\mathbf{r}) \mid^2 - \mid \varphi_{\mathbf{k}}(\mathbf{r}) \mid^2] \tag{2.26}$$

The integral is over a single core volume Ω_m, so that ρ_d represents the depletion charge at a single ion site. The corresponding depletion charge density associated with site i is $\rho_{di}(\mathbf{r}) = \sum_{\mathbf{k} \leq \mathbf{k_F}} [\mid \Psi_{\mathbf{k}}(\mathbf{r}) \mid^2 - \mid \varphi_{\mathbf{k}}(\mathbf{r}) \mid^2]$.

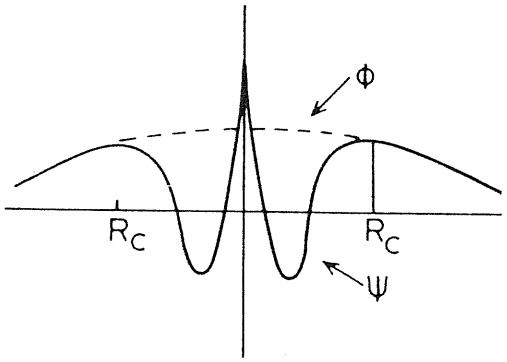

Figure 2.4: Schematic drawing of the un-normalized model wave function $\varphi_{\mathbf{k}}(\mathbf{r})$ and the exact wave function $\psi_{\mathbf{k}}(\mathbf{r})$.

ρ_d can be evaluated in terms of the model pseudopotential as [44,48]

$$\rho_d = -\sum_{\mathrm{k}\leq \mathrm{k_F}} \int_{\Omega_m} \mathrm{d^3 r}\varphi_{\mathrm{k}}^*(\mathrm{r})\frac{\partial \mathrm{W}}{\partial \mathrm{E_k}}\varphi_{\mathrm{k}}(\mathrm{r}). \tag{2.27}$$

2.3.2 Perturbation theory and screening of the model potential

In order to calculate the self-consistent screening of the model potential, we must evaluate the electron potential, which is determined from the electron density by Poisson's equation.

As mentioned in the above section, the total electron density can be written as the sum of two parts,

$$\begin{aligned} n(\mathrm{r}) &= \sum_{k\leq k_F} \psi_k^*(\mathrm{r})\psi_{\mathrm{k}}(\mathrm{r}) \\ &= \sum_{k\leq k_F} \varphi_k^*(\mathrm{r})\varphi_{\mathrm{k}}(\mathrm{r}) + \sum_{\mathrm{i}} \rho_{\mathrm{di}}(\mathrm{r}-\mathrm{r_i}) \end{aligned} \tag{2.28}$$

where ρ_{di} is the depletion charge density at the ith ion site.

The model wave function $\varphi_k(\mathrm{r})$ in Eqn. (2.11) can be determined by perturbation theory. For most applications of the model potential it is sufficient to know the energy eigenvalues to second order in W. Therefore, we obtain the wave function to first order. We expand the model wave function in plane waves,

$$\mid \varphi_k > = \mid \mathrm{k} > + \sum_{\mathrm{q}} \mathrm{a_q(k)} \mid \mathrm{k+q} > \tag{2.29}$$

From the perturbation calculation we obtain[38]

$$a_q(\mathrm{k}) = \frac{< \mathrm{k+q} \mid \mathrm{W} \mid \mathrm{q} >}{\frac{1}{2}(\mathrm{k}^2 - \mid \mathrm{k+q} \mid^2)}, \qquad \mathrm{q} \neq 0. \tag{2.30}$$

$a_0(\mathrm{k})$ can be found as [44]

$$a_0(\mathrm{k}) = \frac{1}{2}\mathrm{N} < \mathrm{k} \mid \partial \mathrm{W}/\partial \mathrm{E_k} \mid \mathrm{k} >_{\Omega_m} \tag{2.31}$$

The results enable us to write a first order expression for the electron density. Since $\partial W/\partial E$ is manifestly first order, the depletion charge becomes

$$\rho_d = -\sum_{k\leq k_F} < \mathrm{k} \mid \partial \mathrm{W}/\partial \mathrm{E_k} \mid \mathrm{k} >_{\Omega_\mathrm{m}} . \tag{2.32}$$

to first order. The electron density is then

$$\begin{aligned} n(\mathbf{r}) \;=\; & \sum_{k\leq k_F} (\frac{1}{\Omega}) + \sum_{k\leq k_F} \frac{N}{\Omega} < \mathrm{k} \mid \partial \mathrm{W}/\partial \mathrm{E_k} \mid \mathrm{k} >_{\Omega_\mathrm{m}} \\ & +2 \sum_{k\leq k_F} \sum_{q} \prime a_q(\mathbf{k}) \mathrm{e}^{\mathrm{iq\cdot r}} + \sum_{\mathrm{i}} \rho_{\mathrm{di}}(\mathbf{r}-\mathbf{r}_\mathrm{i}) \end{aligned} \tag{2.33}$$

Here, the first term in (2.33) is the uniform plane-wave density; the second is a uniform density which, when integrated over the metal, exactly cancels the integrated depletion charge;[44] the third term is the screening charge density; and the fourth still involves the depletion charge density $\rho_d(\mathbf{r})$.

We can now proceed with the self-consistent screening calculation using a standard procedure. We Fourier transform the electron charge density (2.33) and obtain for $\mathbf{q} \neq 0$:

$$n_q = 2 \sum_{k\leq k_F} a_q(k) + S(q)\rho_{dq}. \tag{2.34}$$

Here, ρ_{dq} is the Fourier transform of the depletion charge density at a single ion,

$$\rho_{dq} = \frac{1}{\Omega} \int_{\Omega_m} d^3 r e^{-i\mathbf{q}\cdot\mathbf{r}} \rho_d(\mathbf{r}), \tag{2.35}$$

and $S(q)$ is the ionic structure factor for the system being considered,

$$S(q) = \frac{1}{N} \sum_i e^{-i\mathbf{q}\cdot\mathbf{r}_\mathrm{i}} \tag{2.36}$$

We substitute Eqn. (2.34) into Poisson's equation and solve self-consistently for the electron potential. This is (with $W_\mathbf{q}(\mathbf{k}) \equiv < \mathrm{k}+\mathrm{q} \mid W \mid \mathrm{k} >=$

$\mathrm{w_q(k)S(q)}$)

$$v_e(q) = \frac{2}{\pi^2 q^2} \int_{k \leq k_F} d\mathrm{k} \frac{\mathrm{w_q(k)}}{\mathrm{E^0_k - E^0_{k+q}}} + \mathrm{v_d(q)} \tag{2.37}$$

where E^0_{k} is the free electron kinetic energy and $v_d(q) = \frac{4\pi}{q^2}\rho_{dq}$. From $w_{\mathrm{q}}(\mathrm{k}) = \mathrm{v_q} + \mathrm{f(k,q)} + \mathrm{v_e(q)}$, where v_{q} and $f(\mathrm{k,q})$ are the local and non-local parts of the electron-core potential, respectively, we finally find the screened form factor as

$$W_{\mathrm{q}}(k) = < k+q \mid \mathrm{W} \mid \mathrm{k} > = (\mathrm{V_q} + \mathrm{V_{dq}})/\varepsilon(\mathrm{q}) + \mathrm{F(k,q)} + \mathrm{G(q)} \tag{2.38}$$

Here, $\varepsilon(q)$ is the Hartree dielectric function (for exchange and correlations, see Chapter 3), $V_q = v_q S(q)$, $F(\mathrm{k,q}) = \mathrm{f(k,q)S(q)}$, and $G(q)$ is given by

$$G(q) = \frac{2}{\pi^2 q^2 \varepsilon(q)} \int_{k \leq k_F} d^3k \frac{F(\mathrm{k,q})}{\frac{1}{2}(\mathrm{k}^2 - \mid \mathrm{k+q} \mid^2)} \tag{2.39}$$

Finally, V_{dq} in Eqn. (2.38) is the depletion charge potential,

$$V_{dq} = \frac{4\pi}{q^2}\rho_{dq} S(q). \tag{2.40}$$

We note that [38,44] W can be written as a sum of potentials centered on individual ion sites,

$$W = \sum_i w_i. \tag{2.41}$$

The form factor $w_q(\mathrm{k})$ can be written explicitly as

$$w_q(\mathrm{k}) = (\mathrm{v_q} + \mathrm{v_{dq}})/\varepsilon(\mathrm{q}) + \mathrm{f(k,q)} + \mathrm{g(q)} \tag{2.42}$$

with $v_{dq} = 4\pi\rho_{dq}/q^2$.

2.3.3 The total energy and the effective ion-ion interaction

First of all, the energy eigenstates can be obtained by writing the usual time independent perturbation expansion[38,49],

$$E_{\mathrm{k}} = E^0_{\mathrm{k}} + < \mathrm{k} \mid \mathrm{w} \mid \mathrm{k} > + \sum_{\mathrm{q}}{}' \frac{< \mathrm{k} \mid \mathrm{w} \mid \mathrm{k}+\mathrm{q} >< \mathrm{k}+\mathrm{q} \mid \mathrm{w} \mid \mathrm{k} >}{\frac{1}{2}(\mathrm{k}^2 - \mid \mathrm{k}+\mathrm{q} \mid^2)} \tag{2.43}$$

where E^0_{k} is the free electron kinetic energy, $k^2/2$ and w is the quantity entering the sum in Eqn. (2.41).

The total energy per ion is the sum of the electron energies, evaluated to second order in the model potential, plus the direct ion-ion interaction, minus the electron-electron interaction energy [50]:

$$\begin{aligned} E_T \;=\; & \frac{1}{N}\sum_{k \le k_F}(\frac{k^2}{2}) + \sum_{k} < \mathrm{k} \mid \mathrm{w} \mid \mathrm{k} > + \mathrm{N}\sum_{\mathrm{k}}\sum_{\mathrm{q}}{}' \mid \mathrm{S(q)} \mid^2 \\ & \frac{< \mathrm{k} \mid \mathrm{w} \mid \mathrm{k}+\mathrm{q} >< \mathrm{k}+\mathrm{q} \mid \mathrm{w} \mid \mathrm{k} >}{\frac{1}{2}(\mathrm{k}^2 - \mid \mathrm{k}+\mathrm{q} \mid^2)} + \frac{1}{2N}\sum_{i,j}{}' V_d(\mid \mathrm{r_i} - \mathrm{r_j} \mid) \\ & -\frac{1}{2N}\int d^3r n(\mathrm{r}) \mathrm{V_e(r)} \end{aligned} \tag{2.44}$$

We must subtract the electron-electron interaction because this contribution has been counted twice in screening the model potential. $V_d(\mid \mathrm{r_i} - \mathrm{r_j} \mid)$ is the direct ion-ion interaction potential, $n(\mathrm{r})$ and $V_e(\mathrm{r})$ are the density of valence electrons and the corresponding potential, respectively.

Equation (2.44) is a basic equation for the calculations of metallic properties. We will give the extension of Eqn. (2.44) to the case of binary alloy and the derivation of some related equations in Chapter 3.

As we have seen in Eqn. (2.33), the total electron density separates naturally into four terms, a uniform plane-wave background, a uniform

Table 2.4: Shorthand notation used in the total energy calculation.

Contributions to total charge	Short hand symbol	
	charge	potential
valence charge Z at ion sites	n_{val}	V_{val}
uniform plane-wave charge compensating valence	n_{vu}	V_{vu}
depletion charge uniform charge compensating	n_d	V_d
depletion charge	n_{du}	V_{du}
total uniform charge	$n_u = n_{vu} + n_{du}$	$V_u = V_{vu} + V_{du}$
screening charge	n_{sc}	V_{sc}
effective valence at ion sites	$Z^* = Z - \rho$	
potential due to a single depletion charge interacting with itself		v_d

depletion charge background, a screening charge density, and a depletion charge density at each ion site. In addition there is at each ion site a valence charge Z. In the following we will give the explicit expressions of all the terms in Eqn. (2.44). In Table (2.4) we define the symbols, which are introduced by Harrison[38], for each of these charge densities and for the corresponding potentials. The interaction energy between two charge densities will be represented symbolically as:

$$nV = \int d^3r n(\mathbf{r})\mathrm{V}(\mathbf{r})$$

A prime on the potential is to indicate that the interaction of a charge density with itself is excluded. For example the ion-ion interaction term in Eqn. (2.44) is written

$$\frac{1}{2N} n_{val} V'_{val} \tag{2.45}$$

To evaluate Eqn. (2.44) explicitly, we see that the first term is simply Z times the average kinetic energy of an electron; the second term can

be written as (see Appendix A):

$$\begin{aligned}\sum_k < \mathbf{k} \mid w \mid \mathbf{k} > \;&=\; \frac{1}{N}(n_u + n_d)(V_u + V_d') + \frac{1}{2N} n_{val}(V_u + V_d) \\ &+ \frac{1}{2N}(n_u + n_d)V_{val} + \frac{1}{N} n_d V_{sc} + \rho_d v_d \\ &+ \frac{1}{N}\sum_k f(k) - \sum_k \sum_{l=0}^{l_0} \frac{\partial A_l}{\partial E} < \mathbf{k} \mid P_l \mid \mathbf{k} > \\ &\{f(k) - f(k_F)\}; \qquad (2.46)\end{aligned}$$

the electron-electron interaction energy per ion (the last term in (2.44)) may be rewritten as

$$E_e = \frac{1}{2N}(n_u + n_d + n_{sc})(V_u + V_d + V_{sc}). \qquad (2.47)$$

Since V_{sc} times a uniform charge distribution gives no contribution, we may rewrite (2.47) as

$$E_e = \frac{1}{2N}(n_u + n_d)(V_u + V_d') + \frac{1}{2}\rho_d v_d + \frac{1}{N} n_d V_{sc} + \frac{1}{2N} n_{sc} V_{sc}. \qquad (2.48)$$

The resulting expression for the total energy may be written conveniently as a sum of three contributions,

$$E_T = E_{fe} + E_{es} + E_{bs} \qquad (2.49)$$

The *free electron energy* E_{fe} is the average kinetic energy of a free electron plus the structure-independent terms from (2.46) and (2.48). This contribution to the total energy depends only on the total volume, not on the ionic structure.

We are primarily interested in the structure-dependent contributions to the total energy, namely E_{es} and E_{bs}. The term E_{es} may be written in the compact form from Eqns. (2.45), (2.46) and (2.48) as

$$E_{es} = \frac{1}{2N}(n_u + n_d + n_{val})(V_u + V_d' + V_{val}'). \qquad (2.50)$$

This is the just the *electrostatic energy* of a system of point charges Z^* embedded in a uniform compensating background. There are two remaining contributions to the total energy. We combine them and refer to the result as the *band-structure energy,*

$$E_{bs} = 2N \sum_k \sum_q{}' \mid S(\mathrm{q}) \mid^2 \frac{< \mathrm{k} \mid \mathrm{w} \mid \mathrm{k}+\mathrm{q} >< \mathrm{k}+\mathrm{q} \mid \mathrm{w} \mid \mathrm{k} >}{\mathrm{k}^2 - \mid \mathrm{k}+\mathrm{q} \mid^2} - \frac{1}{2N} n_{sc} V_{sc}. \tag{2.51}$$

If we Fourier transform the screening term we can write the band-structure energy as

$$E_{bs} = \sum_q{}' \mid S(\mathrm{q}) \mid^2 \mathrm{F(q)}. \tag{2.52}$$

The function

$$F(q) = \frac{2\Omega_0}{(2\pi)^3} \int_{k \le f_F} d^3k \frac{2\{w_q(\mathrm{k})\}^2}{\mathrm{k}^2 - \mid \mathrm{k}+\mathrm{q} \mid^2} - \frac{\Omega_0 q^2}{8\pi} (v_{scq})^2 \tag{2.53}$$

is called the *energy-wave-number characteristic,* and it depends only on the atomic volume Ω_0 and not on the ionic structure.

If we write Eqn. (2.52) by writing the structure factor explicitly, we have[38]

$$\begin{aligned} E_{bs} &= \sum_q{}' S^*(q) S(q) F(q) \\ &= \sum_q{}' \sum_{i,j} N^{-2} F(q) exp[-i\mathbf{q} \cdot (\mathbf{r}_i - \mathbf{r}_j)] \\ &= \frac{1}{2N} \sum_{i,j}{}' V_{ind}(r_i - r_j) + \frac{1}{N} \sum_q{}' F(q), \end{aligned} \tag{2.54}$$

where the indirect interaction is given by

$$V_{ind} = \frac{2}{N} \sum_q{}' F(q) e^{-i\mathrm{q} \cdot \mathrm{r}} \tag{2.55}$$

If we convert the sum over q to an integral and do the angle integrations we obtain

$$V_{ind}(r) = \frac{\Omega_0}{\pi^2} \int_0^\infty F(q) \frac{sin\, qr}{qr} q^2 dq. \tag{2.56}$$

We see that V_{ind} is a two body, central force interaction between ions just as the direct interaction is. The two may be added to give a total "effective ion-ion interaction". If we add to Eqn. (2.56) the direct interaction between ions with an effective valence Z^* (the choice of an effective valence is required due to the definition of electrostatic energy), then we get

$$V_{eff} = \frac{(Z^*)^2}{r}[1 - \frac{2}{\pi}\int_0^\infty F_N(q)\frac{sin\, qr}{qr}dq] \tag{2.57}$$

where the normalized energy-wavenumber characteristic has been used, which is,

$$F_N(q) = -\frac{q^2\Omega_0}{2\pi Z^{*2}}F(q). \tag{2.58}$$

The extension of the equations derived in this section to the binary alloy systems will be given in Chapter 3.

2.4 Applications of model potentials

In this section we will give some of applications of the model potentials which we have introduced in Section 2.2. Here we just give some examples but do not attempt to cover the whole field of this subject.

2.4.1 Applications of Ashcroft empty-core model potential

In Section 1.1.3 we have seen that there is a relation between long wavelength limit of structure factor, $S(0)$, and the isothermal compressibility κ_T (Eqn. (1.28)). In the work of Chaturvedi *et.al.*[51], they consider the usual model of a liquid alkali metal as constituted of a fluid of classical

ions and degenerate electrons. In such a system the ionic liquid and the electron gas are assumed weakly coupled through a pseudopotential $v(k)$. The structure factor $S(k)$ of the liquid metal can be written as (for details and references see [51]):

$$S(k) = S_0(k)[1 - c_s(k)S_0(k)]^{-1} \tag{2.59}$$

or equivalently the direct correlation function $c(k)$ is given by

$$c(k) = c_0(k) + c_s(k). \tag{2.60}$$

Here, $S_0(k)$ and $c_0(k)$ are, respectively, the structure factor and the direct correlation function of the bare ionic system on a rigid neutralizing background, which forms a one-component classical plasma (OCP), while

$$c_s = \frac{nk^2v^2(k)}{4\pi k_B T}[1 - 1/\varepsilon(k)] \tag{2.61}$$

is given by the usual expression for the contributions of electronic screening to the effective ion-ion potential in terms of $v(k)$ and of the dielectric function $\varepsilon(k)$ of the homogenous electron gas. The one component plasma (OCP) structure factor $S_0(k)$ and the dielectric function are given, respectively, in the long wavelength limit:

$$\lim_{k\to 0} S_0(k) = \frac{k_B T k^2}{4\pi n e^2}(1 + k^2/k_i^2)^{-1} \tag{2.62}$$

$$\lim_{k\to 0} \varepsilon(k) = 1 + k_e^2/k^2 \tag{2.63}$$

where k_e is the inverse screening length of the electron gas, related to its compressibility, and k_i is given in terms of the excess internal energy u per particle of the OCP, in units of $k_B T$, as[51]

$$\frac{k_D^2}{k_i^2} = 1 + \frac{1}{3}u + \frac{1}{9}\Gamma\frac{du}{d\Gamma} \tag{2.64}$$

where

$$k_D = (4\pi n e^2/k_B T)^{1/2}$$

is the Debye-Hűckel inverse screening length and the plasma parameter Γ is given by $\Gamma = (Ze)^2/ak_BT$ with a being the atomic radius. The simulated expressions for u are available[52–54]. The pseudopotential is taken as the Ashcroft empty-core model potential, which is given by (in the k-space),

$$v(k) = -\frac{4\pi}{k^2} cos(kr_c) \tag{2.65}$$

where r_c is the empty-core radius.

The use of Eqns. (2.62)-(2.64) in Eqn. (2.59) leads to

$$S(0) = (\frac{k_D^2}{k_c^2} + \frac{k_D^2}{k_i^2} + k_D^2 r_c^2)^{-1}. \tag{2.66}$$

The theoretical and the experimental results of $S(0)$ are given in Table 2.5[51]. The good agreement with experiment shows that the theory is quite successful.

For the alkali alloys, the same approximations yields the following

Table 2.5: Structure factor at long wavelength for liquid alkali metals (the references cited in this table refer to the original paper [51]).

	T(K)	e^2/ak_BT	r_c(Å)	r_s	$S(0)_{calc}$[a])	$S(0)_{expt}$[b])
Li	453	211	0.741	3.299	0.0158(0.0201)	-
Na	371	208	0.894	4.049	0.0215	0.0240(0.0233)
	437	163	0.894	4.085	0.0289	0.0322(0.0308)
K	337	186	1.18	5.030	0.0231(0.0212)	0.0247(0.0225)
	408	153	1.18	5.072	0.0295(0.0270)	0.0312(0.0283)
Rb	312	188	1.27	5.388	0.0236(0.0207)	(0.0220)
Cs	301	181	1.39	5.786	0.0235(0.0202)	(0.0237)

[a]) Values in parenthesis include an effective mass correction in the calculation of k_c^2, as discussed by Price et al. [17].
[b]) Values in parentheses are deduced from the sound velocities reported by Webber and Stephens [27], with a correction for the difference between the adiabatic and isothermal compressibilities. The other values are from Greenfield et al. [2].

equations for the thermodynamic properties:

$$nk_BT\kappa_T = [\frac{k_D^2}{k_e^2} + \frac{k_D^2}{k_i^2} + k_D^2(c_1r_1^2 + c_2r_2^2)]^{-1} \tag{2.67}$$

$$(v_2 - v_1)/(k_BT\kappa_T) = \frac{1}{2}k_D^2(r_2^2 - r_1^2) \tag{2.68}$$

and

$$S_{cc} = c_1c_2[1 - 2c_1c_2w/k_BT]^{-1} \tag{2.69}$$

with

$$w = \frac{1}{2}n(v_2 - v_1)^2/\kappa_T. \tag{2.70}$$

Here v_α are the partial molar volumes of the two components of the alloy, r_α are the empty-core radius and c_α the concentration of the αth component of the alloy.

For the $Na-K$ alloy, Eqn. (2.67) leads to an essentially linear dependence of the isothermal compressibility on concentration, in substantial accord with experiment. The calculated variation of molar volume with concentration from (2.68) is also in reasonable agreement with experiment, the largest discrepancies being of the order of 20%[51]. For what concerns the concentration fluctuations, we see that w in Eqn. (2.70) contains only an elastic term, which gives a value too large by about an order of magnitude when compared with that deduced from the experimental data. In Chapter 3 we will see that there is another term in w when we use a non-local model potential other than Ashcroft empty-core potential in the calculations. This term will cancel a lot the elastic term and give a value w closer to the experimental data.

2.4.2 Applications of the EIMP

In recent years, the EIMP has been used to calculate the electrical resistivities[55,56] and to carry out variational thermodynamic calculations[57,58] for some liquid metals and alloys. Here we give an example of the calculations of the isothermal compressibility of the alkali alloys.

By the idea of the Gibbs-Bogoliubov inequality[59], one may begin with an upper bound to the Helmholtz free energy, F, per ion for a metallic system. If the hard sphere (HS) is used as a reference system, one has [57]

$$F = F_{HS} + F_{eg} + F_d + F_b + F_M \tag{2.71}$$

where the free energy of the HS reference system, F_{HS}, is given by $\frac{3}{2}k_BT - TS_{HS}$ with S_{HS} being the entropy of the HS system; F_{eg} is the free energy of the electron gas. The explicit expressions for S_{HS} and F_{eg} can be found in references [60] and [61], respectively; F_d is the diagonal term, arising from the deviation of the electron-ion pseudopotential from purely Coulombic form, and $F_b + F_M$ is the sum of the band-structure term and the Madelung term, *i.e.* the electrostatic energy. The last three terms depend on the poseudopotential theory used and can be written for the binary alloys as

$$F_d = \Omega_0\pi^{-2}\sum_{\alpha=1}^{2} c_\alpha \int_0^{k_F} dk k^2 N < \mathbf{k} \mid \Delta \mathrm{w}_\alpha^{\mathrm{b}}(\mathbf{r}) \mid \mathbf{k} > \tag{2.72}$$

and

$$\begin{aligned} F_b + F_M &= -\pi^{-1}\sum_{\alpha=1}^{2}\sum_{\beta=1}^{2} Z_{eff,\alpha}Z_{eff,\beta}(c_\alpha c_\beta)^{1/2} \\ &\quad \int_0^\infty dq[a_{\alpha\beta}(q)(F_{\alpha\beta}(q)-1)+\delta_{\alpha\beta}] \end{aligned} \tag{2.73}$$

Here, c_α stands for the concentration of the αth component of the alloy, $\Delta w_\alpha^b(\mathbf{r})$ denotes the deviation of the bare EIMP from pure Coulom-

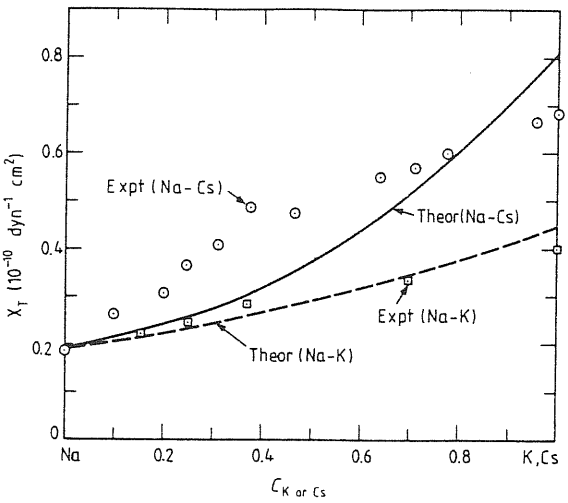

Figure 2.5: Isothermal compressibilities, κ_T calculated in EINMP for $Na - K$ (100 C) and $Na - Cs$ (100 C) alloys, comparing with the experiments (for references, see [56]) (from [56]).

bic for a valence electron at r due to an αth-type ion, and k_F is the Fermi momentum given by $[3\pi^2\Omega_0^{-1}(c_1 n_{v_1} + c_2 n_{v_2})]^{1/3}$ with n_{v_α} and Ω_0 being, respectively, the number of valence electrons around an αth-type ion and the mean volume occupied by one ion; $Z_{eff,\alpha}Z_{eff,\beta}$ represents an effective valence of the product of the ionic valences Z_α and Z_β, $F_{\alpha\beta}(q)$ denotes the normalized energy-wavenumber characteristic in the low order perturbation pseudopotential theory and $a_{\alpha\beta}(q)$ is the partial structure factor.

The variational calculation of F is to minimize F with respect to the HS diameters, σ_α, using the EIMP. The isothermal compressibility of the alloy, κ_T, can be expressed theoretically as[62] (for HS system)

$$\kappa_T(c_\alpha) = \Omega_0 a(0)(k_B T)^{-1} \tag{2.74}$$

with

$$a(0) = \frac{a_{11}(0)a_{22}(0) - a_{12}^2(0)}{c_1 a_{22}(0) + c_2 a_{11}(0) - 2(c_1 c_2)^{1/2} a_{12}(0)} \tag{2.75}$$

which is usually written in terms of η and σ_α. Here η is the packing density and is given by

$$\eta = \frac{\pi}{6\Omega_0}(c_1\sigma_1^3 + c_2\sigma_2^3) \tag{2.76}$$

Figure 2.5 shows the calculations and experimental data of the isothermal compressibilities for $Na-Cs$ and $Na-K$ alloys. The results shows that the calculated κ_T is in good agreement with experiment for $Na-K$ alloy, whereas for $Na-Cs$ alloy the theory gives a correct trend of the concentration dependence of κ_T.

We summarize this chapter by remarking that the replacement of the deep core potential by a shallow pseudopotential enables us to calculate rather easily such properties as lattice dynamics, cohesive energy, optical absorption, transport properties and thermodynamic properties of metals and alloys by low order perturbation theory. We also note that, in the calculations of the physical properties, different forms of model potentials may give different results. Therefore the choice of a suitable model potential is very important.

Chapter 3

Pseudopotential Theory of Thermodynamic Properties of Simple Liquid Alloys

In Chapter 2 we introduced the formulation of pseudopotential theory and some of the model potentials in common use, giving some examples of applications. In this chapter we shall focus on our application of the model potential theory to the thermodynamic property for simple liquid metal alloys[63].

3.1 The relation between long wavelength structure factors and pair potentials in a binary alloy

3.1.1 Exact relations between thermodynamic properties and Ornstein-Zernike correlations in an alloy

We have reviewed the structure factors and correlation functions for monatomic liquids and mixtures in Chapter 1. However, we shall see in this section that it is convenient to use the direct correlation functions $c_{\alpha\beta}(r)$ to rewrite the relations between the partial structure factors in a binary alloy and the pair potentials. The $c_{\alpha\beta}(q)$ are related to the inverse of the matrix of partial structure factors by (see, for instance, [51])

$$c_{\alpha\beta}(q) = \delta_{\alpha\beta} - S^{-1}_{\alpha\beta}(q). \tag{3.1}$$

The connection to thermodynamic fluctuation theory[1] in the long wavelength limit is conveniently made through the correlation functions of total density fluctuations and concentration fluctuations in the alloy[2], defined by

$$\begin{aligned} c_{NN}(q) &= c_1 c_{11}(q) + c_2 c_{22}(q) + 2(c_1 c_2)^{1/2} c_{12}(q), & (3.2)\\ c_{cc}(q) &= c_2 c_{11}(q) + c_1 c_{22}(q) - 2(c_1 c_2)^{1/2} c_{12}(q), & (3.3)\\ c_{Nc}(q) &= c_{11}(q) - c_{22}(q) + (c_2 - c_1)(c_1 c_2)^{-1/2} c_{12}(q). & (3.4) \end{aligned}$$

The relations of Kirkwood and Buff can then be written as

$$\rho k_B T \kappa_T = \lim_{q\to 0}[1 - c_{NN}(q)]^{-1}, \tag{3.5}$$

$$\rho(v_2 - v_1) = \lim_{q\to 0}\{c_{Nc}(q)/[1 - c_{NN}(q)\}, \tag{3.6}$$

$$\frac{1}{1-c}\left(\frac{\partial \mu_2}{\partial c}\right)_{T,P,N} = \frac{-\rho(v_2 - v_1)^2}{\kappa_T} + \frac{k_B T}{c(1-c)} \lim_{q\to 0}[1 - c_{cc}(q)]. \tag{3.7}$$

Here v_α are the partial molar volumes of the two components of the alloy and μ_2 is the chemical potential of the second component, in concentration c. The quantity on the left hand side of Eqn. (3.6) is in fact the relative variation of the volume of the alloy with the concentration, $\delta = V^{-1}(\partial V/\partial c)_{T,P,N}$. On the other hand, the left hand side of Eqn. (3.7) is related to the long wavelength limit of the concentration-concentration structure factor, S_{cc}, through

$$S_{cc} = (1-c)k_B T/(\partial \mu_2/\partial c)_{T,P,N} \tag{3.8}$$

Combining Eqns. (3.7) and (3.8) we can write S_{cc} as

$$S_{cc} = \frac{c(1-c)}{1 - 2c(1-c)w/k_B T} \tag{3.9}$$

where w is defined by

$$w = \frac{\rho(v_2 - v_1)^2}{2\kappa_T} + \frac{1}{2} k_B T \lim_{q\to 0} \frac{c_{cc}(q)}{c(1-c)}. \tag{3.10}$$

We stress that we did not introduce any approximations in deriving the above equations and therefore all the results are exact. In particular, Eqn. (3.10) gives an exact definition for the "interchange free energy" w, which is introduced as an approximate concept in the model of conformal solutions (see Section 1.3) in order to arrive at the expression (3.9) for S_{cc}. Our derivation shows that the expression (3.9) for S_{cc} is exact, with w defined through Eqn. (3.10) as the sum of a positive-definite elastic strain term and of an "effective interaction" between concentration fluctuations, which is described by the long-wavelength limiting value of the concentration-concentration Ornstein-Zernike function.

3.1.2 Approximate relations to pair potentials

Eqns. (3.2)-(3.10) show that the calculation of w (and hence S_{cc}) and of the other thermodynamic properties requires calculation of the direct correlation functions $c_{\alpha\beta}$ in the long wavelength limit. Following the work of Postogna and Tosi[64], we resort to an approximation in which, for a binary alloy of equi-valent elements such as Na-K, we adapt the one-component classical plasma (OCP) as the reference liquid and treat all the effects of the electron-ion and electron-electron interactions by low order perturbation theory. The ions in the reference liquid are taken to have the true valence (Z, say) of the ions in the alloy of equi-valent elements. It is then easily shown that the partial direct correlation functions at long wavelength limit can be expressed as

$$\lim_{q\to 0} c_{\alpha\beta}(q) = (c_\alpha c_\beta)^{1/2}(c_0(0) - V_{\alpha\beta}/k_B T). \tag{3.11}$$

Here, $c_0(0)$ is the long wavelength limit of the regular part of the direct correlation function of the OCP for ions of valence Z and

$$V_{\alpha\beta} = \lim_{q\to 0}[\rho V_{\alpha\beta}(q)] \tag{3.12}$$

where $V_{\alpha\beta}(q)$ are the effective interionic pair potentials. As already noted in Section 2.4.1, $c_0(0)$ can be expressed as

$$c_0(0) = 1 - \frac{k_D^2}{k_i^2} \tag{3.13}$$

with k_D^2/k_i^2 defined in Eqn. (2.64).

We can now see from Eqns. (3.11) and (3.12) that all the calculations are focussed on the evaluation of the long wavelength limit of the effective interionic pair potentials.

3.2 Pair potentials in the alloy and their long wavelength limit

In this section we will use Shaw's optimized model potential in the system of simple liquid alloys to derive the effective ion-ion interaction potential $V_{\alpha\beta}(q)$ and finally we will derive the long wavelength limit $V_{\alpha\beta}$.

3.2.1 Effective pair potentials $V_{\alpha\beta}(q)$

From the discussions and the formula given in Section 2.3, we can easily write the total energy and the effective ion-ion interactions for a binary alloy. The total energy can be written, for a binary alloy, as

$$\begin{aligned} E_T &= \frac{1}{N}\sum_{\mathbf{k}\le\mathbf{k}_F}\frac{1}{2}k^2 + \frac{1}{N}\sum_{\mathbf{k}\le\mathbf{k}_F}\sum_{\alpha=1}^{2} c_\alpha N < \mathbf{k}|w_\alpha|\mathbf{k} > + \frac{1}{N}\sum_{\mathbf{k}\le\mathbf{k}_F}\sum_{\mathbf{q}}{}' \\ &[\sum_{\alpha=1}^{2}|S_\alpha(\mathbf{q})|^2 w_{\alpha,-\mathbf{q}}(\mathbf{k}+\mathbf{q})w_{\alpha,\mathbf{q}}(\mathbf{k}) + S_{12}(\mathbf{q})w_{1,-\mathbf{q}}(\mathbf{k}+\mathbf{q})w_{2,\mathbf{q}}(\mathbf{k}) \\ &+S_{12}^*(\mathbf{q})w_{2,-\mathbf{q}}(\mathbf{k}+\mathbf{q})w_{1,\mathbf{q}}(\mathbf{k})](\frac{k^2}{2} - \frac{|\mathbf{k}+\mathbf{q}|^2}{2})^{-1} \\ &+\frac{1}{2N}\sum_{\alpha,\beta}\sum_{\lambda}\sum_{\mu}{}' V(|\mathbf{R}_{\mu(\beta)} - \mathbf{R}_{\lambda(\alpha)}|) - \frac{1}{2N}\int d^3r n(\mathbf{r})V_e(\mathbf{r}) \end{aligned} \tag{3.14}$$

where $S_\alpha(q)$ is given by

$$S_\alpha(q) = \frac{1}{N}\sum_{\lambda} exp(-i\mathbf{q}\cdot\mathbf{R}_{\lambda(\alpha)}) \tag{3.15}$$

in which the summation over λ extends over all the position $\mathbf{R}_{\lambda(\alpha)}$ of the αth type ions and $N = \sum_\alpha N_\alpha$, N_α being the numbers of the αth type ions in the alloy under considered. $w_{\alpha,-\mathbf{q}}(\mathbf{k}+\mathbf{q})$ is the form factor derived from $< \mathbf{k}|w(r)|\mathbf{k}+\mathbf{q} >$ and $S_{12} = S_1^*(\mathbf{q})S_2(\mathbf{q})$.

The effective ion-ion interactions in an alloy can be derived by the similar procedure as that for a metal (see Section 2.3). The resulting expression is[55]

$$V_{\alpha\beta}(r) = \frac{Z^*_\alpha Z^*_\beta}{r}\{1 - \frac{1}{\pi}\int_0^\infty [F^N_{\alpha\beta}(q) + F^N_{\beta\alpha}(q)]\frac{sin\, qr}{q}dq\} \tag{3.16}$$

and in wave-number space

$$V_{\alpha\beta}(q) = \frac{4\pi Z^*_\alpha Z^*_\beta}{q^2}\{1 - \frac{1}{2}[F^N_{\alpha\beta}(q) + F^N_{\beta\alpha}(q)]\} \tag{3.17}$$

Here, Z^*_α and $F^N_{\alpha\beta}(q)$ are, respectively, the effective charge and the normalized energy wavenumber characteristic, which are defined by

$$Z^*_\alpha = Z_\alpha - \rho_{d\alpha} \tag{3.18}$$

and

$$F^N_{\alpha\beta}(q) = -\frac{\Omega_0 q^2}{2\pi Z^*_\alpha Z^*_\beta}F_{\alpha\beta}(q). \tag{3.19}$$

Z_α and $\rho_{d\alpha}$ are the valence and depletion charge of the αth component in the alloy and $F_{\alpha\beta}(q)$ are given by

$$\begin{aligned} F_{\alpha\beta}(q) &= \frac{2\Omega_0}{(2\pi)^3}\int_{\mathbf{k}\le\mathbf{k}_F}\frac{w_{\alpha,-\mathbf{q}}(\mathbf{k}+\mathbf{q})w_{\beta,\mathbf{q}}(\mathbf{k})}{\frac{1}{2}(k^2 - |\mathbf{k}+\mathbf{q}|^2)} \\ &\quad -\frac{\Omega_0 q^2}{8\pi}v_{\alpha,sc}v_{\beta,sc} \end{aligned} \tag{3.20}$$

where $v_{\alpha,sc}$ are defined by

$$\begin{aligned} v_{\alpha,sc} &= \frac{2}{\pi^2 q^2}\int_{\mathbf{k}\le\mathbf{k}_F} d^3k\frac{w_{\alpha,\mathbf{q}}(\mathbf{k})}{\frac{1}{2}(k^2 - |\mathbf{k}+\mathbf{q}|^2)} \\ &= -[4\pi Z^*_\alpha/(\Omega_0 q^2)]\frac{1-\varepsilon(q)}{\varepsilon(q)} + g_\alpha(q) \end{aligned} \tag{3.21}$$

Here,

$$\begin{aligned} \varepsilon(q) &= 1 - \frac{2}{\pi^2 q^2}\int_{\mathbf{k}\le\mathbf{k}_F} d^3k\frac{1}{\frac{1}{2}(k^2 - |\mathbf{k}+\mathbf{q}|^2)} \\ &= 1 + \frac{1}{2\pi k_F \eta^2}(1 + \frac{1-\eta^2}{2\eta}ln|\frac{1+\eta}{1-\eta}|) \\ \eta &= q/2k_F \end{aligned} \tag{3.22}$$

in the Hartree approximation (for the inclusion of exchange and correlations, see Section 3.4 below), and $g_\alpha(q)$ is defined by

$$g_\alpha(q) = \frac{2}{\pi^2 q^2 \varepsilon(q)} \int_{\mathbf{k}\le\mathbf{k}_F} d^3k \frac{f_\alpha(\mathbf{k}+\mathbf{q},\mathbf{k})}{\frac{1}{2}(k^2 - |\mathbf{k}+\mathbf{q}|^2)} \tag{3.23}$$

Here, $f_\alpha(\mathbf{k}+\mathbf{q},\mathbf{k})$, the nonlocal contribution to the bare model potential of the αth component in the alloy, is given, for Shaw's optimized model potential, by

$$\begin{aligned} f_\alpha(\mathbf{k}+\mathbf{q},\mathbf{k}) &= -N < \mathbf{k}+\mathbf{q}| \sum_{l=0}^{l_0} \{A_l^\alpha(E) - Z_\alpha/r\} P_l |\mathbf{k}> \qquad (3.24) \\ &= -\frac{4\pi}{\Omega_0} \sum_{l=0}^{l_0} (2l+1) A_l^\alpha(E) [R_l^\alpha(E)]^3 \\ &\quad \int_0^1 dx\, x(x-1) j_l(k' R_l^\alpha x) j_l(k R_l^\alpha x). \qquad (3.25) \end{aligned}$$

$$(x = r/R_l^\alpha(E), k' = |\mathbf{k}+\mathbf{q}|)$$

In the above equations $A_l^\alpha(E)$ and $R_L^\alpha(E)$ are energy dependent model potential parameters related by the optimization condition $A_l^\alpha(E) = Z_\alpha/R_l^\alpha(E)$; j_l is the l-order spherical Bessel function and l_0 is the largest angular quantum number for which there are core states.

3.2.2 Long wavelength limit

We finally come to the main point of our calculation, that is the derivation of the long wavelength limit of the effective ionic pair potentials $V_{\alpha\beta}(q)$. From Eqn. (3.22) we have

$$\lim_{q\to 0} \varepsilon(q) = 1 + \frac{4k_F}{\pi q^2}. \tag{3.26}$$

The long wavelength limit of $g_\alpha(q)$ can be shown to be[44]

$$g_\alpha = \lim_{q\to 0} g_\alpha(q) = -f_\alpha(k_F) - \frac{\pi^2}{\Omega_0 k_F} \rho_{d\alpha} \tag{3.27}$$

Substituting Eqns. (3.26) and (3.27) into Eqn. (3.21), we obtain

$$\lim_{q\to 0} v_{\alpha,sc}(q) = \frac{4\pi Z_\alpha^*}{\Omega_0 q^2} - f_\alpha(k_F) - \frac{\pi^2 Z_\alpha}{\Omega k_F}. \tag{3.28}$$

Finally we get the long wavelength limit of the effective pair potentials by Eqns. (3.17), (3.19) and (3.20),

$$\begin{aligned} V_{\alpha\beta} &= \rho \lim_{q\to 0} V_{\alpha\beta}(q) \\ &= \frac{\pi^2 Z_\alpha^* Z_\beta^*}{\Omega_0 k_F} - (Z_\alpha^* g_\beta + Z_\beta^* g_\alpha) + \frac{\Omega_0}{\pi^2} k_F g_\alpha g_\beta + I_{\alpha\beta} \end{aligned} \tag{3.29}$$

where $I_{\alpha\beta}$ is defined by

$$\begin{aligned} I_{\alpha\beta} &= \lim_{q\to 0} \frac{\Omega_0}{4\pi^3} \int_{k\le k_K} d^3k [f_\alpha(\mathbf{k}+\mathbf{q},\mathbf{k}) f_\beta(\mathbf{k},\mathbf{k}+\mathbf{q}) \\ &\quad + f_\alpha(\mathbf{k},\mathbf{k}+\mathbf{q}) f_\beta(\mathbf{k}+\mathbf{q},\mathbf{k})][\frac{1}{2}(k^2 - |\mathbf{k}+\mathbf{q}|^2)]^{-1} \\ &= \frac{\Omega}{\pi^2} k_F f_\alpha(k_F) f_\beta(k_F) - \frac{\Omega}{\pi^2} \int_0^{k_F} k dk [f_\alpha(k) N \sum_{l=0}^{l_0} < \mathbf{k}| \frac{\partial A_l^\beta(E_k)}{\partial k} P_l |\mathbf{k}> \\ &\quad + f_\beta(k) N \sum_{l=0}^{l_0} < \mathbf{k}| \frac{\partial A_l^\alpha(E_k)}{\partial k} P_l |\mathbf{k}>]. \end{aligned} \tag{3.30}$$

We stress at this point (see also the discussion in Section 2.4.1) that there are two terms entering the determination of the exchange energy w when we use a nonlocal model poseudopotential. From Eqns. (3.3) and (3.11) we have

$$\lim_{q\to 0} c_{cc}(q) = c(1-c)(2V_{12} - V_{11} - V_{22})/k_B T. \tag{3.31}$$

This expression, which vanishes when one uses a local model potential such as the empty-core one, describes the "effective interaction" between concentration fluctuations within our approximate treatment and is soon shown to be non-vanishing on account of nonlocality. Indeed, substituting Eqns. (3.29) and (3.30) into Eqn. (3.31) and rearranging

the terms, we get the compact form

$$(2V_{12} - V_{11} - V_{22}) = \frac{2\Omega_0}{\pi^2}\int_0^{k_F} kdk[\sum_{l=0}^{l_0} < \mathrm{k}|(A_l^{(2)} - A_l^{(1)})P_l|\mathrm{k} >] \\ [\sum_{l=0}^{l_0} < \mathrm{k}|(\frac{\partial A_l^{(1)}}{\partial k} - \frac{\partial A_l^{(2)}}{\partial k})P_l|\mathrm{k} >] \qquad (3.32)$$

We can see from Eqn. (3.32) that the first factor in the integrand is the difference in non-local contributions to the unscreened form factor $f_\alpha(k)$ at long scattering wavelength, which is defined by (see Eqn. (3.24))

$$f_\alpha = N\sum_{l=0}^{l_0} < \mathrm{k}|(\frac{Z}{r} - A_l^{(\alpha)})P_l|\mathrm{k} > . \qquad (3.33)$$

On the other hand, the second factor in the integrand also determines the difference in depletion charge, since

$$\rho_{d,\alpha} = \frac{\Omega_0}{\pi^2}\int_0^{k_F} kdk\sum_{l=0}^{l_0} < \mathrm{k}|\frac{\partial A_l^{(\alpha)}}{\partial k}P_l|\mathrm{k} > . \qquad (3.34)$$

Therefore, if $A_l^{(1)} > A_l^{(2)}$ for all relevant values of l (namely, if the model potential is deeper inside the core for the first alloy component), one has $f_1(k) - f_2(k) < 0$ and at the same time one expects that less charge will be excluded from the core (namely, $\rho_{d,1} > \rho_{d,2}$). The argument suggests that the integral in Eqn. (3.32) has a definite *negative* sign, at least when the behaviour of the two integrand factors with wave number is sufficiently smooth. We conclude that the effective interaction between concentration fluctuations (a) is due in the case of homovalent elements to non-local terms reflecting differences in core levels and (b) is likely to be an attraction arising from the fact that the alloy component with deeper core potential undergoes less exclusion of electronic charge from the core. Clearly, if the "effective interaction" between concentration fluctuations is indeed attractive, it will be at least partially cancel the positive-definite elastic strain contribution to w in Eqn. (3.10).

3.3 Calculations of thermodynamic properties of simple liquid alloys

In the last section we have derived the expressions for $V_{\alpha\beta}$. We can now calculate the thermodynamic quantities $S_{cc}(0), \delta$ and κ_T by Eqns. (3.5)-(3.8). In this section, numerical calculations of these quantities for the liquid binary alloys Na-K and Na-Cs will be given.

With reference to the discussions given by Shaw[45,50], we assume a linear dependence of the parameters $A_l^\alpha(E_k)$ on the energy E_k,

$$A_l^\alpha(E_k) = A_l^\alpha(E_F^0) + \frac{1}{2}(k^2 - (k_F^0)^2)\frac{\partial A_l^\alpha}{\partial E}, \tag{3.35}$$

where E_F^0 and k_F^0 are, respectively, the Fermi energy and the Fermi wavenumber of the pure α component. This equation has been used by Shaw[50] in his model potential calculations for pure metals. In the alloy, however, we first use this equation to get $A_l^\alpha(E_F)$ at the Fermi energy of the alloy. Then we can get the required parameters in the alloy by

$$A_l^\alpha(E_k) = A_l^\alpha(E_F) + \frac{1}{2}(k^2 - k_F^2)\frac{\partial A^\alpha}{\partial E}, \tag{3.36}$$

where E_F and k_F are, respectively, the Fermi energy and the Fermi wavenumber of the αth component in the alloy.

$c_0(0)$ is evaluated by Eqns. (2.64) and (3.13) with u given by the simulated result[59]

$$u = a\Gamma + b\Gamma^{1/4} + c\Gamma^{-1/4} + d \tag{3.37}$$

with

$$\begin{aligned} a &= -0.898004 \\ b &= 0.96786 \end{aligned}$$

$$c = 0.220703$$

$$d = -0.86097$$

3.3.1 $Na - K$ alloys

Two sets of parameters are used in the calculations for Na-K alloys: one is taken from Shaw[45] and the other is taken from Ese and Reissland[65]. We give these parameters in Table 3.1.

Based on the experimental data of Ω_0 for liquid $Na - K$ alloys[66], we use a linear relation to calculate the atomic volume of the alloy, that is

$$\Omega_0 = c\Omega_{0K} + (1 - c)\Omega_{0Na} \tag{3.38}$$

where c refers to the concentration of K and $\Omega_{0\alpha}$ are the atomic volumes of pure α metal, which are taken as $\Omega_{0Na} = 278.4(au)$ and $\Omega_{0K} = 546.0(au)$ in our calculations. The calculated results are given in Table 3.2, in which $\rho_{d,\alpha}$ refers to the depletion charge of αth component in

Table 3.1: Model potential parameters in atomic units ((a): from Shaw[45] (b): from Ese and Reissland [65])

	$R_0(E_F^0)$	$A_0(E_F^0)$	$\partial A_0/\partial E$	$R_1(E_F^0)$	$A_1(E_F^0)$	$\partial A_1/\partial E$
(a):						
Na	3.26	0.307	-0.231	2.71	0.369	-0.196
K	4.20	0.238	-0.294	4.00	0.250	-0.120
(b):						
Na	3.209	0.312	-0.187	2.802	0.357	-0.117
K	4.025	0.248	-0.240	4.033	0.248	-0.287

the alloy while w^e denotes the second term in Eqn. (3.10) ; $\kappa_{T,Na}$ is the isothermal compressibility of pure Na ($c_K = 0$) and (a) and (b) correspond to the two different sets of model potential parameters.

The results given in Table 3.2 shows that the magnitude and the concentration dependence of depletion charges $\rho_{d,Na}$ and $\rho_{d,K}$ are similar to those already reported by Wang and Lai[55]. As discussed by these authors, the behaviour of the two depletion charges can be interpreted as reflecting electronic charge transfer to the more electronegative Na atom on alloying. This appears in their results for the effective pair potentials in the alloy through a deepening of the main minimum in $V_{NaNa}(r)$ with increasing Na concentration. We have checked that the integrand in Eqn. (3.34) is indeed negative and monotonic for both components at all compositions, in confirmation of the argument given above for an effective attraction between concentration fluctuations. The calculated contribution to w (w^e in Table 3.2) is negative and cancels almost one half of the elastic term at all compositions. We will give in later section the discussions of the other calculated thermodynamic properties with comparison to the experiments. We also notice that only minor changes are found in Table 3.2 by using the two sets of model potential parameters.

Table 3.2: The calculated results for liquid $Na-K$ alloy at 100°C.

(a):	c_K	$-\rho_{d,Na}$	$-\rho_{d,K}$	$\kappa_T/\kappa_{T,Na}$	δ	$\frac{\delta^2}{2\kappa_T}(k_BT)$	$-w^e(k_BT)$
	0.0	0.092		1.00			
	0.1	0.084	0.217	1.11	0.51	14.8	5.6
	0.2	0.078	0.201	1.23	0.48	12.7	4.7
	0.3	0.073	0.188	1.34	0.45	11.0	4.1
	0.4	0.068	0.176	1.46	0.43	9.7	3.6
	0.5	0.063	0.165	1.57	0.40	8.5	3.1
	0.6	0.060	0.156	1.69	0.38	7.6	2.8
	0.7	0.056	0.148	1.81	0.36	6.8	2.5
	0.8	0.054	0.140	1.93	0.35	6.1	2.2
	0.9	0.051	0.134	2.05	0.33	5.5	2.0
	1.0		0.128	2.17			
(b):	c_K	$-\rho_{d,Na}$	$-\rho_{d,K}$	$\kappa_T/\kappa_{T,Na}$	δ	$\frac{\delta^2}{2\kappa_T}(k_BT)$	$-w^e(k_BT)$
	0.0	0.072		1.00			
	0.1	0.066	0.216	1.11	0.51	14.2	5.8
	0.2	0.061	0.198	1.23	0.47	12.0	4.8
	0.3	0.057	0.182	1.35	0.44	10.2	4.0
	0.4	0.053	0.168	1.48	0.41	8.8	3.4
	0.5	0.050	0.157	1.59	0.39	7.7	2.9
	0.6	0.047	0.146	1.73	0.37	6.8	2.6
	0.7	0.045	0.137	1.85	0.35	6.0	2.2
	0.8	0.042	0.129	2.00	0.33	5.4	2.0
	0.9	0.040	0.122	2.12	0.32	4.8	1.8
	1.0		0.118	2.27			

3.3.2 $Na - Cs$ alloys

As we mentioned in Section 2.2.3, Hallers *et.al.*[46] pointed out that for Cs the optimized model potential gives rise to an unphysically large core radius for the $l = 2$ level, so that the small core approximation is violated. Like Hallers *et.al.* have done, we drop the dependence of $R_l(E)$ on angular momentum l and energy E by taking $R_{Na} = 3.4(au)$ and $R_{Cs} = 4.75(au)$. The other model potential parameters, which are used in the calculations, are given in Table 3.3.

The atomic volumes of the liquid $Na - Cs$ alloys are taken from the experimental measurements[16] (Table 3.4). All the following calculations for the liquid $Na - Cs$ alloys are the same as that for the liquid $Na - K$ alloys. The calculated results are given in Table 3.5.

As already discussed in Section 3.3.1 for Na-K alloys, we also have the calculated results of depletion charges $\rho_{d,Na}$ and $\rho_{d,Cs}$ similar to those reported by Wang and Lai[55].

Table 3.3: Model potential parameters in atomic units (taken from [46]).

	A_0	A_1	A_2	$\frac{\partial A_0}{\partial E}$	$\frac{\partial A_1}{\partial E}$	$\frac{\partial A_2}{\partial E}$
Na	0.3056	0.3399		-0.2464	-0.0323	
Cs	0.2058	0.1808	0.3676	-0.4414	-0.0578	0.9467

Table 3.4: Atomic volumes of liquid $Na - Cs$ alloys at 110°C[16]

c_{Cs}	0.0	0.1	0.2	0.3	0.4	0.5
Ω_0(au)	278.9	325.3	370.7	418.6	469.7	523.4
c_{Cs}	0.6	0.7	0.8	0.9	1.0	
Ω_0(au)	579.9	639.0	701.2	765.8	832.9	

Table 3.5: The calculated results for liquid $Na - Cs$ alloy at 110°C.

c_{Cs}	$-\rho_{d,Na}$	$-\rho_{d,Cs}$	$\kappa_T/\kappa_{T,Na}$	δ	$\frac{\delta^2}{2\kappa_T}(k_BT)$	$-w^e(k_BT)$
0.0	0.112		1.00			
0.1	0.099	0.314	1.20	0.82	38.2	15.8
0.2	0.088	0.296	1.40	0.79	33.1	13.4
0.3	0.079	0.278	1.61	0.73	28.3	11.3
0.4	0.072	0.261	1.83	0.68	24.0	9.5
0.5	0.065	0.244	2.08	0.63	20.4	8.1
0.6	0.059	0.228	2.35	0.59	17.3	6.8
0.7	0.054	0.213	2.64	0.55	14.8	5.8
0.8	0.050	0.200	2.97	0.52	12.7	5.0
0.9	0.046	0.187	3.34	0.49	11.0	4.3
1.0		0.176	3.73			

3.4 Effective mass and exchange correlation corrections

3.4.1 Effective mass correction

It has been shown by Shaw[67] that the energy dependence and the non-locality of the diagonal matrix element $< \mathbf{k}|w|\mathbf{k} >$ can be taken into account by introducing two k-dependent functions $m_E(\mathbf{k})$ and m_k. In deriving these two functions Shaw assumed that the model potential $W(E_k)$ is a linear function of energy, that is

$$W(E_k) = W_0 + E_k \frac{\partial W}{\partial E}. \tag{3.39}$$

The two functions are defined, respectively, by

$$m_E(\mathbf{k}) = 1 - < \mathbf{k}|\frac{\partial W}{\partial E}|\mathbf{k} > \tag{3.40}$$

and

$$\frac{k^2}{2m_k} = \frac{k^2}{2} + < \mathbf{k}|W_0|\mathbf{k} > . \tag{3.41}$$

The energy E_k of electronic states then can be calculated by perturbation theory as

$$E_k = E_k^0 + \sum_{q \neq 0} \frac{< \mathbf{k}|W(E_k^0)|\mathbf{k}+\mathbf{q} >< \mathbf{k}+\mathbf{q}|W(E_k^0)|\mathbf{k} >}{m_E(\mathbf{k}) m_E(\mathbf{k}+\mathbf{q})(E_{\mathbf{k}}^0 - E_{\mathbf{k}+\mathbf{q}}^0)}, \tag{3.42}$$

where

$$E_k^0 = \frac{k^2}{2m_k m_E(\mathbf{k})}. \tag{3.43}$$

We can now renormalize the quantities derived in section 3.2 as in the following:

$$\rho_d^* = - \sum_{\mathbf{k} \leq \mathbf{k_F}} \{< \mathbf{k}|\frac{\partial W}{\partial E}|\mathbf{k} >_{\Omega_m} / m_E(\mathbf{k})\} \tag{3.44}$$

$$w_{\mathbf{q}}^*(\mathbf{k}) = \frac{4\pi Z^*}{\Omega_0 \varepsilon^*(q) q^2} + f(\mathbf{k}+\mathbf{q}, \mathbf{k}) + g^*(q) \tag{3.45}$$

where

$$Z^* = Z - \rho_d^* \tag{3.46}$$

$$\varepsilon^*(q) = 1 - \frac{2}{\pi^2 q^2} \int_{k \le k_F} d^3k \frac{1}{m_E(\mathbf{k}) m_E(\mathbf{k}+\mathbf{q})(E^0_{\mathbf{k}} - E^0_{\mathbf{k}+\mathbf{q}})} \tag{3.47}$$

and

$$g^*(q) = \frac{2\Omega_0}{(2\pi)^3} \int_{k \le k_F} d^3k \frac{f(\mathbf{k}+\mathbf{q}, \mathbf{k})}{m_E(\mathbf{k}) m_E(\mathbf{k}+\mathbf{q})(E^0_{\mathbf{k}} - E^0_{\mathbf{k}+\mathbf{q}})}. \tag{3.48}$$

The renormalized energy-wavenumber characteristic is then given by

$$F^*(q) = \frac{2\Omega_0}{(2\pi)^3} \int_{k \le k_F} d^3k \frac{N^2 | < \mathbf{k}+\mathbf{q} | w(E^0_k) | \mathbf{k} > |^2}{m_E(\mathbf{k}) m_E(\mathbf{k}+\mathbf{q})(E^0_{\mathbf{k}} - E^0_{\mathbf{k}+\mathbf{q}})} - \frac{\Omega_0 q^2}{8\pi} (v^*_{sc})^2 \tag{3.49}$$

where v^*_{sc} is given by

$$\begin{aligned} v^*_{sc} &= \frac{2}{\pi^2 q^2} \int_{k \le k_F} d^3k \frac{N < \mathbf{k}+\mathbf{q} | w(E^0_k) | \mathbf{k} >}{m_E(\mathbf{k}) m_E(\mathbf{k}+\mathbf{q})(E^0_{\mathbf{k}} - E^0_{\mathbf{k}+\mathbf{q}})} \\ &= \frac{4\pi Z^*}{\Omega_0 q^2} \frac{1 - \varepsilon^*(q)}{\varepsilon^*(q)} + g^*(q). \end{aligned} \tag{3.50}$$

The above expressions for the renormalized quantities are derived for simple metals. We can simply write these expressions for a binary alloy. The renormalized energy-wavenumber characteristic $F^*_{\alpha\beta}(q)$ in a binary alloy can be written as

$$F^*_{\alpha\beta}(q) = \frac{2}{\pi^2 q^2} \int_{k \le k_F} d^3k \frac{w^*_{\alpha,-\mathbf{q}}(\mathbf{k}+\mathbf{q}) w^*_{\beta,\mathbf{q}}(\mathbf{k})}{m_E(\mathbf{k}) m_E(\mathbf{k}+\mathbf{q})(E^0_{\mathbf{k}} - E^0_{\mathbf{k}+\mathbf{q}})} - \frac{\Omega_0 q^2}{8\pi} v^*_{\alpha,sc} v^*_{\beta,sc}. \tag{3.51}$$

$m_E(k)$ and m_k are given by

$$m_E(k) = 1 - < \mathbf{k} | \{ c_1 \frac{\partial W^{(1)}}{\partial E} + c_2 \frac{\partial W^{(2)}}{\partial E} \} | \mathbf{k} > \tag{3.52}$$

and

$$m_k = [1 + \frac{2}{k^2} < \mathbf{k} | \{ c_1 W_0^{(1)} + c_2 W_0^{(2)} \} | \mathbf{k} >]^{-1}. \tag{3.53}$$

Here, W^α and W_0^α are defined by Eqn. (3.39) and c_α refers to the concentration of α component in the alloy.

As discussed by Shaw[67], the effective mass $m_E(\mathbf{k})$ and m_k can be evaluated with the approximation that $R_l(E)$ are evaluated at the Fermi energy for Shaw's optimized model potential. So we can rewrite Eqns. (3.52) and (3.53) as

$$m_E(\mathrm{k}) = 1 + \frac{4\pi}{\Omega_0}\sum_{l=0}^{l_0}(2l+1)\sum_{\alpha=1}^{2} c_\alpha \frac{\partial A_l^\alpha}{\partial E}\int_0^{R_l^\alpha(E_F)} r j_l^2(kr)dr \qquad (3.54)$$

and

$$\begin{aligned} m_k^{-1} &= 1 - \frac{2}{k^2}\frac{4\pi}{\Omega_0}\sum_{l=0}^{l_0}(2l+1)\sum_{\alpha=1}^{2} c_\alpha \\ &\int_0^{R_l^\alpha(E_F)} r^2\{A_l^\alpha(E_F) - E_F\frac{\partial A_l^\alpha}{\partial E} - Z/r\}j_l^2(kr)dr. \end{aligned} \qquad (3.55)$$

3.4.2 Long wavelength limit calculations with effective mass corrections

Similar to the calculations of $V_{\alpha\beta}$ we can calculate the long wavelength limit of the renormalized pair potential $V_{\alpha\beta}^*$ straightforwardly. The final result is

$$\begin{aligned} V_{\alpha\beta}^* &= \rho \lim_{q\to 0} V_{\alpha\beta}^*(q) \\ &= \frac{\pi^2 Z_\alpha^* Z_\beta^*}{\Omega_0} - (Z_\alpha^* g_\beta^* + Z_\beta^* g_\alpha^*) + \frac{\Omega_0}{\pi^2} k_F^* g_\alpha^* g_\beta^* + I_{\alpha\beta}^*. \end{aligned} \qquad (3.56)$$

Here $V_{\alpha\beta}^*(q)$ are given by Eqn. (3.29) with Z_α^* and $F_{\alpha\beta}^N$ taking the corresponding renormalized forms. k_F^* is given by

$$k_F^* = \frac{\pi q^2}{4}\lim_{q\to 0}[\varepsilon^*(q) - 1] \qquad (3.57)$$

and g_α^* is given by

$$g_\alpha^* = \lim_{q\to 0} g_\alpha^*(q) \qquad (3.58)$$

Z^*_α is evaluated by Eqn. (3.46) and $I^*_{\alpha\beta}$ is given by

$$I^*_{\alpha\beta} = \lim_{q\to 0}\frac{\Omega_0}{4\pi^3}\int_{k\le k_K} d^3k[f_\alpha(\mathbf{k}+\mathbf{q},\mathbf{k})f_\beta(\mathbf{k},\mathbf{k}+\mathbf{q}) + f_\alpha(\mathbf{k},\mathbf{k}+\mathbf{q})f_\beta(\mathbf{k}+\mathbf{q},\mathbf{k})][m_E(\mathbf{k})m_E(\mathbf{k}+\mathbf{q})(E^0_{\mathbf{k}}-E^0_{\mathbf{k}+\mathbf{q}})]^{-1} \tag{3.59}$$

We do the calculations with effective mass corrections of the thermodynamic properties for liquid alloys Na-K and Na-Cs as we have done in Section 3.3. The results are given in Tables 3.6 and 3.7.

The calculated results with the effective mass corrections in Tables 3.6 and 3.7 show that the magnitude of depletion charges are increased by about 10% and the magnitude of the electron charge transfer contribution to the exchange energy, w^e, are increased by about 15% over all concentrations for Na-K alloys. For Na-Cs alloys the increment of the magnitude of depletion charges and w^e are larger (about 20%). In tables 3.6 and 3.7 we can also see that the other thermodynamic properties, *i.e.* the compressibility (scaled by $\kappa_{T,Na}$) and the difference in partial molar volumes δ, are not changed appreciably for Na-K alloys. For Na-Cs alloys, however, the effective mass correction give wrong variation trends for δ when $c_{Cs} < 0.5$ in comparison with experiment, to be discussed below.

Table 3.6: The calculated results with effective mass corrections for liquid $Na-K$ alloy at 100°C.

(a):	c_K	$-\rho_{d,Na}$	$-\rho_{d,K}$	$\kappa_T/\kappa_{T,Na}$	δ	$\frac{\delta^2}{2\kappa_T}(k_BT)$	$-w^e(k_BT)$
	0.0	0.102		1.00			
	0.1	0.095	0.243	1.10	0.57	16.7	6.2
	0.2	0.088	0.227	1.20	0.53	14.3	5.3
	0.3	0.082	0.213	1.30	0.50	12.4	4.6
	0.4	0.077	0.201	1.40	0.47	10.9	4.0
	0.5	0.073	0.189	1.50	0.44	9.6	3.6
	0.6	0.069	0.180	1.60	0.41	8.5	3.2
	0.7	0.065	0.171	1.71	0.39	7.6	2.8
	0.8	0.062	0.162	1.81	0.37	6.8	2.6
	0.9	0.059	0.155	1.92	0.36	6.2	2.3
	1.0		0.148	2.02			
(b):	c_K	$-\rho_{d,Na}$	$-\rho_{d,K}$	$\kappa_T/\kappa_{T,Na}$	δ	$\frac{\delta^2}{2\kappa_T}(k_BT)$	$-w^e(k_BT)$
	0.0	0.078		1.00			
	0.1	0.073	0.237	1.10	0.56	15.7	6.3
	0.2	0.068	0.219	1.22	0.52	13.3	5.2
	0.3	0.064	0.203	1.33	0.48	11.3	4.4
	0.4	0.060	0.189	1.45	0.45	9.8	3.8
	0.5	0.057	0.177	1.57	0.43	8.6	3.3
	0.6	0.054	0.166	1.69	0.40	7.5	2.9
	0.7	0.051	0.156	1.81	0.38	6.7	2.5
	0.8	0.048	0.148	1.93	0.36	6.0	2.2
	0.9	0.046	0.140	2.06	0.35	4.5	2.00
	1.0		0.133	2.18			

Table 3.7: The calculated results with effective mass corrections for liquid $Na - Cs$ alloy at 110°C.

c_{Cs}	$-\rho_{d,Na}$	$-\rho_{d,Cs}$	$\kappa_T/\kappa_{T,Na}$	δ	$\frac{\delta^2}{2\kappa_T}(k_BT)$	$-w^e(k_BT)$
0.0	0.126		1.00			
0.1	0.113	0.361	1.25	0.39	16.0	19.1
0.2	0.102	0.345	1.50	0.45	19.8	17.0
0.3	0.092	0.327	1.74	0.47	21.1	15.0
0.4	0.084	0.309	2.00	0.47	20.8	13.1
0.5	0.077	0.291	2.27	0.46	19.8	11.4
0.6	0.071	0.274	2.56	0.45	18.6	9.9
0.7	0.066	0.258	2.88	0.44	17.5	8.6
0.8	0.061	0.242	3.22	0.43	16.4	7.4
0.9	0.056	0.228	3.58	0.43	15.5	6.4
1.0		0.215	3.95			

3.4.3 Exchange and correlation corrections

According to Shaw[68], the conduction electron contribution to the form factor including exchange and correlation effects, v_e^{EX}, is given by

$$v_e^{EX} = [1 - G(q)](4\pi/q^2)n_e^{EX}(q). \tag{3.60}$$

Here, $G(q)$ is a function which describes the effects of exchange and correlation among conduction electrons[69,70] and $n_e^{EX}(q)$ is given by

$$n_e^{EX}(q) = \frac{1}{2\pi^3}\int_{\mathbf{k}\leq\mathbf{k}_F} d^3k \frac{w_{\mathbf{q}}^{EX}(\mathbf{k})}{\frac{1}{2}(k^2 - |\mathbf{k}+\mathbf{q}|^2)} + n_d(q) \tag{3.61}$$

where $n_d(q)$ is the depletion charge density and $w_{\mathbf{q}}^{EX}(\mathbf{k})$ is given by

$$w_{\mathbf{q}}^{EX}(\mathbf{k}) = v_q + f(\mathbf{k}+\mathbf{q},\mathbf{k}) + v_e^{EX}(q). \tag{3.62}$$

Since $w_{\mathbf{q}}^{EX}(\mathbf{k})$ depends on $\mathbf{k}$ we must solve Eqns. (3.61) and (3.62) self-consistently. The result we obtain is

$$w_{\mathbf{q}}^{EX}(\mathbf{k}) = w_{\mathbf{q}}(k) - \frac{G(q)}{\tilde{\varepsilon}(q)} v_e(q) \tag{3.63}$$

with

$$\tilde{\varepsilon}(q) = 1 + [\varepsilon(q) - 1][1 - G(q)]. \tag{3.64}$$

As we have seen in previous sections a fairly complete description of metallic properties can be obtained from the pseudopotential form factor and energy-wavenumber characteristic. For convenience we define the form factor $w_{\mathbf{q}}^{EX}(\mathbf{k})$, and the modified energy-wavenumber characteristic $F^{EX}(q)$, which include exchange and correlations, in terms of the corresponding Hartree results $w_{\mathbf{q}}(\mathbf{k})$ and $F(q)$ (namely, the results obtained in Section 3.2) by the relations

$$w_{\mathbf{q}}^{EX}(\mathbf{k}) = w_{\mathbf{q}}(\mathbf{k}) + \Delta w \tag{3.65}$$

and

$$F^{EX}(q) = F(q) + \Delta F. \tag{3.66}$$

After some algebraic manipulation by using the formula given in Section 3.2, the expression of ΔF in Eqn. (3.66) can be written as[68]

$$\Delta F(q) = -\frac{\Omega_0 q^2}{8\pi} \varepsilon(q) \frac{G(q)}{\tilde{\varepsilon}(q)} [v_e(q)]^2 \tag{3.67}$$

For a binary alloy we can write Eqn. (3.66) as

$$F_{\alpha\beta}^{EX}(q) = F_{\alpha\beta}(q) + \Delta F_{\alpha\beta} \tag{3.68}$$

where $\Delta F_{\alpha\beta}$ is given by

$$\Delta F_{\alpha\beta}(q) = -\frac{\Omega_0 q^2}{8\pi} \varepsilon(q) \frac{G(q)}{\tilde{\varepsilon}(q)} v_{e,\alpha}(q) v_{e,\beta}(q) \tag{3.69}$$

Table 3.8: The calculated results with exchange and correlation corrections for liquid $Na-K$ alloy at 100°C.

(a):	c_K	$-\rho_{d,Na}$	$-\rho_{d,K}$	$\kappa_T/\kappa_{T,Na}$	δ	$\frac{\delta^2}{2\kappa_T}(k_BT)$	$-w^e(k_BT)$
	0.0	0.092		1.00			
	0.1	0.084	0.217	1.10	0.83	23.8	5.6
	0.2	0.078	0.201	1.20	0.77	20.3	4.7
	0.3	0.073	0.188	1.29	0.71	17.4	4.1
	0.4	0.068	0.176	1.39	0.66	15.1	3.6
	0.5	0.063	0.165	1.49	0.62	13.2	3.1
	0.6	0.060	0.156	1.58	0.58	11.6	2.8
	0.7	0.056	0.148	1.68	0.55	10.3	2.5
	0.8	0.054	0.140	1.78	0.52	9.2	2.2
	0.9	0.051	0.134	1.88	0.49	8.3	2.0
	1.0		0.128	1.97			
(b):	c_K	$-\rho_{d,Na}$	$-\rho_{d,K}$	$\kappa_T/\kappa_{T,Na}$	δ	$\frac{\delta^2}{2\kappa_T}(k_BT)$	$-w^e(k_BT)$
	0.0	0.072		1.00			
	0.1	0.066	0.216	1.10	0.84	23.4	5.8
	0.2	0.061	0.198	1.20	0.77	19.4	4.8
	0.3	0.057	0.182	1.30	0.71	16.4	4.0
	0.4	0.053	0.168	1.41	0.66	14.0	3.4
	0.5	0.050	0.157	1.52	0.62	12.2	2.9
	0.6	0.047	0.146	1.63	0.58	10.6	2.6
	0.7	0.045	0.137	1.74	0.55	9.4	2.2
	0.8	0.042	0.129	1.86	0.52	8.3	2.0
	0.9	0.040	0.122	1.97	0.49	6.0	1.8
	1.0		0.118	2.09			

Table 3.9: The calculated results with exchange and correlation corrections for liquid $Na - Cs$ alloy at 110°C.

c_{Cs}	$-\rho_{d,Na}$	$-\rho_{d,Cs}$	$\kappa_T/\kappa_{T,Na}$	δ	$\frac{\delta^2}{2\kappa_T}(k_BT)$	$-w^e(k_BT)$
0.0	0.112		1.00			
0.1	0.099	0.314	1.18	1.32	60.4	15.8
0.2	0.088	0.296	1.34	1.21	51.1	13.4
0.3	0.079	0.278	1.51	1.10	42.7	11.3
0.4	0.072	0.261	1.69	1.01	35.6	9.5
0.5	0.065	0.244	1.88	0.92	29.8	8.1
0.6	0.059	0.228	2.10	0.85	25.1	6.8
0.7	0.054	0.213	2.35	0.79	21.3	5.8
0.8	0.050	0.200	2.64	0.74	18.2	5.0
0.9	0.046	0.187	2.95	0.69	15.6	4.3
1.0		0.176	3.30			

and $v_{e,\alpha}(q)$ is given by Eqn. (2.37).

The pair potential $V_{\alpha\beta}^{EX}$ can then be calculated by using Eqns. (3.17), (3.19) and (3.69). We finally take the long wavelength limit ($q \to 0$) and calculate the thermodynamic properties of the liquid alloys Na-K and Na-Cs as before. In the calculations $G(q)$ is taken from the interpolation results given by Singwi *et.al.*[69] We present the results in Tables 3.8 and 3.9 for liquid alloys Na-K and Na-Cs, respectively. The effective mass corrections are not included in the calculations.

We see in Tables 3.8 and 3.9 that the exchange and correlation corrected calculations give very good results for the partial volumes change δ when compared with experiments (see Section 3.5). The electron

charge transfer contribution to w and the scaled compressibility are almost the same as those obtained in the Hartree calculations in Section 3.3 although the absolute value of the isothermal compressibility κ_T are apparently increased (see Figure 3.1 in Section 3.5).

3.5 Comparison with experiment and discussion

In previous sections we have calculated the thermodynamic properties of liquid Na-K and Na-Cs alloys. In this section we shall compare the calculated results with the experimental data systematically. Figure 3.1 gives the compressibility of the Na-K alloy. Here and in all the following figures, the dots refer to the experimental data, the full lines denote the Hartree calculations (namely without effective mass and exchange and correlation corrections), the short dashed lines refer to the calculations with effective mass corrections and the long dashed lines are for the exchange and correlation corrections. As we have seen in the above section, the two sets of model potential parameters give almost the same results for Na-K alloys. Here, we just give the results calculated by using the model potential parameters of set (a). Figures 3.1-3.3 are the results for Na-K alloys while Figures 3.4-3.6 are the results for the Na-Cs alloys.

Figure 3.1 shows that in the Na-K alloy the calculations cannot predict the measured isothermal compressibility accurately but only give the correct trend with concentration. We stress this point by scaling the results with the compressibility of pure Na ($c_K = 0$) in Figure 3.2. On the other hand, in the case of the Na-Cs alloys (Figures 3.4 and 3.5) both the absolute magnitude of the compressibility and the shape of its

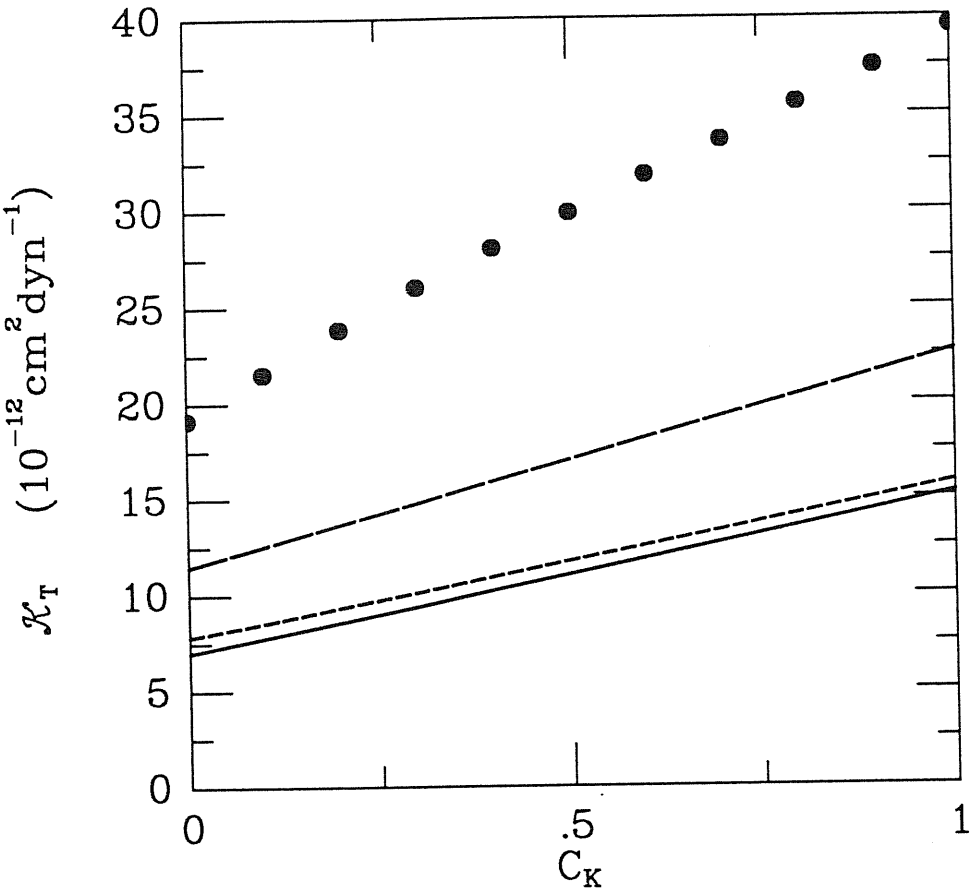

Figure 3.1: Compressibility of Na-K liquid alloys at 100 °C.

relative relative magnitude as a function of concentration are in error. The calculations of Wang *et.al.* are also affected by similar errors (see Figure 2.5).

Figure 3.3 gives the difference in partial molar volumes for the Na-K alloy, and Figure 3.6 for the Na-Cs alloys. In both systems the agreement with experiment is satisfactory when the corrections for exchange and correlation are included. On the other hand, the effective mass corrections for Na-Cs alloys give an incorrect trend at low Cs concentration.

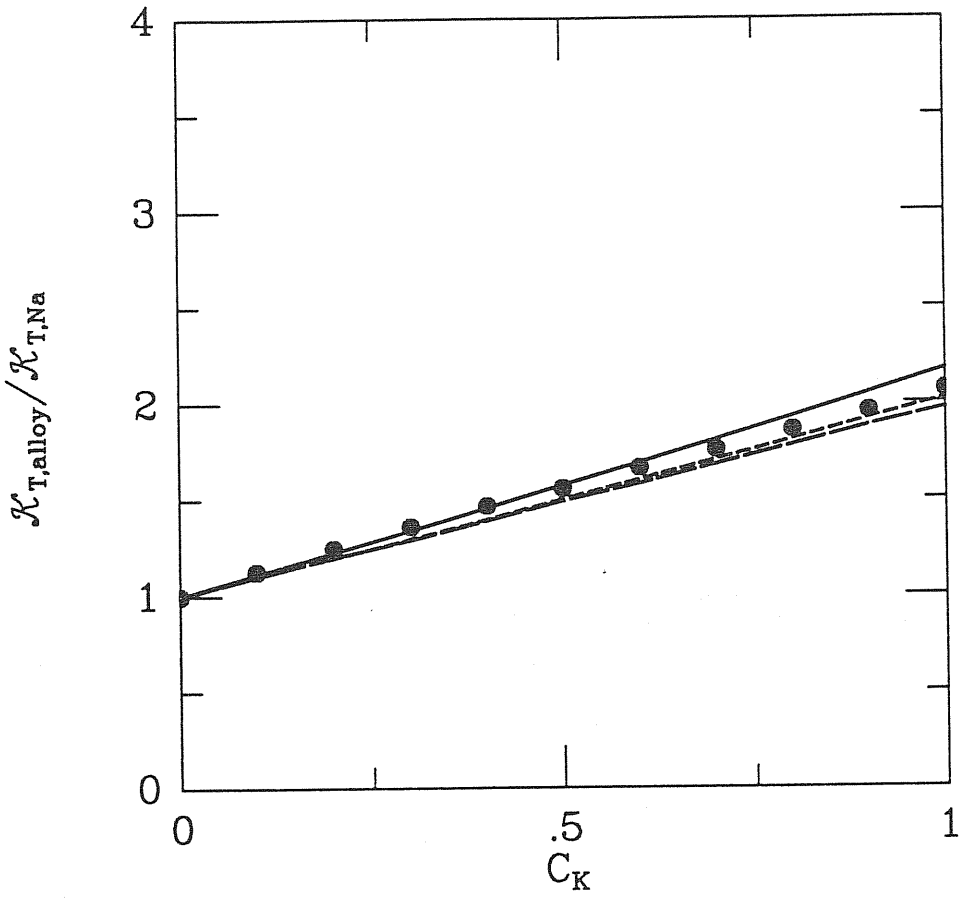

Figure 3.2: Scaled compressibility of Na-K liquid alloys at 100 °C.

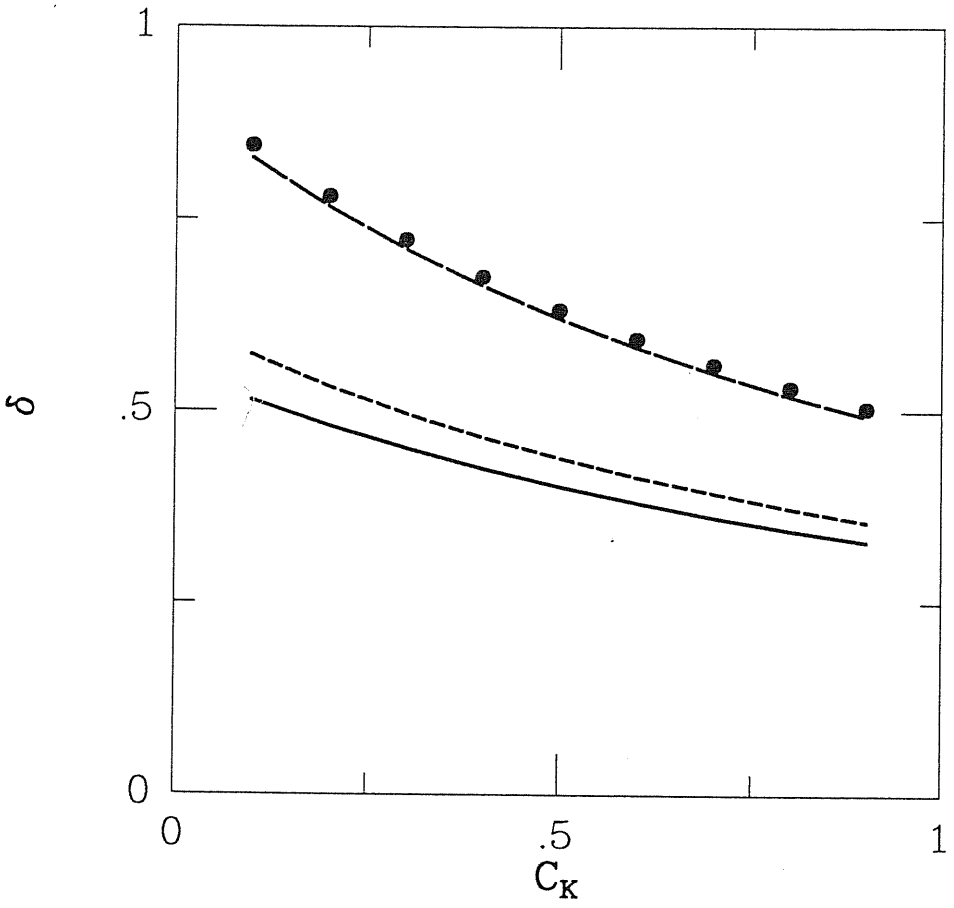

Figure 3.3: The difference in partial molar volumes of the alloy components, δ, for Na-K liquid alloys at 100 °C.

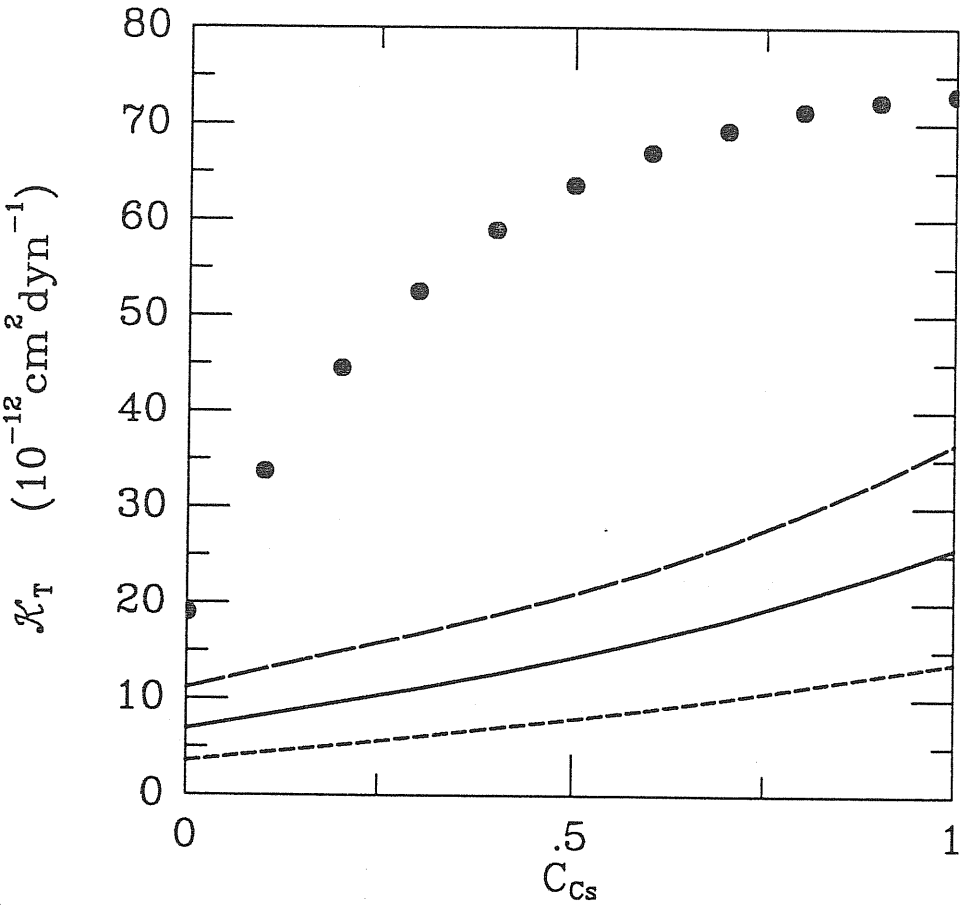

Figure 3.4: Compressibility of Na-Cs liquid alloys at 110 °C.

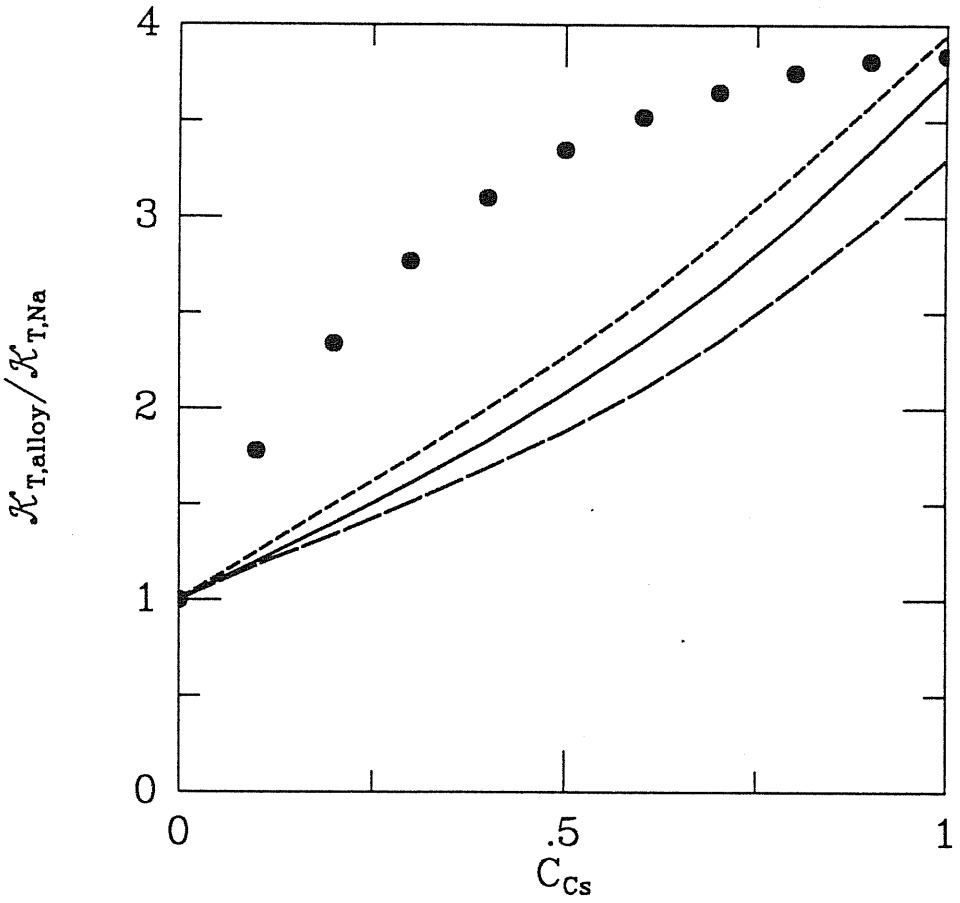

Figure 3.5: Scaled compressibility of Na-Cs liquid alloys at 110 °C.

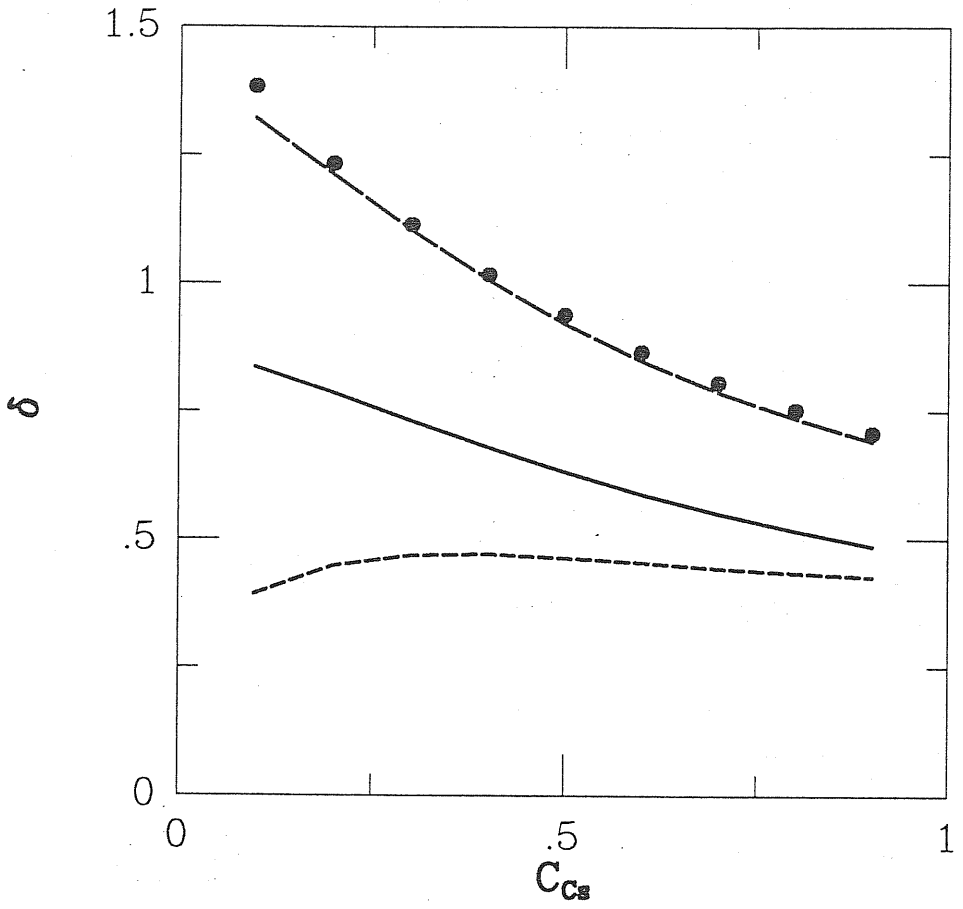

Figure 3.6: The difference in partial molar volumes of the alloy components, δ, for Na-Cs liquid alloys at 110 °C.

Finally in Tables 3.10 (Na-K alloys) and 3.11 (Na-Cs alloys) we give the results for the interchange energy w, as defined in Eqn. (3.10). To evaluate w we use the the experimental data to calculate the first, elastic strain term. The reason for doing so is to see how electron charge transfer enters the determination of w, since the theoretical results do not give reliable values for κ_T and δ. In these Tables we also give the values of w which are deduced from measurements. The main points of our results is to show that strong cancellations exists between elastic and charge transfer contributions. The results are rather weakly affected by the inclusion of effective mass or exchange-correlation corrections and are clearly not sufficiently accurate for a theoretical prediction of the magnitude of w.

Table 3.10: The interchange energy w of Na-K liquid alloys at 100 °C. The elastic strain term is calculated from the measured δ and κ_T and the three columns for w^e and for w refer to the calculations (i) in the Hartree approximation, (ii) with inclusion of effective mass corrections and (iii) with inclusion of exchange and correlation corrections , respectively.

c_K	$\frac{\delta^2}{2\kappa_T}(k_BT)$ (expt.)	$-w^e(k_BT)$			$w(k_BT)$			$w(k_BT)$ (expt.)
0.1	12.5	5.6	6.2	5.6	6.9	6.3	6.9	1.1
0.2	12.3	4.7	5.3	4.7	7.6	7.0	7.6	1.1
0.3	9.9	4.1	4.6	4.1	5.8	5.3	5.8	1.1
0.4	8.6	3.6	4.0	3.6	5.0	4.6	5.0	1.1
0.5	8.0	3.1	3.6	3.1	4.9	4.4	4.9	1.1
0.6	6.7	2.8	3.2	2.8	3.9	3.5	3.9	1.1
0.7	6.3	2.5	2.8	2.5	3.8	3.5	3.8	1.1
0.8	6.2	2.2	2.6	2.2	4.0	3.6	4.0	1.2
0.9	4.8	2.0	2.3	2.0	2.8	2.5	2.8	1.2

Table 3.11: The interchange energy w of Na-Cs liquid alloys at 110 °C. The elastic strain term are calculated from the measured δ and κ_T and the three columns for w^e and for w have the same meaning as in Table 3.10.

c_{Cs}	$\frac{\delta^2}{2\kappa_T}(k_BT)$	$-w^e(k_BT)$			$w(k_BT)$			$w(k_BT)$
	(expt.)							(expt.)
0.1	25.7	15.8	19.1	15.8	9.9	6.6	9.9	4.5
0.2	17.7	13.4	17.0	13.4	4.3	0.7	4.3	2.7
0.3	13.9	11.3	15.0	11.3	2.6	-1.1	2.6	2.3
0.4	11.5	9.5	13.1	9.5	2.0	-1.6	2.0	1.9
0.5	10.2	8.1	11.4	8.1	2.1	-1.2	2.1	1.3
0.6	9.1	6.8	9.9	6.8	2.3	-0.8	2.3	0.8
0.7	8.4	5.8	8.6	5.8	2.6	-0.2	2.6	0.5
0.8	7.8	5.0	7.4	5.0	2.8	0.4	2.8	0.3
0.9	7.4	4.3	6.4	4.3	3.1	1.0	3.1	0.3

Chapter 4

Summary and Conclusions

In this thesis we have used pseudopotential theory to calculate those thermodynamic properties of liquid Na-K and Na-Cs alloys, which are related to the long-wavelength limit of the partial structure factors or equivalently of the Ornstein-Zernike functions. We have, in particular, derived an exact formula for the concentration-concentration structure factor at long wavelengthes, showing how a mechanical stress contribution and an effective interaction between concentration fluctuations enter to determine it. The latter contribution has been shown to be related to electron charge transfer between the alloy components, within the framework of the pseudopotential theory of metals. For these calculations we have derived expressions for the long wavelength limit of the effective ion-ion interactions in the alloy, considering first a simple Hartree treatment and then evaluating effective mass and exchange-correlation corrections.

Numerical calculations within the optimized Heine-Abarenkov model potential, which is nonlocal, have been carried out for the above thermodynamic properties, namely the concentration-concentration structure

factor $S_{cc}(0)$, the isothermal compressibility κ_T and the difference in partial molar volumes of the alloy components. Our results for simple alkali-metal liquid alloys show that microscopic approach based on pseudopotential theory still has difficulties in reaching quantitative predictive value. Nevertheless, a number of qualitative trends shown by the available experimental data can be reproduced. In particular, a strong cancellation between the increase of free energy associated with elastic strains and the decrease associated with electron charge transfer has been demonstrated in the "interchange energy" w regulating the fluctuations of concentration in a liquid alloy of homovalent metallic elements. This implies, of course, that electron charge transfer acts in a liquid metal alloy to stabilize it against phase separation.

In relation to future continuations of this work, one may hope for some improvements of our results if the calculations are carried out with more refined model potentials. It would also be of relevant interest to extend the present approach to alloys of heterovalent elements, especially in relation to the alloys with chemical short-range order that we have briefly reviewed in Section 1.4 of this thesis.

Appendix A

Evaluation of $\Sigma_k < \mathbf{k} \mid w \mid \mathbf{k} >$

Here we use Shaw's optimized model potential to derive the explicit expression of the sum over diagonal matrix elements in Eqn. (2.44). We write the model potential as the sum of a bare electron-core potential w_0, given by Eqn. (2.21) as

$$w_0 = -Z/r - \sum_{l=0}^{l_0} \theta(R_l - r)(A_l(E) - Z/r)P_l \qquad \text{(A.1)}$$

and a potential $v_e(\mathbf{r})$ due to all the conduction electrons. The diagonal matrix elements of the local terms are k independent so the sum over occupied states gives simply NZ. We may write the average value of the valence and electron potentials as the electrostatic energy of these potentials in a uniform background charge normalized by the effective valence $Z^* = Z - \rho_d$. Note that the screening charge distribution gives no contribution to the average electron potential. The contribution to Eqn. (2.44) due to the diagonal matrix elements may now be written explicitly as[50]

$$\sum_k < \mathrm{k}|w|\mathrm{k} >= \frac{n_u}{NZ^*}(V_{val} + V_u + V_d) - \sum_k \sum_{l=0}^{l_0} < \mathrm{k}|\{A_l(E) - \frac{Z}{r}\}P_l|\mathrm{k} >_{\Omega_m} \qquad \text{(A.2)}$$

Here, we use the same symbols as in the text.

It has been shown[45] that, for most simple metals, $A_l(E)$ is a linear function of energy over the range of conduction-band energies and the well depth $A_l(E)$ appropriate to a conduction state with energy E_k is determined by evaluating $A_l(E)$ at energy $(E_k - V_0)$ on an energy scale with the free-ion vacuum chosen as the zero. Here V_0 is the potential at a particular site due to all the other ions and the conduction electrons.

For simplicity in determining the well depths, it has been customary to replace V_0 by an average equal to the electrostatic energy of the contributing potentials embedded in a uniform charge,

$$< V_0 >= \frac{n_u}{NZ^*}(V_{val} + V_u + V_d). \tag{A.3}$$

Having determined $< V_0 >$, we may then evaluate $A_l(E_F)$ using the relation

$$A_l(E_F) = A_l(- < V_0 >) + E_F \frac{\partial A_l}{\partial E}. \tag{A.4}$$

The well depth appropriate to an arbitrary electron energy E_k is then given by the linear relation

$$A_l(E_k) = A_l(E_F) + (E_k - E_F)\frac{\partial A_l}{\partial E}. \tag{A.5}$$

However, it is not correct to use (A.5) to calculate (A.2). If we do so, we will be overlooking structure-dependent terms which must be included if our total energy calculation is to be accurate to to second order in W. There are two corrections must be made. First we must include the true overlap potential V_0. This is done by subtracting out the $< V_0 >$ contribution to $A_l(E_F)$ and adding the correct overlap term. And secondly, we must evaluate the energies in (A.5) to first order in

W. The expression of $A_l(E_k)$ now can be written as[50]

$$A_l(E_k) = A_l(E_F) + (< V_0 > -V_0)\frac{\partial A_l}{\partial E} + (\frac{1}{2}k^2 + N < \mathbf{k} \mid w \mid \mathbf{k} > - \frac{1}{2}k^2 + N < \mathbf{k_F} \mid w \mid \mathbf{k_F} >)\frac{\partial A_l}{\partial E}. \quad (A.6)$$

The overlap potential is given by the electrostatic energy of an electron charge $-n_{val}/NZ$ at the nucleus in question interacting with the ion potentials at all other sites and with the total electron potential

$$V_0 = -\frac{n_{val}}{NZ}(V'_{val} + V_u + V_d + V_{sc}) + v_d \quad (A.7)$$

We may now write the expression of $\sum_k < \mathbf{k} \mid w \mid \mathbf{k} >$ explicitly by combining Eqns. (A.2), (A.3) and (A.7) and then recalling that the depletion charge is given by

$$\rho_d = Z - Z^* = \sum_k \sum_{l=0}^{l_0} \frac{\partial A_l}{\partial E} < \mathbf{k} \mid P_l \mid \mathbf{k} >_{\Omega_m} . \quad (A.8)$$

The resulting expression may then be simplified by noting that

$$V_d = -\frac{Z - Z^*}{Z} V_{val} \quad (A.9)$$

and that n and V may be interchanged in the symbolic expressions. Finally we obtain (Eqn. (2.46))

$$\sum_k < \mathbf{k} \mid w \mid \mathbf{k} > = \frac{1}{N}(n_u + n_d)(V_u + V'_d) + \frac{1}{2N} n_{val}(V_u + V_d) + \frac{1}{2N}(n_u + n_d)V_{val} + \frac{1}{N} n_d V_{sc} + \rho_d v_d + \frac{1}{N}\sum_k f(k) - \sum_k \sum_{l=0}^{l_0} \frac{\partial A_l}{\partial E} < \mathbf{k} \mid P_l \mid \mathbf{k} > \{f(k) - f(k_F)\}. \quad (A.10)$$

An explicit expression for the function $f(k)$ is given by Eqns. (3.24) and (3.25).

References

1. J.G. Kirkwood and F. Buff, *J. Chem. Phys.*, **19**, 774(1951).

2. A.B. Bhatia and D.E. Thornton, *Phys. Rev.*, **B2**, 3004(1970).

3. N.H. March and M.P. Tosi, *Atomic Dynamics in Liquids,* (McMillan Press , London and Basingstoke, 1976).

4. N.H. March, *Amorphous Solids and Liquid State*, P. 53 (eds. N. H. March, R.A. Street and M.P. Tosi; Plenum Press, New York, 1985).

5. J.P. Hansen and I.R. McDonald, *Theory of Simple Liquids,* (Academic Press, London, 1986)

6. M.J. Huijben and W. van der Lugt, *Acta Cryst.,* **A35**, 431(1979); N.H. March and M.P. Tosi, *Coulomb Liquids,* (Academic Press, London, 1984).

7. M. Hasegawa and M. Watabe, *Proc. Second Int. Conf. Liquid Met.,* P. 439 (1972); N.W. Ashcroft and D. Stroud, *Solid State Physics,* **33**, 1(1978).

8. J.E. Enderby and P.A. Egelstaff, *Phil. Mag.*, **14**, 961(1966).

9. H. Ruppersberg, *Phys. Letts.*, **A46**, 74(1973).

10. A.B. Bhatia, *Inst. Phys. Conf. Ser.*, No. 30, 21(1977).

11. H.C. Longuet-Higgins, *Proc. Roy. Soc.*, **A205**, 247(1951).

12. S.P. McAlister and R. Turner, *J. Phys.*, **F2**, L51(1972).

13. A.B. Bhatia, W.H. Hargrove and N.H. March, *J. Phys.*, **C6**, 621(1973).

14. A.B. Bhatia and N.H. March, *Phys. Letts.*, **A41**, 397(1972).

15. A.B. Bhatia and N.H. March, *J. Phys.*, **F5**, 1100(1975).

16. K. Ichikawa, S.M. Granstaff and J.C. Thompson, *J. Chem. Phys.*, **61**, 4059(1974).

17. F.E. Neale and N.E. Cusack, *J. Phys.*, **F12**, 2839(1982).

18. W.H. Young, *Can. J. Phys.*, **65**, 241(1987).

19. J.A. Alonso and N.H. March, *Phys. Chem. Liquids*, **11**, 135(1981).

20. A.R. Miedema, P.F. de Chatel and F.G. de Boer, *Physica*, **B100**, 1(1980).

21. L.S. Darken, *Trans. AIME*, **239**, 80(1967).

22. A. Petric, A.D. Pelton and M-L. Saboungi, *J. Chem. Phys.*, **89**, 5070(1988).

23. A. Petric, A.D. Pelton and M-L. Saboungi, *J. phys.*, **F18**, 1473(1988).

24. M-L. Saboungi, J. Ellefson and G.K. Johnson, *J. Chem. Phys.*, **88**, 5812(1988).

25. A. Petric, A.D. Pelton and M-L. Saboungi, *J. Electrochem. Soc.*, **135**, 2754(1988).

26. G. Grube and H. Klaiber, *Z. Electrochem.*, **40**, 745(1934).

27. M-L. Saboungi, J. Marr and M. Blander, *J. Chem. Phys.*, **68**, 1375(1978).

28. J.A. Meijer, *Ph.D Thesis* (Rijifsunnisitet Gronigen, 1988).

29. M. Hansen, *Constitution of Binary Alloys*, (McGraw Hill, New York , 1958).

30. S. Matsunaga, T. Ishiguro and S. Tamaki, *J. Phys.*, **F13**, 527(1983).

31. C. van der Marel, A.B. van Oosten, W. Geertsma and W. van der Lugt, em J. Phys., **F12**, L129(1984)

32. M-L. Saboungi, S. J. Herron and R. Kumar, *Ber. Bunsengs. Phys. Chem.*, **89**, 375(1985).

33. D.N.Shoikheit, A.G.Morachevskii and A.F. Alabyshev, *Russ. J. Inorg. Chem.*, **4**, 728(1959).

34. M-L. Saboungi, S. R. Leonard and J. Ellefson, *J. Chem. Phys.*, **85**, 6072(1986)

35. S. Tamaki, T. Ishiguro and S. Takeda, *J. Phys.*, **F12**, 1613(1982).

36. P. Ramachandrarao, R.N. Singh and S. Lele, *J. Non-Cryst. Solids* , **64**, 387(1984).

37. S. Harada, S. Takahashi, S. Takeda, S. Tamaki, P. Gray and N.E. Cusack , *J. Phys.*, **F18**, 2559(1988).

38. W.A. Harrison, *Pseudopotentials in the Theory of Metals*, (W.A. Benjamin Inc., New York, 1966).

39. N.W. Ashcroft and N.D. Mermin, *Solid State Physics*, (Holt, Rinehart and Winston, Philadelphia, 1976).

40. J.C. Phillips and L.K. Kleinman, *Phys. Rev.*, **116**, 287, 880(1959).

41. M.L. Cohen and V. Heine, *Solid State Physics*, Vol.24, 38(1970).

42. N.W. Ashcroft, Phys. Letts., **23**, 48(1966).

43. I.V.Abarenkov and V. Heine, *Phil. Mag.*, **12**, 529(1965); V. Heine and I.V. Abarenkov, *Phil. Mag.*, **9**, 451(1964).

44. R.W. Shaw,Jr. and W.A. Harrison, *Phys. Rev.*, **163**, 604 (1967).

45. R.W. Shaw,Jr., *Phys. Rev.*, **174**, (1968).

46. J.J. Hallers, T. Marrẽn and W. van der Lugt, *Physica*, **78**, 259(1974).

47. C.H. Woo and S. Wang, *Phys. Rev.*, **B7**, 2810(1973).

48. C.H. Woo, S. Wang and M. Matsuura, *J. Phys.*, **F5**, 1836 (1975).

49. W.A. Harrison, *Phys. Rev.*, **129**, 2503(1963).

50. R.W. Shaw,Jr. *J. Phys.*, **C2**, 2335(1969).

51. D.K. Chatuvredi, M. Rovere, G. Senatore and M.P. Tosi, *Physica*, **111B**, 11(1981).

52. H.E. DeWitt, *Phys. Rev.*, **14A**, 1290(1976)

53. J.P. Hansen, G.M. Torrie and P. Vieillefosse, *Phys. Rev.*, **A16**, 2153(1977).

54. S. Ogata and S. Ichimaru, *Phys. Rev.*, **36A**, 5451(1987).

55. S. Wang and S.K. Lai, *J. Phys.*, **F10**, 2717(1980)

56. S. Wang, S.K. Lai and C.B. So, *J. Phys.*, **F10**, 445(1980)

57. S.K. Lai, M. Matsuura and S. Wang, *J. Phys.*, **F13**, 2033(1983).

58. D.H. Li, X.R. Li and S. Wang, *J. Phys.*, **F16**, 309(1986).

59. T. Lukes and R. Jones, *J. Phys.*, **A1**, 29(1968).

60. I. Yokoyama, A. Meyer, M.J. Stott and W.H. Young, *Phil. Mag.*, **35**, 1021(1977).

61. I.H. Umar, A. Meyer, M. Watabe and W.H. Young, *J. Phys.*, **F4**, 1619(1974).

62. N.W. Ashcroft and D.C. Langreth, *Phys. Rev.*, **156**, 685(1967).

63. Wang Li and M.P. Tosi, *N. Cimento*, **D11**, 1509(1989).

64. F. Postogna and M.P. Tosi, *N. Cimento*, **B55**, 399(1980).

65. O. Ese and J.A. Reissland, *J. Phys.*, **F3**, 2066(1973).

66. G. Abowitz and R.B. Gordon, *J. Chem. Phys.*, **37**, 125(1962).

67. R.W. Shaw,Jr., *J. Phys.*, **C2**, 2356(1969).

68. R.W. Shaw,Jr., *J. Phys.*, **C3**, 1140(1970).

69. K.S. Sigwi, A Sjölander, M.P. Tosi and R.H. Land, *Phys. Rev.*, **B1**, 1044(1970).

70. K.S. Singwi and M.P. Tosi, *Solid State Physics*, Vol.36, 177(1981).